JOANNES A.A. REIJERS

STICKY & DIRTY PROTEINS

or
on the poorly characterised peculiar pharmacokinetic and immunostimulatory aspects of biopharmaceuticals

COLOFON

The publication of this thesis was financially supported by the foundation Centre for Human Drug Research (CHDR) in Leiden, the Netherlands.

DESIGN

Caroline de Lint, Voorburg (caro@delint.nl)
(*featuring graphical art by the author*)

ISBN

978-90-828304-0-8

STICKY & DIRTY PROTEINS

or on the poorly characterised, peculiar, pharmacokinetic and immunostimulatory aspects of biopharmaceuticals

PROEFSCHRIFT

ter verkrijging van de graad van Doctor aan de Universiteit Leiden, op gezag van Rector Magnificus Prof. Mr. C. J. J. M. Stolker, volgens besluit van het College voor Promoties te verdedigen op woensdag 14 maart 2018 klokke 15:00 uur

DOOR

Joannes Albertus Antonius Reijers
geboren te Dordrecht in 1985

PROMOTORES
Prof. Dr. J. Burggraaf
Prof. Dr. A.F. Cohen

COPROMOTOR
Dr. M. Moerland

PROMOTIECOMMISSIE
Prof. Dr. T.W.J. Huizinga
Prof. Dr. H.J. Guchelaar
Prof. Dr. E.L. Swart (*VU Medisch Centrum, Amsterdam*)
Prof. Dr. H. Schellekens (*Universiteit Utrecht*)

STELLINGEN

1 Een zogenaamde non-compartimentele analyse van de plasmaconcentratie van veel biofarmaceutica is ongeschikt voor het aantonen van biosimilariteit. (*dit proefschrift*)

2 Adsorptie van eiwitten aan endotheel gedurende intraveneuze toediening, gevolgd door desorptie, kan verklaren waarom de maximumplasmaconcentratie van sommige biofarmaceutica geruime tijd na het einde van toediening optreedt. (*dit proefschrift*)

3 De huidige farmacokinetische modellen zijn ontoereikend in hun verklaring van de (fluctuerende) plasmaconcentratie van biofarmaceutica. (*dit proefschrift*)

4 Immunostimulatie veroorzaakt door biofarmaceutica is soms lastig *in vitro* te voorspellen door onvoldoende kennis van het onderliggende mechanisme, zoals ook het geval is bij trastuzumab. (*dit proefschrift*)

5 De veelgebruikte teststrategie voor nieuwe en bestaande geneesmiddelen, die ten doel heeft de veiligheid van patiënten en deelnemers aan klinisch onderzoek te waarborgen, kan (ernstige) immunostimulatie missen, zelfs als bekende pro-inflammatoire stoffen (bijvoorbeeld endotoxine of flagelline) de bron zijn. (*dit proefschrift*)

6 Biofarmaceutica hebben een inherent risico op (soms letale) immunostimulatie; daarom moeten de richtlijnen worden aangepast. (*dit proefschrift*)

7 Het onbedachtzaam toepassen van farmacologische concepten die in het verleden nuttig bleken, kan tot foutieve conclusies leiden. (*dit proefschrift*)

8 'Regressie naar het gemiddelde' is een bedreiging voor de ontwikkeling van nieuwe inzichten, zeker indien dit fenomeen gepaard gaat met een inquisitie.

9 Onderzoek waarin het vinden van associaties centraal staat, is geassocieerd met een hoog risico op *confounding*, hetgeen kan worden voorkomen door integratie van de resultaten met basale wetenschap en door het uitvoeren van interventieonderzoek met een goede controlegroep.

10 Mensgebonden onderzoek kan nooit volledig worden vervangen door laboratoriumonderzoek, tenzij de laborant ook als proband fungeert.

11 Wetenschap draait om weten en weten om kennis vergaren; selectieve publicatie van observaties bevordert alleen het ego van de auteurs.

12 De stelling 'Als mensen een verband leggen tussen het beoefenen van de voetbalsport en geringe intelligentie, zijn ze te dom zijn om het spel te begrijpen.' [J. Burggraaf, 1998, *sic*] behoeft geen toelichting; immers, het getuigt van een groot abstractievermogen als men een verband ziet tussen het najagen van opgeblazen lucht en een hoogleraar.

INTRODUCTION

Clinical pharmacology focuses on 'all aspects of the study and use of drugs in humans' with the objective to treat patients rationally. Rational pharmacotherapy revolves around two core questions: 'How does a drug reach its site of action in sufficient quantities?' (*i.e.* pharmacokinetics) and 'How does a drug exert an effect?' (*i.e.* pharmacodynamics), which relates both to intended and unintended effects. Typically, answering these question involves an integration of various areas of knowledge on a pharmaceutical, including molecular mechanisms (sub-cellular level), (patho)physiology of the intended indication(s), drug distribution, interactions, epidemiology, and individual characteristics.[1]

Although the execution of experiments with pharmacologically active substances in living beings dates back to ancient times, this practice became a more scientifical character starting in the renaissance and progressing throughout the 19th century.[2] Conversely, clinical pharmacology is a relatively young discipline with its roots in the 1950s.[3] At that time, the majority of pharmaceuticals was chemically derived, meaning that raw materials are converted to the active (drug) substance by a series of chemical reactions. It is therefore not surprising that pharmacological knowledge and theories are largely based on experience with these so-called 'small molecules'.

Since the 1980s biotechnologically derived drug substances have emerged.[4,5] These 'biopharmaceuticals' (or 'biologicals') are produced by manipulated organisms or living cell systems, usually via recombinant DNA techniques. Naturally occurring human proteins – including coagulation factors, hormones, enzymes, and plasma constituents – have been manufactured that way, as well as tailored or specifically developed proteins, mostly monoclonal antibodies (MABs), which can be directed against signal peptides, blocking receptors, or targeting cell types for destruction.[4–8]

Admittedly, drugs that could qualify as biopharmaceuticals, such as insulin, were already in use by the 1920s. However, these drugs were then extracted from animal tissues, which posed additional difficulties in terms of potency and safety.[9] Many other drugs also have an origin in nature; for example, those derived from (medicinal) plants (*e.g.* digitalis, morphine, salicylic acid, cytostatics) or from microbial secretions (*e.g.* many antibiotics and certain oncolytics), but such drugs are nowadays chemically synthesised.[10–14]

Biopharmaceuticals are among the most celebrated drugs; they have offered perspective to patients with previously incurable enzymatic or hormonal deficiencies, they can specifically target cancer cells as opposed to the whole-body cytotoxic attack by chemotherapeutical agents, and they can block the activity of signal peptides that play a role in the pathophysiology of – for example – rheumatological diseases. Because of these benefits and the blockbuster state usually associated therewith, biopharmaceuticals are increasingly being developed, with an expected share of 27% of the total pharmaceutical market in 2020 (73% of the top 20 product sales).[15]

In contrast to small molecules, biopharmaceuticals are much more complex in structure, with molecular weights of 3.5 (calcitonin) to 150 kDa (monoclonal antibodies), and sometimes consist of subunits (quaternary structure). As a result of these differences, biopharmaceuticals display other pharmacokinetic properties compared with small molecules. For example, they distribute more slowly over the body than small molecules, and are mainly eliminated via catabolism into amino-acids and target-mediated pathways.[16–19]

However, the pharmacokinetics of biopharmaceuticals are commonly described by models that were suitably applied to small molecules. In the ***first section*** of this thesis (*Sticky proteins*), some pharmacokinetic aspects of large therapeutical proteins will be explored, especially those that are not adequately covered by current pharmacokinetic models or theory. The focus will be on monoclonal antibodies, which represent the largest class of biopharmaceuticals, and because of their very slow plasma clearance, MABs are particularly useful in investigating the complex pharmacokinetics of biopharmaceuticals.

The ***first chapter*** studies the use of a population modelling approach in testing pharmacokinetic biosimilarity of a monoclonal antibody. This technique

is widely used during drug development to describe and predict drug concentration in the body over time, but in biosimilarity research a non-model approach is still favoured. The benefit of a pharmacokinetic model is that it can deal with the non-linear elimination pathways.

The following two chapters (***2 & 3***) discuss rises in plasma concentration after the cessation of intravenous administration, which have been frequently observed for various biopharmaceuticals. These observations are not in agreement with the current understanding of how infused molecules behave. Even the aforementioned, more sophisticated, mathematical models that incorporate the known complex elimination routes cannot account for these findings.

Apart from the higher level of complexity in pharmacokinetics, biopharmaceuticals are associated with other safety hazards than small molecules. First, as a result of the production in (non-human) host cell systems, other substances than the pharmaceutical (called impurities) are introduced during manufacturing, some of which are harmful when administered (*e.g.* endotoxin, peptidoglycans, or flagellin from bacterial hosts) or possess unintended ('pharmacological') activity. Second, safety pharmacology studies can be misleading, because the target that interacts with the biopharmaceutical or the impurity is exclusively expressed in human beings. Additionally, the toxicity often is the result of an intricate interplay of multiple cell types and effector pathways which can be difficult to simulate in the laboratory. Again, the preclinical testing strategy to detect safety concerns and prevent dangerous drugs from entering the clinical phases of development has not changed much since the introduction of biopharmaceuticals. The ***second section*** of this thesis (*Dirty proteins*) highlights shortcomings in assessments of adverse immunostimulation, which is a propensity of some monoclonal antibodies, but is also encountered as a result of impurities in the drug product.

In ***chapter 4***, an attempt is made to reproduce the observed clinical response following administration of the monoclonal antibody trastuzumab in an *ex vivo* stimulation test, which included material from 'responders' and 'non-responders'. Trastuzumab is an interesting example, because only 40% of patients shows signs of an inflammatory reaction[20] and even lower percentages have been reported in healthy volunteers.[21–23]

Chapter 5 describes the history of a biopharmaceutical where so-called host cell impurities, including flagellin, induced unanticipated adverse immunostimulation, which resulted in a severe delay in clinical development. In this case, an *ex vivo* simulation test could detect cytokine release caused by the impurities. Thus, the question is raised why preclinical testing failed in generating a safety signal, especially since all the applicable guidelines were meticulously followed. The next chapter (***6***) answers this question and illustrates several shortcomings of the current testing strategy based on two examples of adverse immunostimulation caused by impurities.

REFERENCES

1 Aronson JK. A manifesto for clinical pharmacology from principles to practice. *Br J Clin Pharmacol* 2010; **70**: 3–13.
2 Ivy AC. The history and ethics of the use of human subjects in medical experiments. *Science* 1948; **108**: 1–5.
3 Miller RR. History of clinical pharmacy and clinical pharmacology. *J Clin Pharmacol* 1981; **21**: 195–7.
4 Buckel P. Recombinant proteins for therapy. *Trends Pharmacol Sci* 1996; **17**: 450–6.
5 Nagle T, Berg C, Nassr R, Pang K. The further evolution of biotech. *Nat Rev Drug Discov* 2003; **2**: 75–9.
6 Walsh G. Biopharmaceutical benchmarks 2010. *Nat Biotechnol* 2010; **28**: 917–24.
7 Walsh G. Biopharmaceutical benchmarks 2014. *Nat Biotechnol* 2014; **32**: 992–1000.
8 Sanchez-Garcia L, Martín L, Mangues R, Ferrer-Miralles N, Vázquez E, Villaverde A. Recombinant pharmaceuticals from microbial cells: a 2015 update. *Microb Cell Fact* 2016; **15**: 33.
9 Sönksen PH. The evolution of insulin treatment. *Clin Endocrinol Metab* 1977; **6**: 481–97.
10 Wachtel-Galor S, Benzie IFF. Herbal Medicine: An Introduction to Its History, Usage, Regulation, Current Trends, and Research Needs. In: Benzie IFF, Wachtel-Galor S, eds. Herbal Medicine: Biomolecular and Clinical Aspects, 2nd edn. Boca Raton, Florida: CRC Press/Taylor & Francis, 2011.
11 Mann J. Natural products in cancer chemotherapy: past, present and future. *Nat Rev Cancer* 2002; **2**: 143–8.
12 Peláez F. The historical delivery of antibiotics from microbial natural products—can history repeat? *Biochem Pharmacol* 2006; **71**: 981–90.
13 García Jordá E. Sacred herbs. *Clin Transl Oncol* 2008; **10**: 685–7.
14 Zaffiri L, Gardner J, Toledo-Pereyra LH. History of antibiotics. From salvarsan to cephalosporins. *J Invest Surg* 2012; **25**: 67–77.

15 Gene Techno Science. Overview of global pharmaceutical market. 2015. http://www.g-gts.com/en/business/market/ (accessed Aug 1, 2017).
16 Keizer RJ, Huitema ADR, Schellens JHM, Beijnen JH. Clinical pharmacokinetics of therapeutic monoclonal antibodies. *Clin Pharmacokinet* 2010; **49**: 493–507.
17 Dostalek M, Gardner I, Gurbaxani BM, Rose RH, Chetty M. Pharmacokinetics, pharmacodynamics and physiologically-based pharmacokinetic modelling of monoclonal antibodies. *Clin Pharmacokinet* 2013; **52**: 83–124.
18 Shi S. Biologics: an update and challenge of their pharmacokinetics. *Curr Drug Metab* 2014; **15**: 271–90.
19 Tibbitts J, Canter D, Graff R, Smith A, Khawli LA. Key factors influencing ADME properties of therapeutic proteins: a need for ADME characterization in drug discovery and development. *MAbs* 2016; **8**: 229–45.
20 Chung CH. Managing premedications and the risk for reactions to infusional monoclonal antibody therapy. *Oncologist* 2008; **13**: 725–32.
21 Wisman LAB, De Cock EPM, Reijers JAA, *et al.* A phase I dose-escalation and bioequivalence study of a trastuzumab biosimilar in healthy male volunteers. *Clin Drug Investig* 2014; **34**: 887–94.
22 Yin D, Barker KB, Li R, *et al.* A randomized phase 1 pharmacokinetic trial comparing the potential biosimilar PF-05280014 with trastuzumab in healthy volunteers (REFLECTIONS B327-01). *Br J Clin Pharmacol* 2014; **78**: 1281–90.
23 Morita J, Tanaka M, Nomoto M, *et al.* Pharmacokinetic bioequivalence, safety, and immunogenicity of DMB-3111, a trastuzumab biosimilar, and trastuzumab in healthy Japanese adult males: results of a randomized trial. *BioDrugs* 2016; **30**: 17–25.

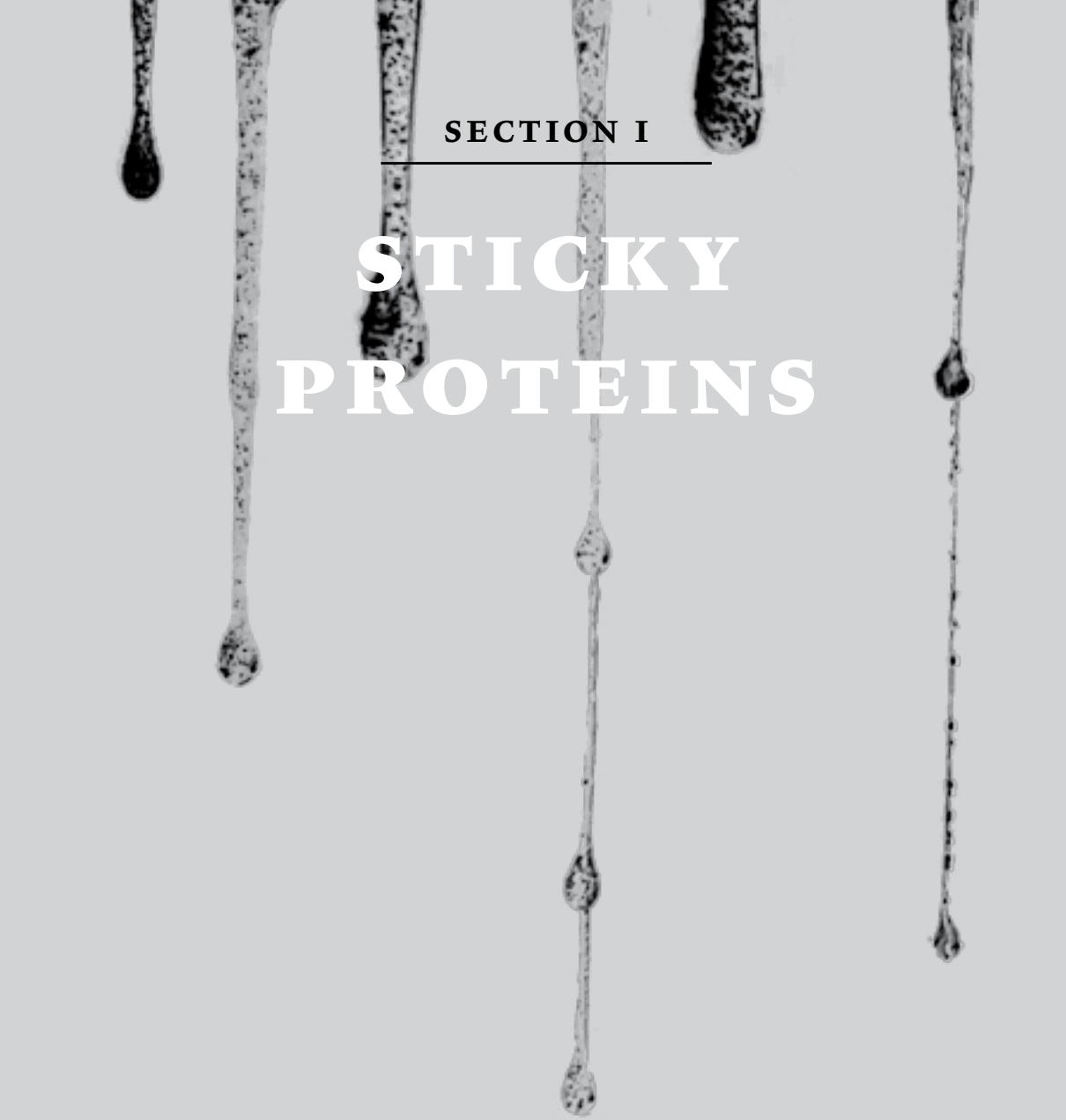

SECTION I

STICKY PROTEINS

CHAPTER I

Use of population approach non-linear mixed effects models in the evaluation of biosimilarity of monoclonal antibodies

J.A.A. Reijers, T. van Donge, F.M.L. Schepers, J. Burggraaf, J. Stevens

Population pharmacokinetic analyses (PPK) have been used to establish bioequivalence for small molecules and some biopharmaceuticals. We investigated whether PPK could also be useful in biosimilarity testing for monoclonal antibodies (MABs).

Data from a biosimilarity trial with two trastuzumab products were used to build population pharmacokinetic models. First, a combined model was developed and similarity between test and reference product was evaluated by performing a covariate analysis with trastuzumab drug product (test or reference) on all model parameters. Next, two separate models were developed, one for each drug product. The model structure and parameters were compared and evaluated for differences.

Drug product could not be identified as statistically significant covariate on any parameter in the combined model and the addition of drug product as covariate did not improve the model fit. A similar structural model described both the test and reference data best. Only minor differences were found between the estimated parameters from these separate models.

PPK can also be used to support a biosimilarity claim for a MAB. However, in contrast to the standard non-compartmental analysis, there is less experience with a PPK approach. Here, we describe two methods of how PPK can be incorporated in biosimilarity testing for complex therapeutics.

During the past decades, many biopharmaceuticals have been marketed, mostly for use in the field of oncology and rheumatology. Although efficacious, high costs often limit the availability of these therapies or greatly burden the health care system. For example, treatment of a rheumatological US patient with biopharmaceuticals costs on average $20,000 to $30,000 annually,[1] and a single cycle of bevacizumab or other monoclonal antibody (MAB) can cost $2,000 or more.[2] In 2014, the top 20 in global medicinal product sales contained 10 biopharmaceuticals, generating revenues between 4.4 and 11.8 billion dollar each.[3] Because of the growing number of patent expirations for the original biopharmaceuticals, it is expected that research of biosimilars will increase.

A first requirement for registration of the novel compound is to establish pharmacokinetic 'biosimilarity'. Although the terminology slightly differs between the regulatory agencies, all agree on the basic concept of biosimilarity, which is that the novel ('test') compound should be highly similar to its originator

('reference') in terms of quality, efficacy, and safety, and that any remaining difference should be clinically insignificant.[4–6]

Notwithstanding specific criteria for biopharmaceuticals, often parts of guidelines for establishing bioequivalence – not biosimilarity – between chemically derived substances ('small molecules') are applied. These guidelines require that similarity should be demonstrated for key pharmacokinetic parameters, most commonly area under the concentration-time curve (AUC) and maximum concentration (C_{max}), based on predefined acceptance limits at the highest dose level used. According to an evaluation by the World Health Organisation, studies proving biosimilarity generally use the 80–125% equivalence range due to lack of specific acceptance criteria for biopharmaceuticals.[4]

Although it is widely recognised that a non-compartmental analysis (NCA) is less appropriate when dealing with complex pharmacokinetics, it is still the most commonly used analytical method for demonstrating biosimilarity. Mentré's group has extensively studied the use of population pharmacokinetic techniques in bioequivalence testing and found that it yielded similar results, with the modelling approach leading to a better understanding of the underlying biological system, and the NCA being a relatively easy approach that does not require modelling and whose results can be used in a statistical analysis. The same was found for two biopharmaceuticals, somatropin and epoetin-α.[7–9]

We investigated whether a population pharmacokinetic analysis (PPK) could also be useful in bioequivalence testing for monoclonal antibodies (MABs), which display complex elimination mechanisms, including non-linear routes, and have a plasma half-life of one to multiple weeks. Two approaches in modelling pharmacokinetic (PK) data were studied. First, we developed a combined model built on all available data for both the test and reference product, and tested whether adding product (test/reference) as a covariate would improve the model, indicating non-similarity. Second, we developed separate models, one for test and one for reference product. This approach does not assume similarity as a starting point and allows comparison of the model structures and parameters. For this exercise, we chose the humanised MAB trastuzumab, which targets the HER2-receptor.

METHODS

Study population and treatment

Data were gathered in a phase I randomised, single dose, parallel group bioequivalence study, preceded by a placebo-controlled dose escalation part.[10] In this study, 110 male volunteers, aged 18–45 years, who were deemed healthy after a full medical screening, received trastuzumab in 250 mL 0.9% NaCl as an intravenous infusion over 90 min. Two trastuzumab products were administered: the biosimilar product (test, T), codenamed FTMB (Synthon BV, Nijmegen, The Netherlands), and the EU-licensed product (reference, R), marketed as Herceptin®.

Studied dose levels of the test product in the dose escalation part were 0.5 mg/kg ($n = 6$), 1.5 mg/kg ($n = 6$), 3 mg/kg ($n = 6$). The bioequivalence part consisted of 92 participants, who randomly received test ($n = 46$) or reference ($n = 46$) product at 6 mg/kg.

Based on the trastuzumab content of the used test and reference product vials, the actual dose levels were determined to be 0.49, 1.48, 2.96, 5.92 mg/kg for T, and 6.44 mg/kg for R.

Bioanalyses

Trastuzumab was quantitated in serum samples collected pre-dose and at 45 min, 1.5, 2, 3, 4, 5, 6, 8, and 24 h, and at 2, 4, 8, 14, 21, 28, 35, 42, 49, and 63 days after start of administration. A detailed description of the assay is given by Wisman *et al.*[10] The lower limit of quantification (LLOQ) was 0.060 µg/mL. All pre-dose trastuzumab concentrations <LLOQ were set to zero prior to analysis. Post-dose concentrations below LLOQ were not included. A serum sample for the quantification of serum HER2 extracellular domain (ECD) was collected prior to administration. This assay had a LLOQ of 0.50 ng/mL.

In the original clinical study protocol, the sample at day 63 was not collected for PK analysis and hence not included in the previously reported NCA results.[10] However, as this sample provided valuable insight in the non-linear clearance of trastuzumab, it was included in the analyses reported in this chapter.

PPK

General modelling approach

Population pharmacokinetic analysis (PPK) followed a stepwise approach. First, a general model for trastuzumab, hereafter referred to as 'combined model',

was developed based on all available PK data for both test and reference product, including dose levels of the dose escalation part (0.49, 1.48, and 2.96 mg/kg). To investigate potential bias in the PK models due to analysing test and reference products simultaneously, PK models were also developed for the test (model T) and reference product (model R) separately and included only data from subjects who were exposed to 6 mg/kg test or reference product. These are hereafter referred to as 'separate models'. The separate models were developed in parallel in order to maintain a structurally similar model for the test and reference product. Consequently, the model was only adopted if the corresponding model in the other treatment arm was preferred over its parent as well.

Model development

Model development was performed using NONLINEAR Mixed Effects Modelling (NONMEM 7.2.0, Icon Development Solutions, Ellicott City, Maryland, USA) and closely followed the FDA and EMA guidelines for PPK.[11,12] Models were built under ADVAN 13 with tolerance (TOL) 9 and the first-order conditional method with interaction (FOCE-I) was used for parameter estimation. NONMEM reports an objective function value (OFV), which is the -2 · log likelihood. Model hypothesis testing used the likelihood ratio test under the assumption that the difference in OFV is χ^2-distributed with degrees of freedom being determined by the number of additional parameters in the more complex model. Hence, with a decrease in OFV of ≥7.88 points ($p < 0.005$), the model is preferred over its parent model. Also, model performance was evaluated by means of goodness-of-fit plots, using the software package R (v3.2.2, R foundation for statistical computing, Vienna, Austria, 2015).

Several structural models with 2 or 3 compartments, including combinations of linear and non-linear clearance, were fitted to the data to determine the best structural model. Log-normal distribution of the between-subject variability (η) was assumed and several residual error (ε) structures were tested (proportional, additive and combined).

Potential covariate correlations, defined as a significant Pearson's product-moment correlation coefficient ($r^2 > 0.5$ with $p < 0.01$), were tested in the model development, in linear and exponential manners, and incorporated based on improvement in model performance. Explored covariates included lean body weight (LBW),[13] body weight, body surface area (BSA),[14] height, BMI, age, HER2-ECD concentration, dose, and product.

Model evaluation and predictive performance

To evaluate the robustness and predictive performance of the developed model, a visual predictive check (VPC) with 500 simulations was performed.[15] Prediction intervals of 95% were obtained by simulating the model results from the original data. Model evaluation was performed by calculating the coefficient of variation to derive the uncertainty in the parameter estimates of the model, which was considered acceptable if lower than 50%. Also, shrinkage, as defined by Karlsson and Savić,[16] was calculated to exclude model misspecification; shrinkage less than 30% was considered acceptable.

Individual pharmacokinetic profiles

Individual pharmacokinetic profiles were simulated in R using the individual participant's model parameter estimates. Integration was performed from the start of administration until the time point when the concentration in the central compartment dropped below 0.01 µg/mL. For the simulations, the following integration intervals were used: 1 s from administration until 24 h, 1 min until day 80, and 1 day thereafter. The concentrations were stored at original sampling times and at every 5 min. Trastuzumab concentration at the start of administration was assumed to be 0 µg/mL.

Comparison to NCA

For comparison to a standard NCA, AUCs were derived using model *simulated* (predicted) individual concentrations at the original sampling times. AUC from administration (time 0) to the time of the last concentration ≥LLOQ (AUC_l) was calculated using the linear trapezoidal method. AUC extrapolated to infinity (AUC_∞) based on the apparent terminal elimination rate constant was calculated as well.

Biosimilarity statistics were performed on AUC_∞ and AUC_l of all participants who were exposed to 6 mg/kg, comparing T to R in an unpaired t-test, using the software package R. AUCs were natural log (ln)-transformed prior to statistical analysis. The estimated difference in means and the corresponding 90% confidence interval (CI) were back-transformed to obtain the relative geometric mean ratio (GMR) of T over R (T/R). These results were then compared to those calculated in a standard NCA.

TABLE 1.1 Demographics

PARAMETER	TEST 0.5 mg/kg ($n=6$)	TEST 1.5 mg/kg ($n=6$)	TEST 3.0 mg/kg ($n=6$)	TEST 6.0 mg/kg ($n=46$)	REFERENCE 6.0 mg/kg ($n=46$)
Age (year)	26.9 (8.9)	33.0 (9.1)	23.4 (2.3)	26.0 (7.3)	24.1 (5.8)
Height (cm)	183 (12.0)	176 (6.5)	184 (3.3)	184 (7.5)	182 (6.2)
Weight (kg)	73.1 (12.6)	73.0 (8.7)	72.0 (7.5)	79.5 (11.2)	77.1 (10.2)
BMI ($kg\,m^{-2}$)	21.7 (3.3)	23.5 (2.6)	21.2 (2.1)	23.4 (2.5)	23.2 (2.7)
LBW (kg)	59.4 (8.4)	57.5 (5.1)	59.1 (3.8)	62.6 (6.6)	61.0 (5.6)
BSA (m^2)	1.93 (0.21)	1.89 (0.13)	1.92 (0.10)	2.01 (0.17)	1.97 (0.15)
ECD ($\mu g\,L^{-1}$)	12.7 (1.8)	11.8 (2.1)	11.4 (1.5)	11.3 (1.8)	11.8 (1.8)

Mean (standard deviation) demographics per treatment arm.
BSA: body surface area | ECD: HER2 extracellular domain | LBW: lean body weight

To correct for the difference between actual (5.92 mg/kg and 6.44 mg/kg) and labelled dose (6 mg/kg), a linear normalisation to 6 mg/kg was applied to the individual AUCs in the NCA. In the PPK, individual profiles were simulated with the actual and labelled dose. Both corrected and uncorrected AUCs were calculated and statistically compared.

RESULTS

Population

Pharmacokinetic data were gathered from 110 healthy male volunteers, whose demographics are presented in *table 1.1*. In total, 1,247 serum trastuzumab concentrations were available for the test product (T), of which 143 were <LLOQ (64 pre-dose). In the 6 mg/kg test group, 60/906 observations were <LLOQ (46 pre-dose) and in the reference product (Herceptin®), 51/912 observations (44 pre-dose).

Model development

First step: combined model

Initial exploration of the data suggested that a 2 or 3 compartment model would describe the data best. Based on the observed non-linear kinetics, Michaelis-Menten kinetics was incorporated, described in terms of maximum rate of elimination (V_{max}), and the concentration where $\frac{1}{2} \cdot V_{max}$ is reached (K_m). Addition of a linear elimination pathway, defined by elimination rate constant (k_e), significantly improved the model fit for both the 2 and 3 compartments models.

Adding the third compartment accounted for a delayed clearance effect. The 3-compartment model, parameterised in terms of a central (V_1) and peripheral volumes (V_2 and V_3) of distribution, and inter-compartmental clearances (Q_1 and Q_2), resulted in a significant improvement compared to the 2-compartment model. This was confirmed by an improved goodness-of-fit, especially for the lower doses of trastuzumab. Thus, the 3-compartment model was considered superior over the 2-compartmental model (*figure 1.1*). A combined residual error structure (ε) proved best fit for purpose.

After identification of the structural model, individual estimates of random effects for between-subject variability were identified for the parameters V_1, K_m, and k_e, with final coefficient of variation values of 14.8, 35.9, and 17.2%, respectively. The residual coefficient of variation of the best model was 14.98%. An omega block was required to correct for the parameter correlation between K_m and k_e in the model.

Significant correlations were found between V_1 and lean body weight (LBW), body weight, body surface area (BSA), height, and BMI, with correlation coefficients of 0.61, 0.55, 0.60, 0.54, and 0.28, respectively. Linear regression analysis of LBW *vs.* BSA resulted in a coefficient of 1, and for LBW *vs.* body weight in 0.96. Furthermore, significant correlation coefficients were observed between BMI and k_e (0.60), between serum concentrations HER2-ECD and k_e (0.29), and between serum concentrations HER2-ECD and K_m (0.18).

Implementing LBW as a linear covariate on V_1 (*equation 1.S1*), significantly improved the objection function value (OFV) and was added to the model. Incorporating other weight-related covariates (body

weight, height and BMI) separately in the model did not result in a significant improvement compared to LBW; accordingly, they were not implemented in the model. Covariate analyses identified BMI as the one most significantly correlated to k_e. Incorporating this covariate linearly on k_e (*equation 1.s2*), further improved the model, and BMI was thus added to the model. Including HER2-ECD as a covariate did not improve the model fit. Interestingly, the model favours lean body weight as a size descriptor to scale trastuzumab dose compared to body weight, which is used clinically in dose calculation.

Adding trastuzumab drug product (test or reference) as a covariate to the model did not explain any relevant variability. A maximum decrease in OFV of only 5.80 points ($p > 0.01$) was observed when treatment was added as a covariate on K_m. Thus, drug product as covariate did not significantly improve model fit. All PK parameter estimates obtained with the best fit of the models are listed in *table 1.2*.

Additionally, the rates of the linear and non-linear elimination pathway *vs.* trastuzumab concentration were calculated. At low trastuzumab concentrations (<10 µg/mL), total elimination was almost independent of serum drug concentration, *i.e.* the non-linear elimination exceeded the linear elimination. At high concentrations, this pathway became saturated and the influence of non-linear elimination seemed negligible (*figure 1.s2*).

Also, a more complex mechanistic model approach was applied to characterise the distribution and clearance of trastuzumab: the target-mediated drug disposition (TMDD) model.[17,18] In addition to receptor and drug-receptor complex quantification, such models are able to provide information on binding affinity of the drug to the receptor. Fitting a TMDD model to our data proved difficult due to over-parameterization. A simplified approximation TMDD model approach with a dissociation constant K_d[19] still resulted in an incorrect fit and instability of the model, and the TMDD model approach was abandoned.

Second step: separate models

Model development of the separate models, including only data from participants who were exposed to 6 mg/kg, followed a similar approach as the combined model to ensure the structural similarity. For both trastuzumab products, a third compartment could be identified, as well as a linear and a non-linear route of elimination, described by Michaelis-Menten kinetics.

For the separate models, individual estimates of random effects for the between-subject variability were identified for the parameters V_1, V_{max}, and k_e, with

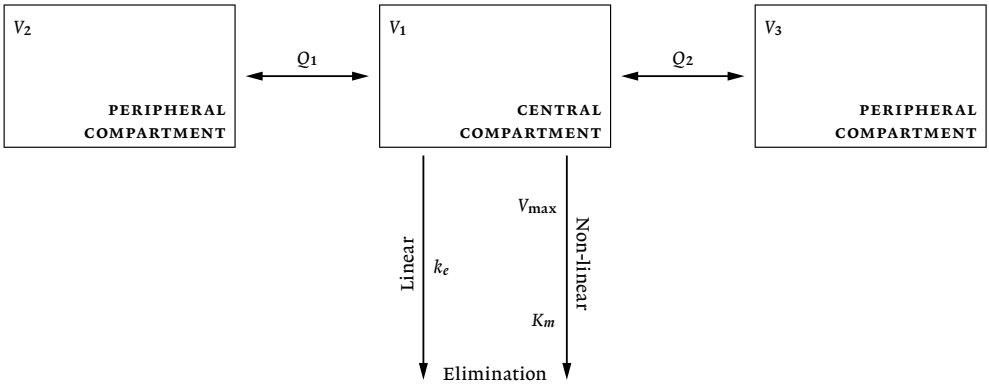

FIGURE 1.1 Schematic representation of the structural PK model with a parallel linear and non-linear elimination pathway | Linear elimination is described by an elimination rate constant (k_e) and non-linear elimination is calculated as

$$\frac{V_{max} \cdot C}{K_m + C},$$

where V_{max} is the maximum rate of elimination, K_m the concentration which produces half of the V_{max}, and C the concentration. V_1, V_2, and V_3 are the distribution volumes; Q_1 and Q_2 are the inter-compartmental clearances to the peripheral compartments.

TABLE 1.2 Population pharmacokinetic parameter estimates from the full covariate model for trastuzumab

PARAMETER[a]	COMBINED MODEL		SEPARATE MODEL T		SEPARATE MODEL R	
Fixed effects, estimate (CI)						
V_1 (L)	3.28	(3.185–3.367)	3.59	(3.418–3.752)	3.13	(3.028–3.232)
V_2 (L)	1.89	(1.325–2.457)	6.82	(-5.572–19.21)	44	(28.18–59.77)
V_3 (L)	1.96	(1.736–2.179)	2.15	(1.858–2.443)	2.09	(1.929–2.244)
Q_1 (L h^{-1})	2.91	(2.02–3.79)· 10^{-3}	2.82	(1.081–4.566)	3.92	(3.58–4.25)· 10^{-3}
Q_2 (L h^{-1})	4.34	(3.66–5.01)· 10^{-2}	3.75	(2.787–4.706)	4.67	(4.12–5.21)· 10^{-2}
V_{max} (µg h^{-1})	178	(162.3–193.1)	172	(138.6–205.7)	127	(111–143.4)
K_m (µg L^{-1})	937	(759.6–1115)	995	(674.6–1316)	1440	(1189–1699)
k_e (h^{-1})	2.20	(2.02–2.38)· 10^{-3}	1.95	(1.33–2.57)· 10^{-3}	1.76	(1.62–1.9)· 10^{-3}
Random effects, estimate (CV)						
Between-subject variability						
$\omega^2 V_1$	0.0217	(14.8%)	0.0270	(16.5%)	0.0122	(11.1%)
$\omega^2 V_{max}$	—		0.0163	(12.8%)	0.0347	(18.8%)
$\omega^2 K_m$	0.121	(35.9%)	—		—	
$\omega^2 k_e$	0.0292	(17.2%)	0.0355	(19.0%)	0.0286	(17.0%)
Residual error						
σ^2 proportional	0.0222		0.0207		0.0198	
σ^2 additive	1520		3090		790	

a. Explanation of parameters is given in *figure 1.1*.
CI: confidence interval | CV: coefficient of variation | σ^2: residual variance | ω^2: between-subject variance

final coefficient of variation values in model T of 16.5, 12.8, and 19%, respectively. The residual coefficient of variation of the best model was 14.5%. In model R, the final coefficients of variation were 11.1, 18.8, and 17%, with a residual coefficient of variation of 14.1%.

As with the combined model, the best model fit with the greatest reduction in OFV was obtained by incorporating LBW as linear covariate on V_1 and BMI on k_e for both separate models.

Model evaluation and predictive performance

Combined model

Goodness-of-fit plots of the combined model (*figure 1.2*) showed that all predictions lay around the line of unity. There was one outlier in the reference group, where one subject had a very low mid-infusion concentration of 0.088 µg/mL. Virtually all conditional weighted residuals with interaction (CWRESI) lay randomly scattered around zero without apparent bias.

The variability of the parameters V_1, K_m, and k_e on the η density histograms (*figure 1.S4*) seemed normally distributed around zero with acceptable coefficient of variation values, indicating correct description of the between-subject variability. Furthermore, no significant shrinkage was observed for parameters for which between-subject variability was identified (<8.04%).

The VPC proved good predictive performance (*figure 1.3*) of the combined model. For the doses >1.48 mg/kg, no signs of bias were apparent and most observations lay within the 95% prediction interval. Only for the lowest dose administered (0.49 mg/kg), a slightly higher prediction of the population mean was observed, especially in the lower concentration range. However, even for this dose group, most of the observations were within the 95% prediction interval.

Separate models

The goodness-of-fit plots of the separate models (*figures 1.S1 & 1.S2*) showed that predictions lay around the line of unity and that the CWRESI were observed near the central line. No bias or trend in the model prediction could be determined. The shrinkage observed for the parameters for which between-subject variability was identified (V_1, V_{max}, k_e) was not significant (<17.80% for model T, <15.50% for model R). Additionally, the variability on the η density plots (*figures 1.S5 & 1.S6*) seemed normally distributed around zero.

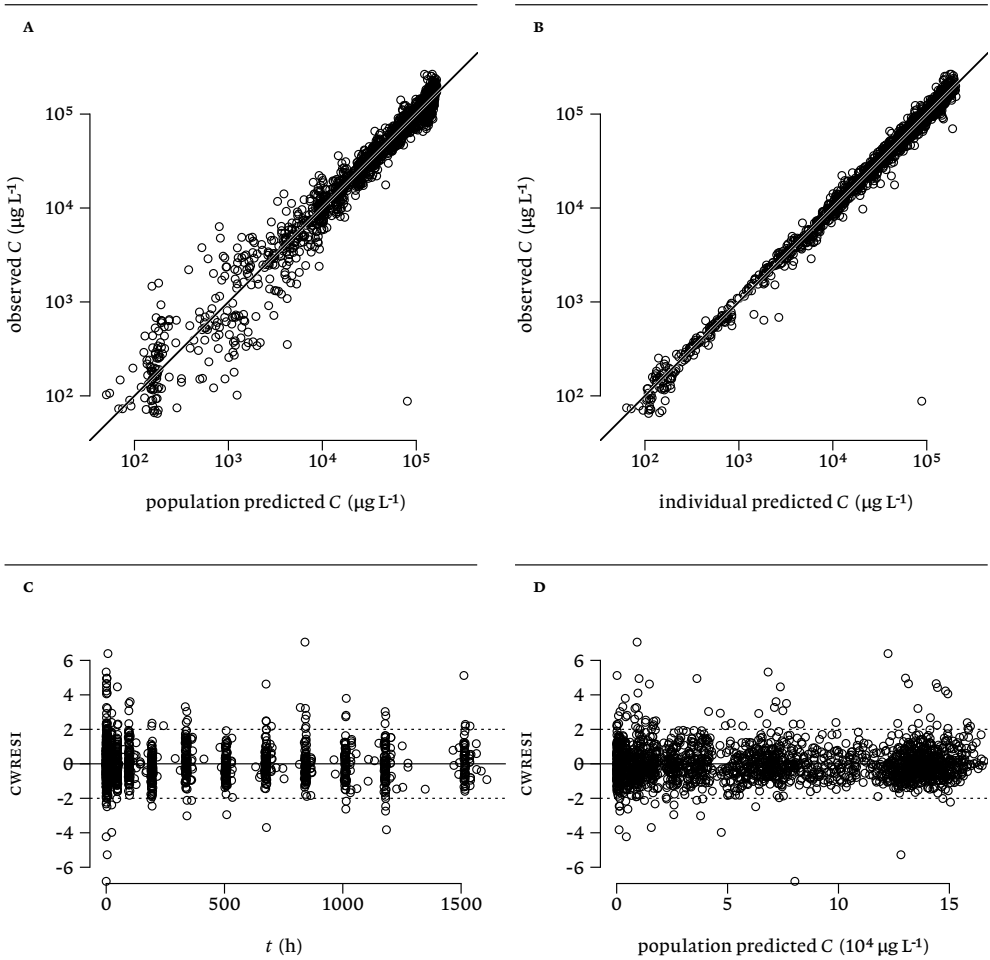

FIGURE 1.2 Goodness-of-fit plots combined model
Observed *vs.* population predicted concentrations (A), observed *vs.* individual predicted concentrations (B), conditional weighted residuals with interaction (CWRESI) *vs.* times (C), and conditional weighted residuals *vs.* population predictions (D) of the combined model.

The population PK parameter estimates from the full covariate model are presented in *table 1.2*. When comparing parameter estimates, most parameter distributions overlapped. The parameter estimates for V_2 differed between model T and model R, but were in the same order of magnitude. However, Q_1 and Q_2 for model T were higher compared to model R. In contrast to the combined model, where between-subject variability was identified for V_1, K_m, and k_e, in the separate models, these were found for V_1, V_{max}, and k_e.

Comparison to NCA

The geometric mean (GM) AUC_1 obtained from the standard NCA was 1,301 µg day mL^{-1} for the test (T) and 1,588 µg day mL^{-1} for the reference (R) product. The AUC_1 remained virtually unchanged when the same calculations were repeated with simulated concentrations, regardless of whether the combined model or the separate models were used (*table 1.3*). Similar results were obtained with regard to AUC_∞. The GM ratio (GMR) T/R with all AUC methods was 81.66-82.54% with the

lower limit (LL) of the associated 90% confidence interval (CI) below the predefined equivalence boundary of 80% (*table 1.3*). Applying a linear correction to the NCA results caused the difference T-R in AUC_t and AUC_∞ to decrease (GMR T/R 89.11-89.55%, LL 90% CI >84.66%). Further reductions were achieved when an equal dosage of 6 mg/kg was *simulated* for both trastuzumab products, which affected the AUCs in the reference product arm more profoundly, and increased the GMR with approximately 2 %-point (*table 1.4*).

Using the entire simulated profile, as opposed to only the simulated concentrations at the original sampling times, generally resulted in a small decrease of 1–2% compared with the NCA for both AUC_t and AUC_∞, with the exception of the AUC_∞ calculated on profiles derived with model R, where an average increase of 1.7% was observed (*tables 1.S1 & 1.S2*). Conversely, with the combined model, lower AUCs were obtained compared with the separate models for T only.

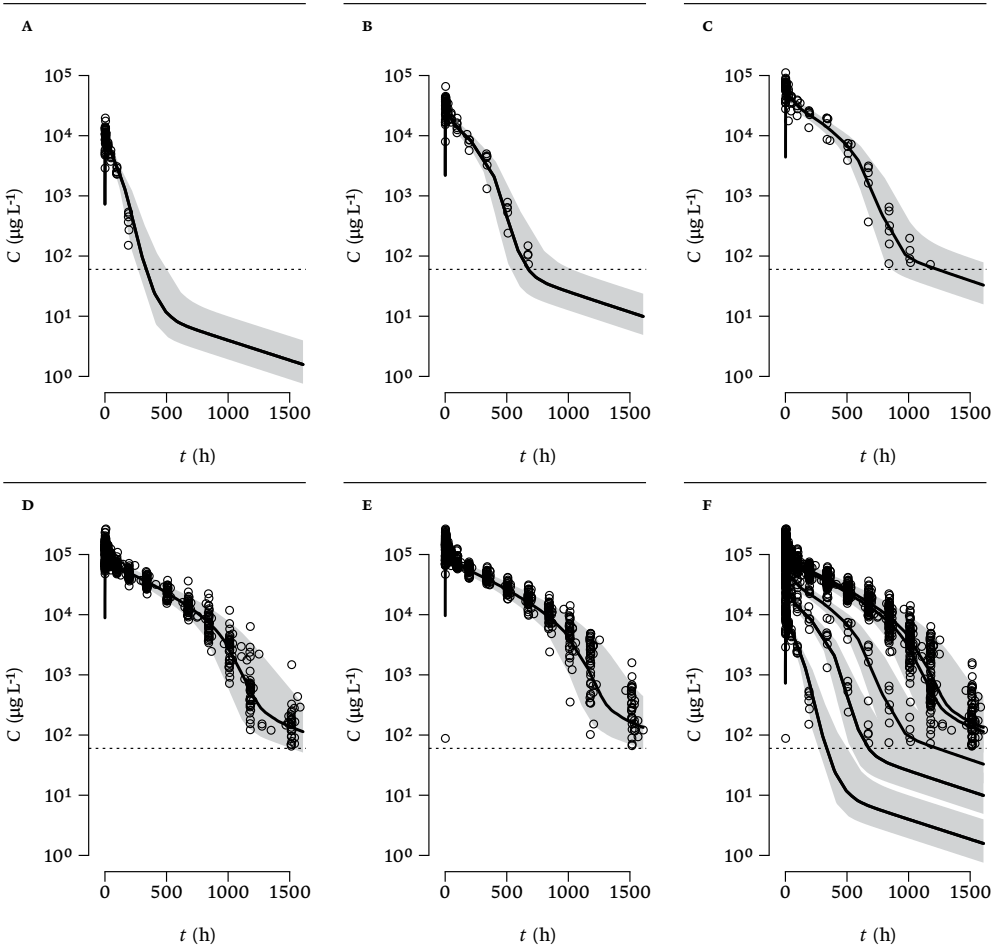

FIGURE 1.3 Visual predictive check (VPC)

Visual predictive check (VPC) of the best combined model, conditioned per dose of test product (0.49 [A], 1.48 [B], 2.96 [C], 5.92 mg/kg [D]) or reference product (6.44 mg/kg, E). In F all doses are displayed. The circles indicate the observations for the different trastuzumab doses administered, the lines are the typical predicted concentrations by the model for each dose, and the grey area is the 95% prediction interval. The dashed line is the assay's lower limit of quantification (LLOQ) for trastuzumab (0.060 µg/mL).

TABLE 1.3 AUC comparison actual dose

	GM		GMR (%)	
	T	R	T/R	
AUC_I				
NCA	1301	1588	81.91	(77.82–86.22)
Separate models	1300	1588	81.86	(78.08–85.82)
Combined model	1296	1588	81.59	(77.88–85.47)
AUC_∞				
NCA	1311	1593	82.32	(78.17–86.69)
Separate models	1313	1591	82.54	(78.70–86.57)
Combined model	1300	1592	81.66	(77.93–85.56)

Geometric mean (GM, μg day mL^{-1}) and GM ratio (GMR) with the 90% confidence interval for the actual dose (5.92 mg/kg for T; 6.44 mg/kg for R) as derived by different methods per treatment arm.

AUC: area under the concentration-time curve | AUC_I: AUC from administration (time 0) to the time of the last concentration ⩾LLOQ (lower limit of quantification) | AUC_∞: AUC_I extrapolated to infinity NCA: non-compartmental analysis | R: reference | T: test

TABLE 1.4 AUC comparison after dose correction

	GM		GMR (%)	
	T	R	T/R	
AUC_I				
NCA	1318	1479	89.11	(84.66–93.79)
Separate models	1323	1455	90.93	(86.72–95.35)
Combined model	1319	1443	91.41	(87.25–95.76)
AUC_∞				
NCA	1329	1484	89.55	(85.03–94.30)
Separate models	1337	1457	91.74	(87.46–96.24)
Combined model	1324	1446	91.54	(87.37–95.92)

Geometric mean (GM, μg day mL^{-1}) and GM ratio (GMR) with the 90% confidence interval for the labelled dose (6 mg/kg) as derived by different methods per treatment arm. For the NCA-results, a linear dose correction was applied; in the models, the labelled dose was used to simulate the individual profiles (see main body).

AUC: area under the concentration-time curve | AUC_I: AUC from administration (time 0) to the time of the last concentration ⩾LLOQ (lower limit of quantification) | AUC_∞: AUC_I extrapolated to infinity NCA: non-compartmental analysis | R: reference | T: test

DISCUSSION

As long as generical products are being developed, controversy and scepticism regarding the claims of therapeutical equality have followed marketed bioequivalent products. Recently, Bate *et al.*[20] advocated that for the more complex pharmaceuticals, two allegedly bioequivalent drug products may not be interchangeable, which could have adverse consequences. MABs are certainly among the most complex therapeutics and establishing similarity to the reference product can thus be challenging.

For demonstrating pharmacokinetic biosimilarity in a human population, a NCA is virtually always performed and its results (AUC and C_{max}) compared statistically, even though it is widely recognised that the NCA is less suitable for drugs with complex non-linear kinetics, as is the case for MABs.

Population approach pharmacokinetic (PK) modelling and simulation techniques have been successfully applied to quantitatively describe the PK of MABs in humans.[21–26] Such an approach has been used in bioequivalence studies, also for biopharmaceuticals,[9] where it was found to give indistinguishable results on the standard NCA-parameters (AUC and C_{max}), as was the case in our analysis. However, as was also argued by Dubois *et al.*,[9] a PK model can provide valuable insight in the biological systems underlying the PK properties. Although the standard NCA-derived parameters, such as C_{max}, AUC_∞, terminal half-life, *etc.*, may seem similar, the two drug products could behave quite differently in terms of PK, a feature that goes undetected in a NCA.[27] Furthermore, similar plasma concentrations do not invariably mean similar concentrations at the site of action.

Here, we describe two methods of incorporating PK modelling in biosimilarity research. The first approach is developing a model on all available data from both test and reference product(s) and carefully examining possible bias in one of the treatment groups. Testing for (statistically) significant differences between drug products can be done for all the model parameters via covariate analysis. Covariate testing follows a well-established statistical distribution that can be used for statistical inference.[28,29] If no significant correlations can be identified between the drug products and if attempts to incorporate treatment as covariate in the model fail to improve it, the biosimilarity claim is supported.

The second method entails the development of different models, one for each test and reference product(s), which in contrast to a combined model does not assume similarity between test and reference product as a starting point. This method allows comparison of the model structure, that should be

identical for biosimilar products, and of model parameters for both test and reference product.

Comparing different PK models inevitably reveals minor differences for which the clinical significance needs to be discussed. For example, in model T the optimal inter-compartmental clearances (Q_1 and Q_2) were estimated to be a factor 10^2–10^3 higher than the corresponding parameters in the other models, while the striking dissimilarity did not seem to affect the descriptive properties of the overall profiles. However, as the (fictive) second and third compartment were not sampled, this finding merely reflects a mathematical solution to a rather complex problem and not necessarily a true (*e.g.* physiological or pharmacological) difference. Additionally, the higher dose administered for the reference product could have allowed a better characterisation of the terminal portion of the PK profile (elimination parameters), which also affects the estimation of remaining parameters, such as Q_1 and Q_2.

This represents an important limitation of the second method, which may be of particular relevance when modelling PK data from two different populations separately. Unfortunately, pharmacokinetic biosimilarity of biopharmaceuticals is regularly investigated in trials of parallel design, because of the long half-life and the potential of anti-drug antibodies development, which could influence the pharmacokinetics.[30] Theoretically, all MABs share common pharmacokinetic properties, *e.g.* small central volume of distribution, no renal excretion due to large molecular size, metabolism into amino-acids and peptides, both specific (non-linear) and non-specific (linear) cellular uptake and degradation elimination mechanisms.[31–35] Thus, the remaining variability is probably determined by patient characteristics. When comparing the model parameters of the separate models, one of the most prominent differences is the population estimate for V_1, which is unlikely caused by a difference between test and reference product.

The combined model equally well described the data, without bias in either the test or reference group. Adding trastuzumab drug product as covariate to the model could not explain any residual variability, which strongly supports the biosimilarity claim, but also indicates that the difference in AUCs must be attributed to population characteristics.

From a regulatory perspective, another limitation of the second method is the lack of proper statistical inference testing on the model parameters. One might consider overlapping confidence intervals for parameter estimates indications for biosimilarity, but many parameters are related, so that – for example – a low inter-compartmental clearance may be 'compensated' in the model by a low volume of distribution. An extension of 'bioequivalence statistics' has been applied to model parameters by Wilkens *et al.*,[36] although their method suffers from the aforementioned limitations as well.

Notwithstanding the limitations of PPK, it has several benefits over a NCA. Importantly, a PPK is not concerned with differences in administered doses. Although the EMA allows a dose correction in the bioequivalence guideline (for chemically derived products) if the difference exceeds 5%, the NCA assumes linearity in its correction, which is not appropriate for MABs, that display non-linear pharmacokinetics. Other benefits of PPK include the possibility to identify and thus correct for certain covariates, and the relative robustness of a PPK against protocol deviations, with regard to timing of sample collection, missing samples, duration of intravenous administration, and incomplete administration.[8,37]

Simulations with model R revealed that the two allowed extremes for protein content per batch (effective doses 5.28 mg/kg and 7.2 mg/kg) would result in a 90% CI for the GMR for AUC_1 of 146.39–147.22% in a crossover design ($n = 46$). If such batch-to-batch variations are not considered relevant, then the consequences on the standard biosimilarity parameters may also be argued to be irrelevant.

With a PK model, multiple scenarios can be simulated within these extremes, which can be used to build the case that the test product achieves therapeutical drug concentrations, similar to the reference product, when administered according to a certain dosing regimen. This approach also circumvents some of the aforementioned limitations of direct comparison of two or more models. If a biomarker or pharmacological effect can be measured in the biosimilarity trial and incorporated in a pharmacokinetic-pharmacodynamic model (pharmacodynamic model), a relevant clinical target may be simulated and lend further support to a biosimilarity claim.

The NCA will most likely remain a gold standard in biosimilarity research, even for the complex MABs. Nonetheless, the model approach can serve as an elegant add-on. Questions that need to be addressed before a PPK can fully substitute the NCA in demonstrating biosimilarity relate to selection of the most

meaningful PK or pharmacodynamic parameter from the model, and the minimal population size to detect with sufficient statistical power relevant (model) differences.

Previously, the benefits of modelling and simulation have been proposed for proof of biosimilarity, to which this chapter adds similar benefits for MABs.

REFERENCES

1 Bonafede M, Joseph GJ, Princic N, Harrison DJ. Annual acquisition and administration cost of biologic response modifiers per patient with rheumatoid arthritis, psoriasis, psoriatic arthritis, or ankylosing spondylitis. *J Med Econ* 2013; **16**: 1120–8.

2 Francis SM, Heyliger A, Miyares MA, Viera M. Potential cost savings associated with dose rounding antineoplastic monoclonal agents. *J Oncol Pharm Pract* 2015; **21**: 280–4.

3 IMS health. IMS Health Top 20 Global Products 2014. 2015. http://www.imshealth.com/files/web/Corporate/News/Top-Line Market Data/2014/Top_20_Global_Products_2014.pdf (accessed April 1, 2016).

4 WHO Expert Committee on Biological Standardization. Guidelines on evaluation of similar biotherapeutic products (SBPs). Genève, 2009.

5 US Food and Drug Administration. Scientific considerations in demonstrating biosimilarity to a reference product. Silver Spring: US Department of Health and Human Services, 2015.

6 Committee for Medicinal Products for Human Use (CHMP). Guideline on similar biological medicinal products. London: European Medicines Agency, 2015.

7 Panhard X, Mentré F. Evaluation by simulation of tests based on non-linear mixed-effects models in pharmacokinetic interaction and bioequivalence cross-over trials. *Stat Med* 2005; **24**: 1509–24.

8 Dubois A, Gsteiger S, Pigeolet E, Mentré F. Bioequivalence tests based on individual estimates using non-compartmental or model-based analyses: evaluation of estimates of sample means and type I error for different designs. *Pharm Res* 2010; **27**: 92–104.

9 Dubois A, Gsteiger S, Balser S, *et al.* Pharmacokinetic similarity of biologics: analysis using nonlinear mixed-effects modeling. *Clin Pharmacol Ther* 2012; **91**: 234–42.

10 Wisman LAB, De Cock EPM, Reijers JAA, *et al.* A phase I dose-escalation and bioequivalence study of a trastuzumab biosimilar in healthy male volunteers. *Clin Drug Investig* 2014; **34**: 887–94.

11 US Food and Drug Administration. Population pharmacokinetics. Silver Spring: US Department of Health and Human Services, 1999.

12 Committee for Medicinal Products for Human Use (CHMP). Guideline on reporting the results of population pharmacokinetic analyses. London: European Medicines Agency, 2008.

13 Janmahasatian S, Duffull SB, Ash S, Ward LC, Byrne NM, Green B. Quantification of lean bodyweight. *Clin Pharmacokinet* 2005; **44**: 1051–65.

14 Mosteller RD. Simplified calculation of body-surface area. *N Engl J Med* 1987; **317**: 1098.

15 Post TM, Freijer JI, Ploeger BA, Danhof M. Extensions to the visual predictive check to facilitate model performance evaluation. *J Pharmacokinet Pharmacodyn* 2008; **35**: 185–202.

16 Karlsson MO, Savić RM. Diagnosing model diagnostics. *Clin Pharmacol Ther* 2007; **82**: 17–20.

17 Luu KT, Bergqvist S, Chen E, Hu-Lowe D, Kraynov E. A model-based approach to predicting the human pharmacokinetics of a monoclonal antibody exhibiting target-mediated drug disposition. *J Pharmacol Exp Ther* 2012; **341**: 702–8.

18 Mager DE, Jusko WJ. General pharmacokinetic model for drugs exhibiting target-mediated drug disposition. *J Pharmacokinet Pharmacodyn* 2001; **28**: 507–32.

19 Gibiansky L, Gibiansky E, Kakkar T, Ma P. Approximations of the target-mediated drug disposition model and identifiability of model parameters. *J Pharmacokinet Pharmacodyn* 2008; **35**: 573–91.

20 Bate R, Mathur A, Lever HM, *et al.* Generics substitution, bioequivalence standards, and international oversight: complex issues facing the FDA. *Trends Pharmacol Sci* 2016; **37**: 184–91.

21 Bruno R, Washington CB, Lu J-F, Lieberman G, Banken L, Klein P. Population pharmacokinetics of trastuzumab in patients with HER2+ metastatic breast cancer. *Cancer Chemother Pharmacol* 2005; **56**: 361–9.

22 Charoin J-E, Jacqmin P, Banken L, Lennon S, Jorga K. Population pharmacokinetic analysis of trastuzumab (Herceptin) following long-term administration using different regimens. *PAGE* 2004; **13**: Abstr 489.

23 Fukushima Y, Charoin J-E, Brewster M, Jonsson EN. Population pharmacokinetic analysis of trastuzumab (Herceptin®) based on data from three different dosing regimens. *PAGE* 2007; **16**: Abstr 1121.

24 Kloft C, Graefe E-U, Tanswell P, *et al.* Population pharmacokinetics of sibrotuzumab, a novel therapeutic monoclonal antibody, in cancer patients. *Invest New Drugs* 2004; **22**: 39–52.

25 Kuester K, Kovar A, Lüpfert C, Brockhaus B, Kloft C. Refinement of the population pharmacokinetic model for the monoclonal antibody matuzumab: external model evaluation and simulations. *Clin Pharmacokinet* 2009; **48**: 477–87.

26 Van Hasselt JGC, Boekhout AH, Beijnen JH, Schellens JHM, Huitema ADR. Population pharmacokinetic-pharmacodynamic analysis of trastuzumab-associated cardiotoxicity. *Clin Pharmacol Ther* 2011; **90**: 126–32.

27 Rescigno A, Powers J, Herderick EE. Bioequivalent or nonbioequivalent? *Pharmacol Res* 2001; **43**: 543–7.

28 Khandelwal A, Harling K, Jonsson EN, Hooker AC, Karlsson MO. A fast method for testing covariates in population PK/PD models. *AAPS J* 2011; **13**: 464–72.

29 Meibohm B, Derendorf H. Basic concepts of pharmacokinetic/pharmacodynamic (PK/PD) modelling. *Int J Clin Pharmacol Ther* 1997; **35**: 401–13.
30 Committee for Medicinal Products for Human Use (CHMP). Guideline on similar biological medicinal products containing monoclonal antibodies: non-clinical and clinical issues. London: European Medicines Agency, 2012.
31 Wang W, Wang EQ, Balthasar JP. Monoclonal antibody pharmacokinetics and pharmacodynamics. *Clin Pharmacol Ther* 2008; **84**: 548–58.
32 Tabrizi MA, Tseng CL, Roskos LK. Elimination mechanisms of therapeutic monoclonal antibodies. *Drug Discov Today* 2006; **11**: 81–8.
33 Ternant D, Bejan-Angoulvant T, Passot C, Mulleman D, Paintaud G. Clinical pharmacokinetics and pharmacodynamics of monoclonal antibodies approved to treat rheumatoid arthritis. *Clin Pharmacokinet* 2015; **54**: 1107–23.
34 Dirks NL, Meibohm B. Population pharmacokinetics of therapeutic monoclonal antibodies. *Clin Pharmacokinet* 2010; **49**: 633–59.
35 Keizer RJ, Huitema ADR, Schellens JHM, Beijnen JH. Clinical pharmacokinetics of therapeutic monoclonal antibodies. *Clin Pharmacokinet* 2010; **49**: 493–507.
36 Wilkins JJ, Gautier A, Lowe PJ. Bioequivalence, bootstrapping and case-deletion diagnostics in a biologic: a model-based analysis of the effect of formulation differences in a monoclonal antibody. *PAGE* 2008; **17**: Abstr 1284.
37 Charles B. Population pharmacokinetics: an overview. *Aust Prescr* 2014; **37**: 210–3.

SUPPLEMENT

$$V_{1,i} = \theta_p \frac{x_i}{\tilde{x}} e^{\eta_i} \qquad \textbf{(1.S1)}$$

$$k_{e,i} = \theta_p \frac{x_i}{\tilde{x}} e^{\eta_i} \qquad \textbf{(1.S2)}$$

Here, i is the i^{th} individual, V_1 the volume of distribution, k_e the elimination rate constant, θ_p the population parameter estimate, x the covariate (respectively LBW and BMI), $\tilde{x}$ the median of x, and η the inter-individual variability.

TABLE 1.S1 AUC comparison actual dose

	TEST						REFERENCE					
	AUC		%-change[a]		%-change[b]		AUC		%-change[a]		%-change[b]	
AUC_1												
NCA	1318	(220)					1602	(220)				
Separate models												
Actual time	1315	(211)	100.0	(5.0)			1599	(190)	100.1	(4.5)		
Continuous time	1292	(206)	98.3	(4.9)			1571	(188)	98.4	(4.5)		
Combined model												
Actual time	1310	(204)	99.8	(5.4)	99.7	(1.1)	1599	(193)	100.1	(4.9)	100.0	(1.5)
Continuous time	1287	(199)	98.0	(5.2)	99.7	(1.1)	1571	(191)	98.4	(5.0)	100.0	(1.5)
AUC_∞												
NCA	1328	(225)					1607	(224)				
Separate models												
Actual time	1329	(216)	100.3	(5.2)			1602	(192)	100.0	(4.5)		
Continuous time	1312	(208)	99.0	(5.0)			1630	(201)	101.7	(4.7)		
Combined model												
Actual time	1315	(206)	99.3	(5.7)	99.1	(3.3)	1604	(195)	100.1	(4.9)	100.1	(1.5)
Continuous time	1298	(200)	98.1	(5.3)	99.1	(1.1)	1577	(193)	98.4	(5.0)	96.8	(1.2)

Mean (standard deviation) AUCs (μg day mL^{-1}) and mean (standard deviation) percentage change for the actual dose (test 5.92 mg/kg; reference 6.44 mg/kg), as derived by different methods per treatment arm. AUCs of combined and separate models are compared to the NCA result (a); AUCs of combined model are compared to the AUCs of the separate model (b, actual time compared to actual time, continuous time to continuous time). For comparison to a standard NCA, AUC_1 was calculated using model simulated (predicted) individual concentrations at the original sampling times ('actual time'). Extrapolation to infinity (AUC_∞) was based on the apparent terminal elimination rate constant. Additionally, the AUCs were derived by integration of the simulated concentration-time profiles ('continuous time'); AUC_1 from the administration time to the last concentration used in the NCA, AUC_∞ until infinity.
AUC: area under the concentration-time curve|NCA: non-compartmental analysis

TABLE 1.S2 AUC comparison after dose correction

	TEST						REFERENCE					
	AUC		%-change[a]		%-change[b]		AUC		%-change[a]		%-change[b]	
AUC_t												
NCA	1335	(223)					1493	(205)				
Separate models												
Actual time	1338	(215)	100.5	(5.1)			1465	(176)	98.4	(4.5)		
Continuous time	1315	(210)	98.7	(5.0)			1439	(174)	96.7	(4.4)		
Combined model												
Actual time	1334	(208)	100.2	(5.4)	99.7	(1.1)	1453	(176)	97.7	(4.8)	99.2	(1.2)
Continuous time	1310	(202)	98.5	(5.3)	99.7	(1.2)	1427	(174)	95.9	(4.8)	99.2	(1.3)
AUC_∞												
NCA	1346	(228)					1497	(209)				
Separate models												
Actual time	1353	(220)	100.7	(5.2)			1467	(177)	98.3	(4.5)		
Continuous time	1335	(212)	99.5	(5.0)			1493	(185)	100.0	(4.7)		
Combined model												
Actual time	1339	(210)	99.8	(5.8)	99.1	(3.4)	1456	(177)	97.6	(4.8)	99.2	(1.2)
Continuous time	1322	(204)	98.6	(5.3)	99.1	(1.2)	1432	(175)	96.0	(4.8)	96.0	(1.0)

Mean (standard deviation) AUCs (μg day mL^{-1}) and mean (standard deviation) percentage change for the labelled dose (6 mg/kg), as derived by different methods per treatment arm. For the NCA-results, a linear dose correction was applied; in the models, the labelled dose was used to simulate the individual profiles (see main body). AUCs of combined and separate models are compared to the NCA result (a); AUCs of combined model are compared to the AUCs of the separate model (b, actual time compared to actual time, continuous time to continuous time). For comparison to a standard NCA, AUC_t was calculated using model simulated (predicted) individual concentrations at the original sampling times ('actual time'). Extrapolation to infinity (AUC_∞) was based on the apparent terminal elimination rate constant. Additionally, the AUCs were derived by integration of the simulated concentration-time profiles ('continuous time'); AUC_t from the administration time to the last concentration used in the NCA, AUC_∞ until infinity.

AUC: area under the concentration-time curve | NCA: non-compartmental analysis

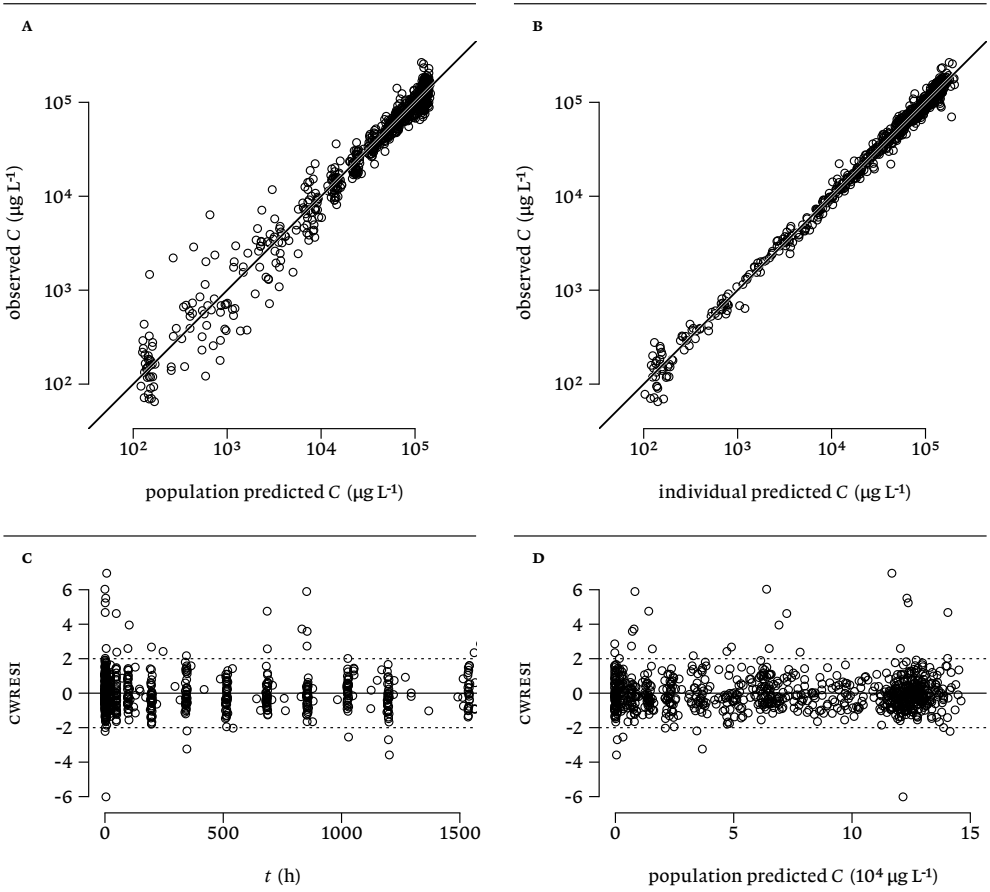

FIGURE 1.S1 Goodness-of-fit plots model T

Observed *vs.* population predicted concentrations (A), observed *vs.* individual predicted concentrations (B), conditional weighted residuals with interaction (CWRESI) *vs.* times (C), and conditional weighted residuals *vs.* population predictions (D) of the separate model for the test product.

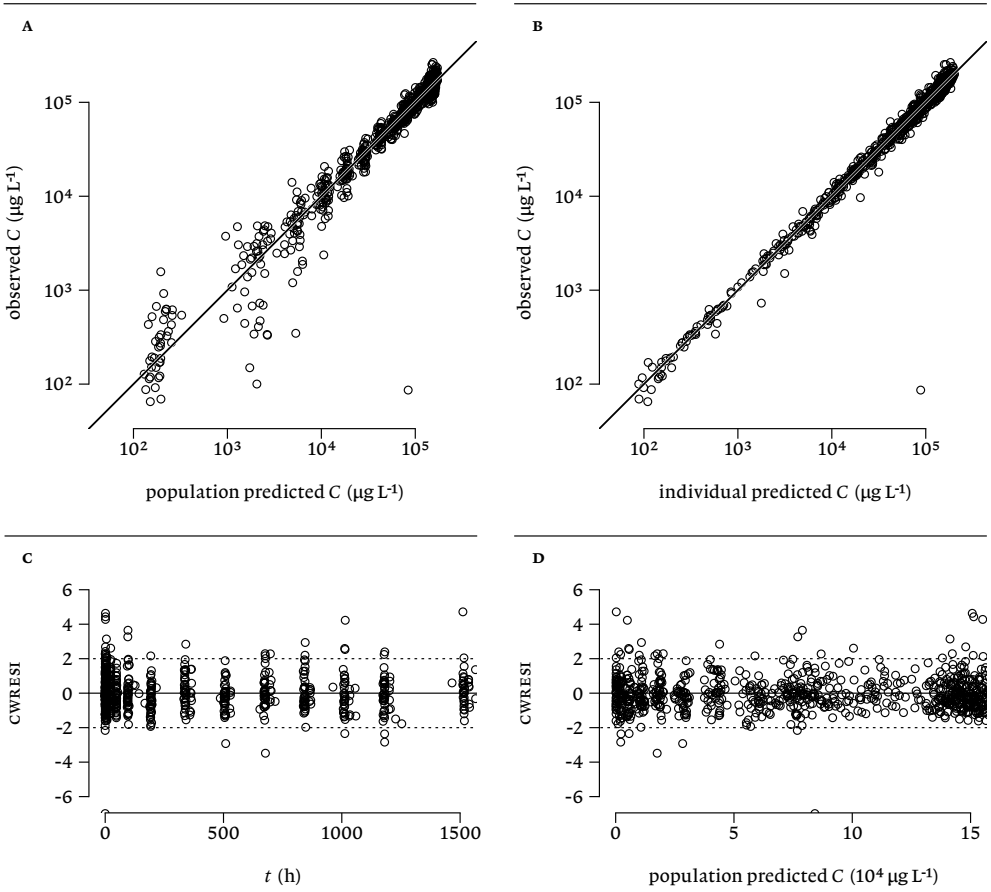

FIGURE 1.S2 Goodness-of-fit plots model R

Observed *vs.* population predicted concentrations (A), observed *vs.* individual predicted concentrations (B), conditional weighted residuals with interaction (CWRESI) *vs.* times (C), and conditional weighted residuals *vs.* population predictions (D) of the separate model for the reference product.

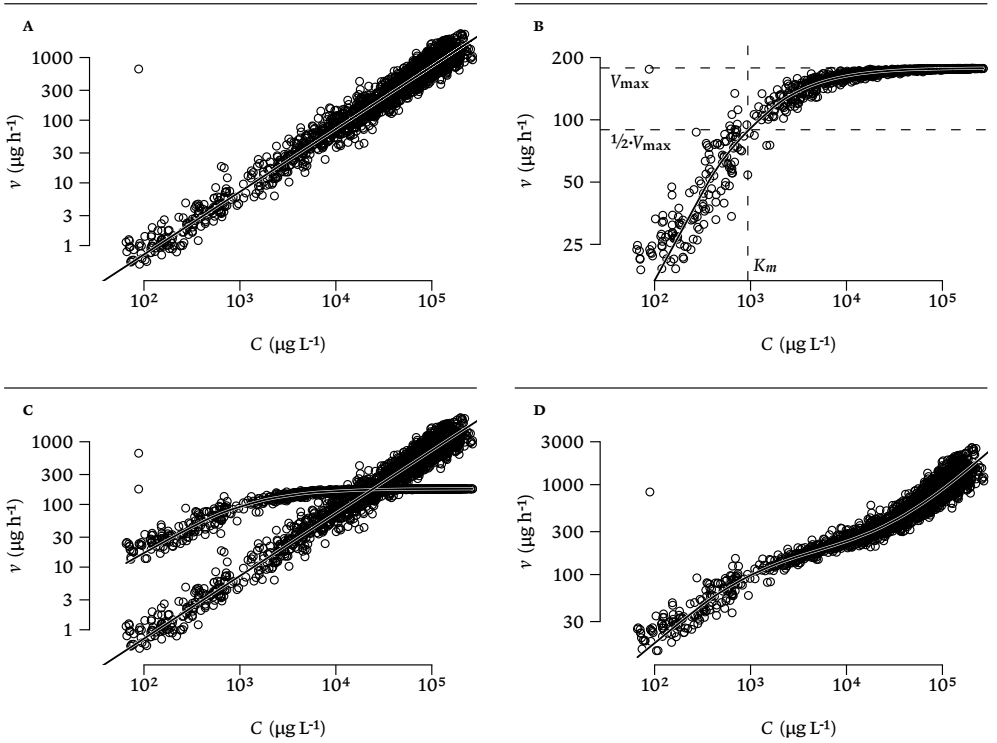

FIGURE 1.S3 Linear and non-linear clearance combined model

The linear clearance (A), the non-linear clearance (B), the combined linear and non-linear clearances (C), and the total clearance (D) of the combined model.

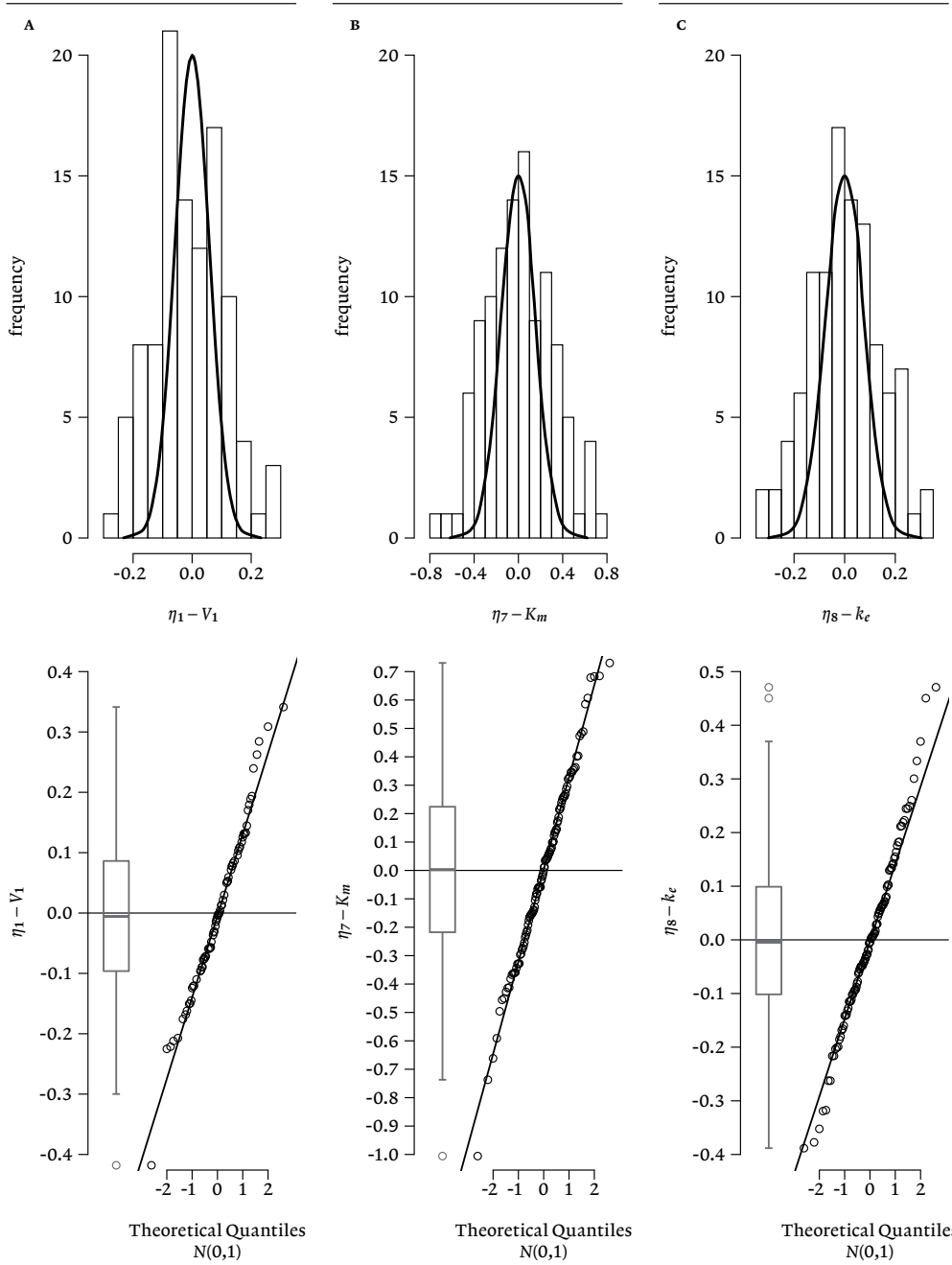

FIGURE 1.S4 η density combined model
Distribution of ηs in the combined model for V_1 (η_1, A), K_m (η_7, B), and k_e (η_8, C).

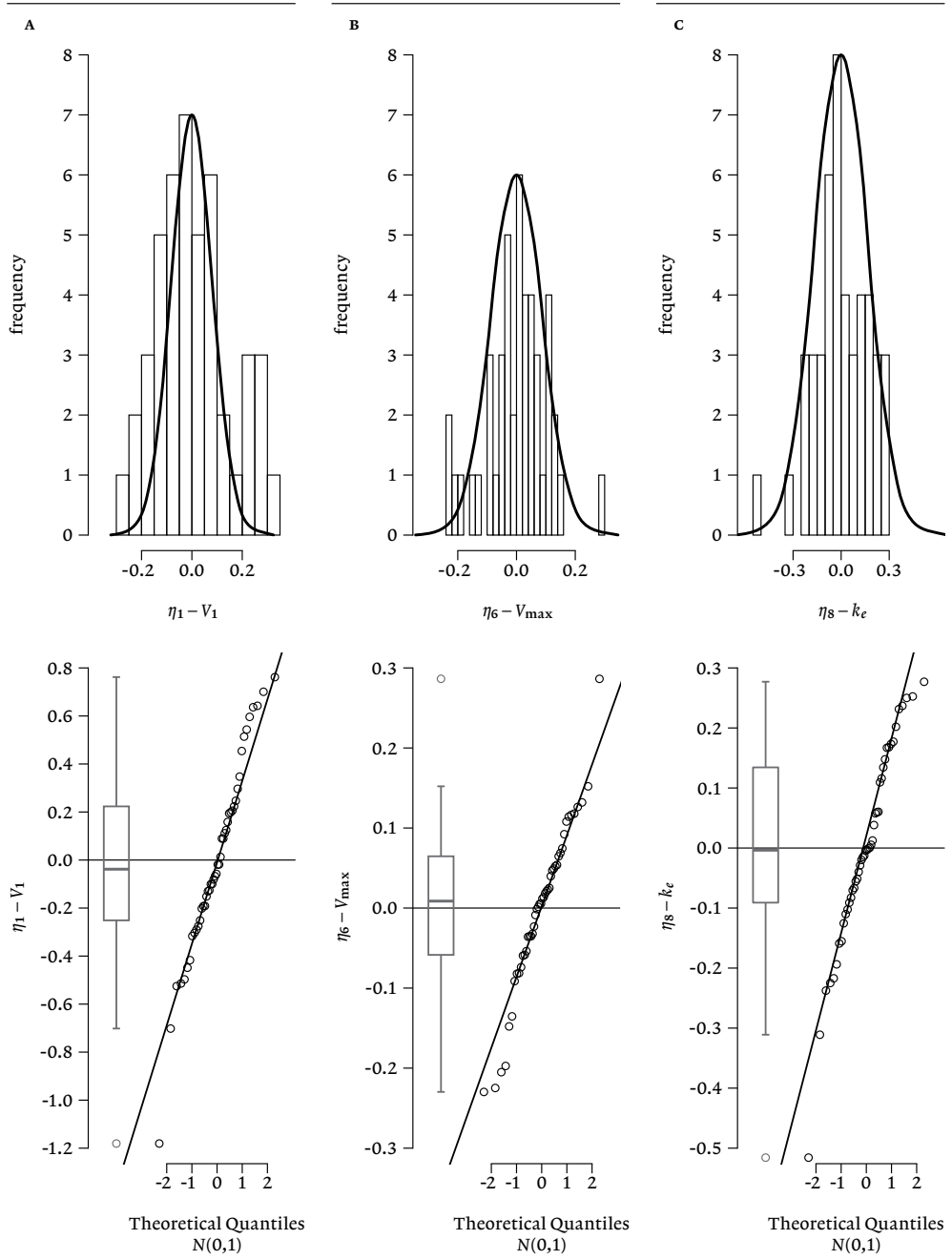

FIGURE 1.S5 η density model T
Distribution of ηs in model T for V_1(η_1, A), V_{max}(η_6, B), and k_e(η_8, C).

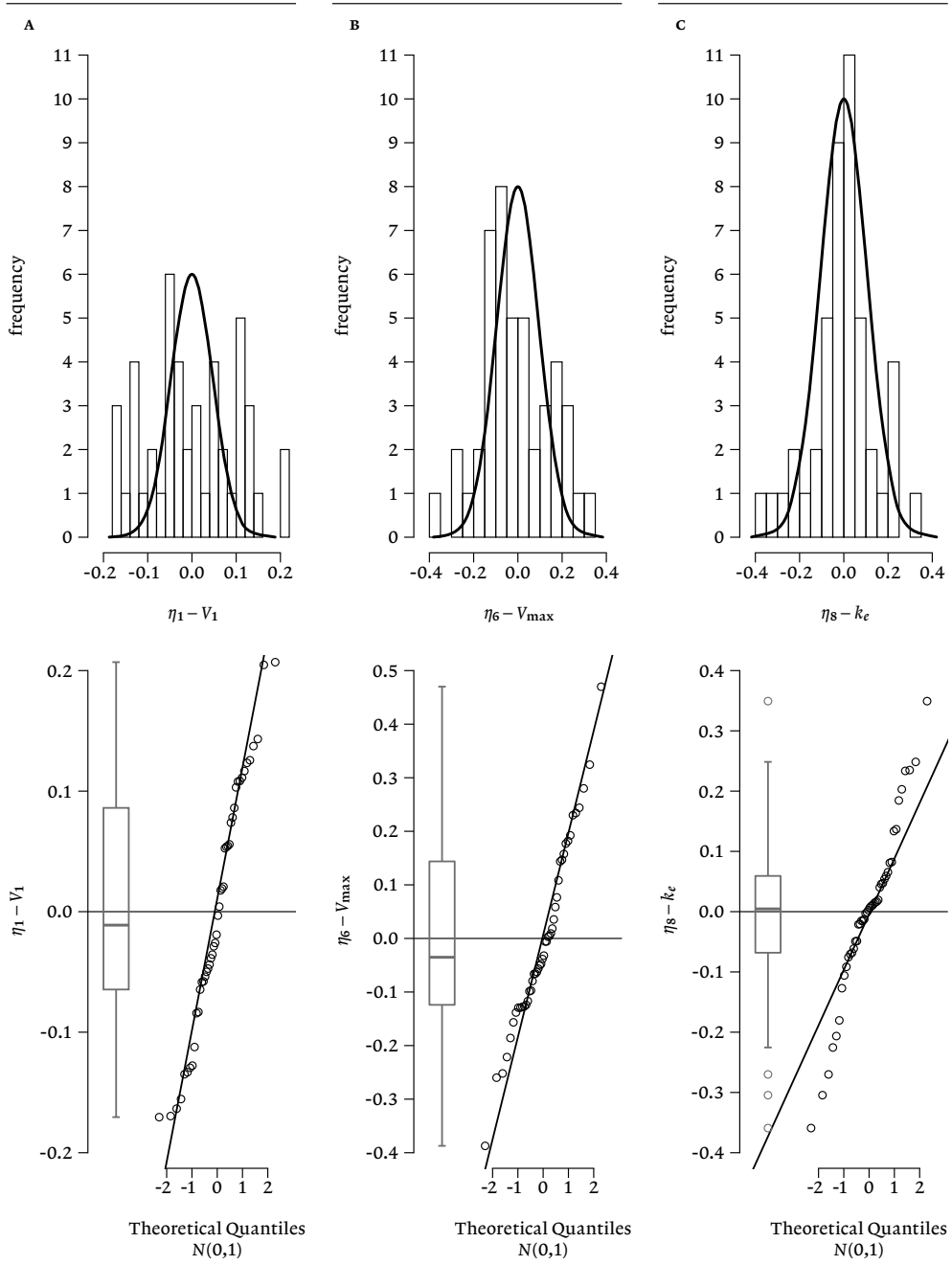

FIGURE 1.S6 η density model R
Distribution of ηs in model R for $V_1(\eta_1, \text{A})$, $V_{max}(\eta_6, \text{B})$, and $k_e(\eta_8, \text{C})$.

CHAPTER II

Potential influence of endothelial adsorption on the delayed time to maximum concentration of biopharmaceuticals

J.A.A. Reijers, M.J.C. Dane, A.J. van Zonneveld, J. Burggraaf, M. Moerland

Maximum plasma concentration of biopharmaceuticals sometimes occurs long after completion of intravenous infusion. The objective of this study was to study the hypothetical adsorption of biopharmaceuticals to endothelium and infusion material, which may theoretically explain this phenomenon.

Infusion procedures were mimicked in an artificial vessel covered with a confluent monolayer of endothelial cells. Three monoclonal antibodies (MABs) and C1-inhibitor were studied.

Adsorption of MABs to endothelium was observed followed by release when the vessel was subsequently perfused with buffer. Adsorption to infusion material also occurred to various degrees and in a seemingly random fashion, with a loss of up to 15% during a single flush of the line, but release from the line was not seen.

Our results indicate that adsorption of biopharmaceuticals to endothelium can occur. This observation can explain the increase in plasma concentration after completion of intravenous administration.

Basic pharmacokinetic principles teach that for the intravenous route of administration, the maximum plasma concentration (C_{max}) is reached at the end of the infusion (EOI). In other words, the time to C_{max} (t_{max}) equals the infusion duration, with a margin of a few minutes, as it is understood that the administered drug requires a finite time to travel to the sampling site. Sufficient evidence exists, however, that this may not always be true. *Table 2.1* provides examples of drugs for which a delayed t_{max} after intravenous administration has been described.

Although this list is not exhaustive, the phenomenon seems to be limited to (poly)peptides, in particular monoclonal antibodies (MABs), for which differences of several hours have been reported between t_{max} and EOI. Although noted and reported, it appears that not much attention has been given to this observation, let alone an explanation.

Based on the reported findings, we considered two hypotheses to explain the findings. First, the drug product may aggregate in the infusate because of the relatively high concentration, which is followed by disaggregation when diluted in plasma upon administration, assuming that the bioassay is unable to measure aggregates. We considered this to be unlikely as protein aggregation is often irreversible. Even if the aggregation were reversible, the physical conditions in the human body determining the equilibrium would not change over time.[1–3] Moreover, it is common practice to tightly control the fraction of drug aggregates below 5%, because of adverse

TABLE 2.1 Drugs with a delayed t_{max}

DRUG PRODUCT	EOI (h)	t_{max} (h)	C_{max}/C_{EOI} (%)	PK SAMPLES (h)	REFERENCE
α1-Antitrypsin	(0.25)	0.7[a], 1.5[a]			28
Bevacizumab	0.67	3.00	123, 134	0.67, 0.83, 1, 2, 3, 4, 5	data on file
C1-inhibitor	bolus	0.5, 1.0		0.25, 0.5, 0.75, 1, 2	29
	(0.17)	2.7[a], 3.9[a]			30
	0.13	0.42[a], 0.60[a]		0.25, 0.5, 1, 2	data on file
Cetuximab	1	2, 7.9		2, 5, 8	31
	1	3.00, 3.63, 3.75, 4.00		1, 4	32
Dalotuzumab	2	3.5, 5	117	2, 5, 8	31
Glucarpidase	0.08	0.25, 0.55		0.08, 0.25, 0.5, 1, 2	33
Pembrolizumab	0.5	1.2, 4.0		~0.5, 6 ± 2	34
Pertuzumab	0.5	1.8			35
	0.5	5.5			36
	1.5	3.2		1.75, 3, 5.5, 9.5	37
Ramucirumab	(1)	1.15[b]		1, 1.5, 2	38
Trastuzumab	1.5	1.7[a], 2.7[a], 4.4[a]		1.5, 3, 4, 6	39
	1.5	3.46[a]	113	1.5, 2, 3, 4, 6	40
	1.5	1.65, 3.00		1.5, 3, 6	41
	1.5	2.083[a], 2.303[a], 2.674[a], 2.683[a], 3.096[a]	(113, 124, 129, 132, 141)	1.5, 2, 3, 4, 5, 6, 8	42

Median, mean (a), or geometric mean (b) t_{max}. In case more than one value is given for t_{max} or C_{max}/C_{EOI}, multiple (combination) treatments or treatment regimens (*e.g.* dosing interval or dosage) are presented in the reference, or parameters were obtained during multiple treatment cycles, each with a different value. Bracketed numbers are not reported in the reference but derived from the package insert.
C_{max}/C_{EOI}: ratio of maximum plasma concentration (C_{max}) over concentration at EOI, based on reported averages | EOI: end of infusion, equals infusion duration | PK samples: scheduled collection times of post-dose pharmacokinetic plasma samples | t_{max}: time to C_{max}

reactions, which seems incompatible with the observed increases in plasma concentration after EOI exceeding 10% (*table 2.1*).

The second hypothesis is that the drug substance is bound to and released from the vessel wall, or taken up and released by endothelial cells, particularly in the presence of a high local concentration at the infusion site. After EOI, the concentration drops, and drug substance is released from the wall or by the cells, causing a rise in plasma concentration and hence a delayed t_{max}. Adsorption to or absorption by circulating blood constituents may also occur, although it is less likely to affect the plasma concentration over time, as these components follow the same route as the infused substance, travelling from a high concentration (infusion site) to a low concentration (sampling site).

Infusion lines are sometimes flushed with normal saline in order to also administer the line content, which is usually done to save the cost of additional (non-administrable) drug product. If – by analogy – binding of a biopharmaceutical to an IV (intravenous) line occurs during the first part of the administration procedure, and the adsorbed fraction is released during flushing, the flushing solution contains drug product as well. Flushing an IV line may thus result in a continuation of administration of a biopharmaceutical after the anticipated EOI and hence an *apparent* delay in t_{max}.

The objective of this study was to find support for the second hypothesis by mimicking the administration procedure on a small scale with therapeutical proteins. These form the largest class of the so-called 'biotechnology-derived products', also commonly known as biopharmaceuticals. Specifically, it was investigated whether biopharmaceuticals could bind to or be taken up by endothelial cells and be subsequently released. In addition, potential adsorption to IV lines during administration followed by desorption during flushing was studied.

Large polypeptides distribute slowly to the extravascular compartment because of their size,[4] which results in a relatively stable plasma concentration during and shortly after infusion. By focussing on drug products in that category, the need to consider

tissue distribution in the experiments was eliminated. Comparison to a negative control was sought; however, to the best of our knowledge, a MAB or other large therapeutical protein with a known t_{max} at EOI does not exist. To further complicate this search, the t_{max} of intravenously administered proteins is only infrequently reported, as is the pharmacokinetic sample density in clinical trials.

METHODS

Biopharmaceuticals

For this experiment, three registered biopharmaceuticals were chosen from *table 2.1*, namely bevacizumab (Avastin®), trastuzumab (Herceptin®), and C1-inhibitor (Berinert®), and one experimental IGG1. These drug products were reconstituted by the Pharmacy of Leiden University Medical Center (LUMC) according to the manufacturer's instruction, with one exception. For the higher concentrations of C1-inhibitor, less dissolvent was used, as reconstitution in the prescribed 10 mL water for injection resulted in a concentration of 4 mg/mL. The experimental human IGG1 was only available diluted in 0.9% NaCl at 3.75 mg/mL.

Cell cultures (artificial vessel)

All *in vitro* experiments were performed with human umbilical vein endothelial cells (HUVECs), freshly isolated (by 0.25% trypsin treatment). After isolation, HUVECs were cultured in EGM2 medium (Lonza, Basel, Switzerland) containing antibiotics and antimycotics (Life Technologies, Carlsbad, California, USA), and used for experiments on passage 3–4. To obtain a confluent, quiescent endothelial monolayer that closely resembles the physiological situation, HUVECs were grown under a constant laminar flow of 10 dyne cm^{-2} for 7 days using a closed perfusion Ibidi flow system (ibiTreat 0.4 µ-Slide VI Luer, Ibidi, Martinsried, Germany). This system is referred to as 'artificial vessel' (AV).

The cells in the AV were exposed to varying concentrations of a single biopharmaceutical in HBSS with 1% bovine serum albumin (BSA) (Life Technologies). Optionally, the AV was pretreated with 15 U/mL heparanase III (HPSE) (Sigma-Aldrich, St. Louis, Missouri, USA) to degrade heparan sulphate proteoglycans from the glycocalyx, or with increasing concentrations of heparin, to examine the role of heparan sulphate proteoglycans on the possible binding of biopharmaceuticals to the AV.

Throughout the experiments, the cell cultures were maintained at 37°C and 5% CO_2. All experiments were executed at least twice in duplicate to minimise culture variability and to confirm the validity of the results. The tested biopharmaceutical concentrations were based on the concentrations observed clinically after administration of the standard intravenous dose of 6 mg/kg for trastuzumab: 2 mg/mL (infusate) and 0.2 mg/mL (C_{max}). Because the experimental IGG1 could only be provided as infusion solution (3.75 mg/mL in 0.9% NaCl), this MAB was not included in any of the cell culture experiments.

Statical experiments

HUVECs from the AV were exposed to varying concentrations of biopharmaceuticals for 30 min under statical conditions. This exposure could be repeated, each instance with a different concentration to simulate increasing and decreasing concentrations during intravenous administration. To mimic the *in vivo* situation following infusion, cells were washed one or more times with HBSS containing 1% BSA.

Dynamical experiments

In the dynamical experiments, the AV was perfused with the biopharmaceutical for a predefined period, followed by perfusion with a lower concentration of the same biopharmaceutical, mimicking the situation during and after administration. The experiment was stopped at various time points and the endothelial monolayer was immediately fixed and imaged. The perfusion rate was 0.2 mL/min (effective velocity 0.2 cm/s).

Staining and imaging

HUVECs (statical or dynamical experiments) incubated with different concentrations of biopharmaceuticals were fixed in 4% paraformaldehyde in HBSS for 10 min at room temperature, washed twice with 1% BSA in HBSS, and blocked with 5% normal goat serum (Dako, Carpinteria, California, USA) in HBSS for 30 min. Cultures were incubated for at least 60 min at 4°C with 10 µg/mL TRITC-labelled wheat germ agglutinin (WGA) (Sigma-Aldrich, 1:100), and Hoechst 33258 (Sigma-Aldrich, 1:5,000), diluted in HBSS with 1% BSA. In the experiments with a MAB, 2 µg/mL of an Alexa Fluor® 488-coupled anti-human-IGG (H + L)

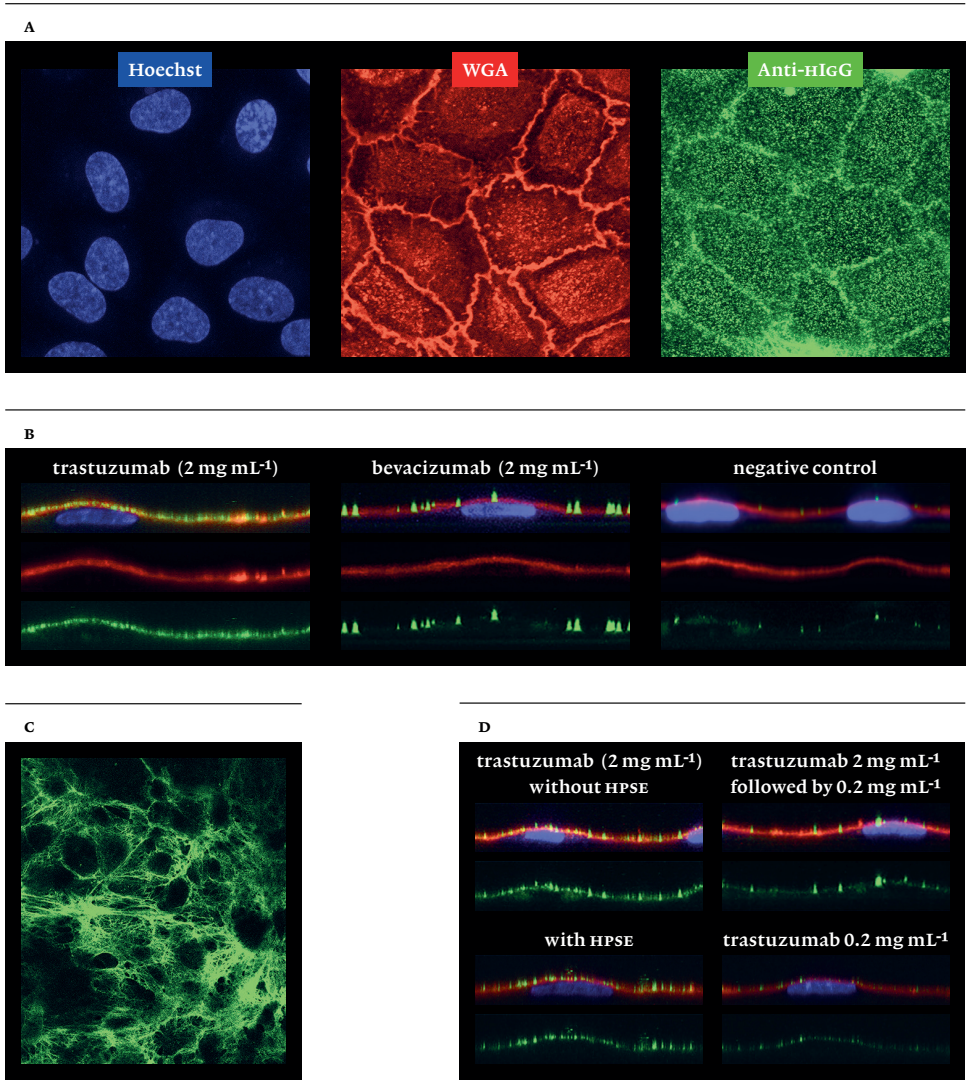

FIGURE 2.1

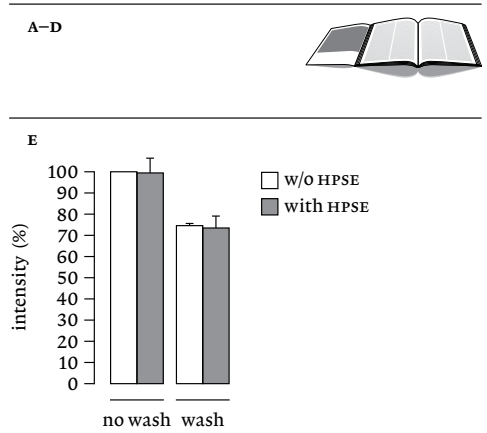

FIGURE 2.1 Statical experiments
After perfusion of the artificial vein with 2 mg/mL trastuzumab or bevacizumab, the human umbilical vein endothelial cells (HUVECs) were stained with Hoechst 33258 (nucleus, *blue*), TRITC-labelled wheat germ agglutinin (WGA) binding the carbohydrate *N*-acetyl galactosamine in the glycocalyx (*red*), and an Alexa Fluor® 488-coupled anti-human-IgG goat IgG (trastuzumab/bevacizumab, *green*). Overview (A) and cross-section (B) for trastuzumab (A&B) and bevacizumab (B).
Where no confluent layer of HUVECs had formed, dense staining of the sub-cellular matrix occurred following incubation with 2 mg/mL trastuzumab (C). Effect of pretreating the HUVECs with heparanase (HPSE) on the binding of 2 mg/mL trastuzumab (D&E) or washing the HUVECs three times with buffer after incubation with trastuzumab (E). The signal intensity was normalised to the 2 mg/mL trastuzumab without HPSE condition and is displayed as mean ± standard deviation ($n = 2$). Perfusing the HUVECs with 2 mg/mL followed by 0.2 mg/mL trastuzumab similarly reduced the signal, but not to the level that was observed when the HUVECs were perfused with 0.2 mg/mL only (D).

goat IgG (Thermo Fisher, Waltham, Massachusetts, USA, 1:500) was included in the incubation. Conversely, in the experiments with C1-inhibitor, an anti-human-C1-inhibitor rabbit IgG (1:25) and a secondary Alexa Fluor® 488-coupled anti-rabbit-IgG goat IgG (Thermo Fisher) were included in the incubation. After washing three times with HBSS + 1% BSA, cells were imaged using a Leica SP5 confocal microscope.

Confocal 12-bit greyscale axial image stacks (*xyz* dimensions, 0.08 × 0.08 × 0.13 µm) that covered 6,724 µm² of surface area per image and a height of 5 to 10 µm above the endothelial cell nuclear plane were recorded using the LAS-AF image software (Leica). The image stacks were analysed with the public domain National Institutes of Health IMAGE program (http://rsb.info.nih.gov/nih-image). Cross-sections of the cell-layer were generated using this software. For quantification, the area of interest was selected (to discard staining which accumulated underneath the cell-layer in the areas of inadequate cell-cell contacts), and the average signal intensity was measured throughout the whole *xyz* area of the recorded image stacks.

Infusion profiling

Infusion procedures were replicated with a standard flexible PVC IV line (CODAN #43.4270, Santa Ana, California, USA) with an inner diameter of 3.0 mm that was cut to hold 10.0 mL. The line was coupled via its Luer-Lock adaptor to a syringe that was placed in a calibrated syringe pump (Omnifuse, Graseby Medical Ltd., Watford, UK).

After the lines were filled with the solution containing the biopharmaceutical ('infusate') and allowed to rest for 1 h, the pump was started at a rate of 2 mL/min. After the IV line was perfused with the infusate at a constant rate for a predefined period ('perfusion'), the IV line was flushed with 50 mL 0.9% NaCl (Baxter BV, Utrecht, The Netherlands) at the same rate ('flushing').

The solution coming out of the IV line was sampled every 2.5 min, corresponding to one-half of the line volume. The wash-out from the line between these samples was collected as well.

To determine the effect of infusion rate and concentration on binding characteristics, the rate was varied from 1 to 3 mL/min (only for trastuzumab) and the concentration from 1.25 to 10 mg/mL (all except the experimental IgG1). This covers the range of commonly encountered infusion rates and concentrations for biopharmaceuticals. The dilutions of the biopharmaceuticals in 0.9% NaCl (Fresenius Kabi, Schelle, Belgium) were prepared by the LUMC Pharmacy.

All experiments with unique combinations of parameters were performed at least twice.

Drug concentration

Drug concentration in the samples from the infusion profile was determined at the Central Clinical Chemical Laboratory (CCCL) of the LUMC as total protein concentration with a colorimetrical assay (Biuret reaction) on a Cobas P800 module (Roche, Penzberg, Germany). This method was validated against spe-

cific immunochemical assays for total human IgG and C1-inhibitor, performed on a BN-Prospec nephelometer (Siemens, Marburg, Germany). These assays use an antibody against the γ-chain of human IgG and antiserum to human C1-inhibitor, respectively. The lower limit of quantification (LLOQ) was 0.04 g/L.

Statistical analysis

Results are presented as mean (standard deviation, SD) for continuous data, and as number (percentage) for categorical data, unless otherwise specified. As this study consisted of multiple hypothesis-generating experiments, no formal inference test was performed.

The cumulative wash-out from the IV lines was calculated as the sum of the biopharmaceutical dose in all the collected samples up to a certain point. The dose per sample was calculated as the product of sample volume and biopharmaceutical concentration in the sample. Samples with a concentration <LLOQ were excluded from the calculation. To estimate the theoretical wash-out, the calculation was repeated with the concentration of the excluded samples (<LLOQ) assumed to be 0.0394 g/L.

Data analysis was performed with R (v2.15.2, R Foundation for Statistical Computing, Vienna, Austria, 2012).

RESULTS

Artificial vessel

Statical experiments

Following incubation of human umbilical cord endothelial cells (HUVECs) with 2 mg/mL trastuzumab for 30 min, binding to the luminal surface of the HUVECs was observed, colocalising with the WGA-signal (binding the carbohydrate N-acetyl galactosamine), whereas in the control samples, the signal of the secondary anti-human-IgG antibody was absent (*figure 2.1A&B*). Translocation to the basal side or internalisation by the endothelial cells was not seen, or was negligible in relation to the apical binding, although the experiments were not specifically designed to detect endocytosis. Where the HUVECs had not formed a confluent monolayer, dense staining of the basal layer in a reticular pattern occurred (*figure 2.1C*).

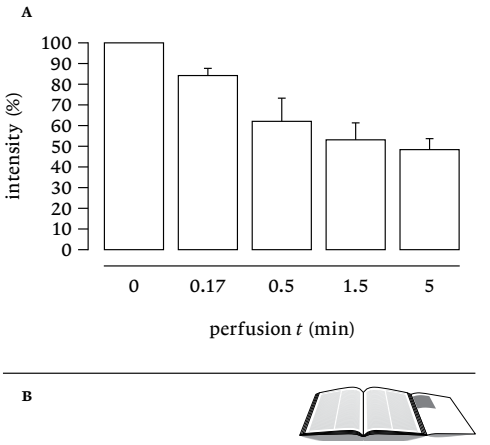

FIGURE 2.2 Dynamical experiments
After perfusing the artificial vein with 2 mg/mL trastuzumab in culture medium for 5 min at 0.2 mL/min, the system was flushed with medium. At this rate, one complete flush of the entire system takes one minute.
At certain moments during the flushing of the artificial vein, the experiment was interrupted and the HUVECs were stained with Hoechst 33258 (nucleus, *blue*), and an Alexa Fluor® 488-coupled anti-human-IgG goat IgG (trastuzumab, *green*): relative Alexa Fluor® 488 signal intensity (mean ± SD [standard deviation]) normalised to baseline (A, $n = 3$), and representative cross-sections of the cell-layer (B).

Washing the cells with buffer alone or with buffer containing a lower concentration of trastuzumab reduced the signal (*figure 2.1D&E*). Comparable results were obtained when varying the duration of the initial incubation with trastuzumab, or when exposing and washing under flow or statical conditions (data not shown).

As trastuzumab was recently demonstrated to interact with heparan sulphate proteoglycans,[5] a major component of the extracellular glycocalyx, their role in the binding of trastuzumab was investigated by pretreating the HUVECs with heparanase (HPSE). No difference was found compared to untreated cells (*figure 2.1D&E*). In addition, escalating concentrations of heparin, which binds competitively to heparan sulphate proteoglycans, did not interfere with the binding of trastuzumab (data not shown).

Bevacizumab was observed to bind to the luminal surface as well, though the pattern differed (*figure 2.1B*). Whereas binding of trastuzumab was characterised by diffuse surface staining with dispersed

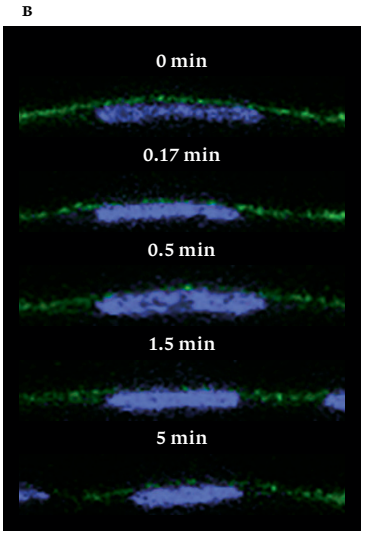

FIGURE 2.2

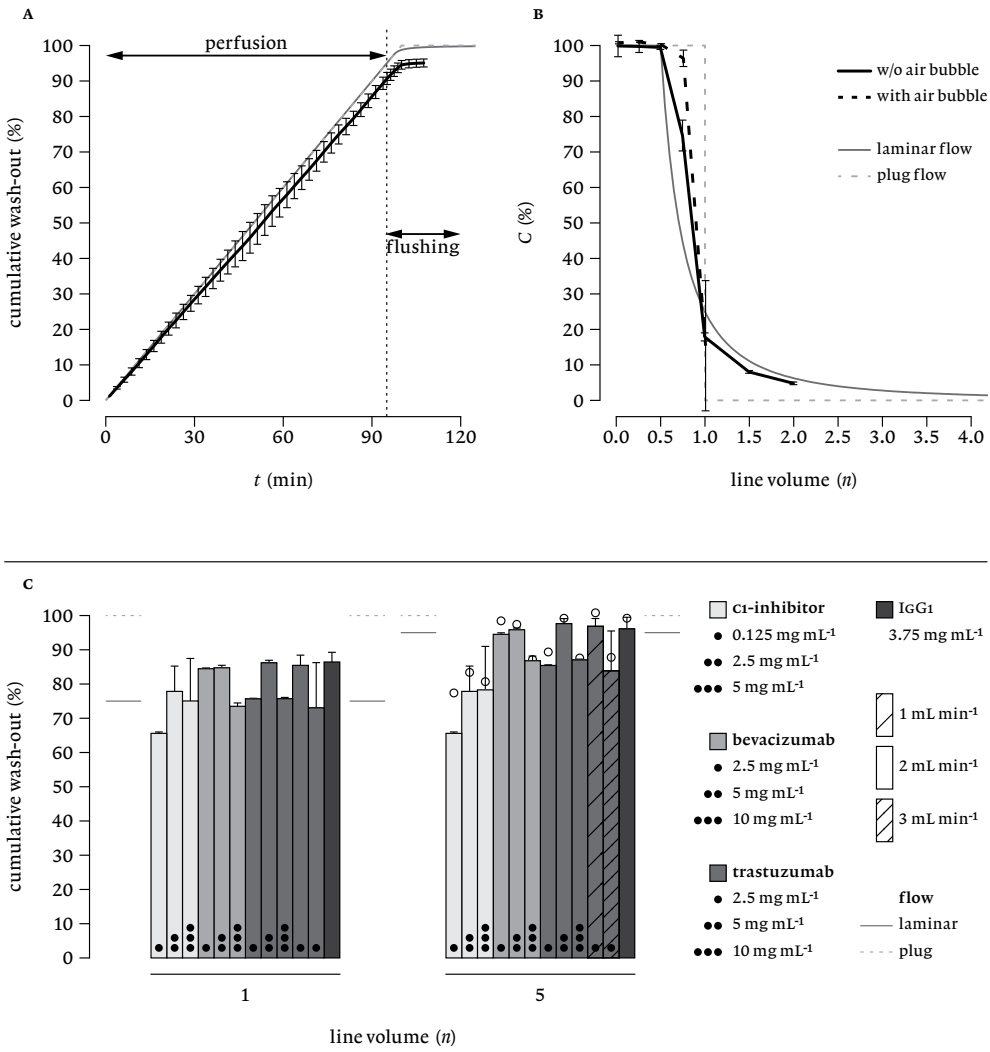

FIGURE 2.3 Infusion profiles

Infusion lines were perfused with a biopharmaceutical ('infusate') for 95 min at 2 mL/min followed by flushing of the line with 0.9% NaCl at the same rate until the protein concentration dropped <LLOQ (0.04 g/L) (A). Alternatively, the infusion line was filled with a biopharmaceutical and flushed immediately (B&C).

Concentration profiles (mean ± SD [standard deviation]) are displayed for the experimental IgG1 (3.75 mg/mL), with or without introducing an air bubble between the infusate and the flushing solution (B). Mean ± SD cumulative wash-out for different biopharmaceuticals at different concentrations and at different perfusion rates (C). The circles in C represent the theoretical cumulative wash-out if it is assumed that the samples with a concentration <LLOQ contained a dose of [sample volume]×[0.0394 g/L].

Data are normalised to either the concentration of the infusate or the maximum theoretical wash-out, which equals the total dose added to the system. Results of duplicate experiments are set against the expected wash-out profile assuming laminar or plug flow through the infusion line. The line volume (*n*) is the number of line volumes (10.0 mL) passing through the IV line during the experiment.

clusters of greater signal intensity in varying degrees, exposure to bevacizumab resulted in intense clusters scattered along the surface.

Locating C1-inhibitor after incubation proved extremely difficult, as the antibody used for staining resulted in a non-specific signal on the entire cell-layer. Hence, the question whether C1-inhibitor adsorbs to endothelium in a similar fashion as the tested MABs could not be answered.

Dynamical experiments

After perfusion of the artificial vessel with 2 mg/mL trastuzumab for 5 min, the system was flushed with buffer solution. Imaging of the cells during flushing revealed a decline in apically bound trastuzumab (*figure 2.2A&B*). After 5 min of flushing (equalling 5 complete flushes), the luminal signal had decreased to approximately 50%.

Infusion profile

Replication of infusion procedures indicated an average recovery of approximately 95% of the anticipated dose at the end of perfusion (similar to the EOI), as well as after flushing the IV line five times (*figure 2.3A*). During the flushing of the IV lines, the wash-out time-course resembled the theoretical profile of laminar flow. The wash-out profiles for bevacizumab, trastuzumab, the experimental IgG1, and C1-inhibitor were similar in shape. Introducing an air bubble between the infusate and the flushing solution to prevent diffusion changed the wash-out profile in the direction of plug flow, with no measurable concentration after the IV line was flushed once (*figure 2.3B*). Flushing the line for longer periods of time did not increase the cumulative wash-out; in all cases, the concentration had dropped <LLOQ (0.04 g/L) after 4 line volumes had been extruded.

A reduced recovery was also observed when prefilled IV lines were flushed immediately, without the 'perfusion' part of the experiment. Interestingly, this reduction did not always occur. The cumulative wash-out ranged roughly between 70 and 85% after five flushes, in cases where a reduced outflow was seen, as opposed to the theoretical 95–100%, even when the potential wash-out in samples with a concentration <LLOQ was taken into account (*figure 2.3C*). There was no apparent relationship between the cumulative wash-out and the tested drug product. Varying the concentration of the infusate or the perfusion rate had no effect on the results. From *figure 2.3C*, it may be suggested that a higher concentration or a higher perfusion rate results in a decreased cumulative wash-out. However, such a relationship was not invariably present to allow definite conclusions to be drawn.

DISCUSSION

THE INITIAL EXPERIMENTS WITH THE artificial vessel demonstrated that bevacizumab and trastuzumab adsorb to the luminal surface of endothelial cells, though the observed pattern differed, with diffuse staining for trastuzumab and a clustered appearance for bevacizumab. Neither the binding nor the difference could be related to the respective targets of these MABs. Trastuzumab targets a membrane receptor (HER2), whereas bevacizumab neutralises a circulating growth factor (VEGF).[6,7] HUVECs contain VEGF-receptors, but these are not distinctly clustered on the cell surface, and – importantly – bevacizumab inhibits receptor engagement by VEGF.[8,9] Moreover, clustering was also observed for trastuzumab, albeit to a lesser extent.

Although detailed sorption studies were beyond the scope of our investigation, the binding seemed to be concentration-dependent and easily reversible upon washing with a lower concentration, which suggests that the two biopharmaceuticals were not tightly bound, *e.g.* to a receptor. The binding of MABs to the extracellular matrix, where the endothelial barrier had been disrupted, further supports the idea of non-specific binding. In contrast, the finding that the apically located MAB could not be completely washed off (*figure 2.2B*) suggests a tighter form of binding, as does the observation that perfusing the artificial vessel with 2 mg/mL followed by 0.2 mg/mL resulted in a higher signal compared to perfusion with 0.2 mg/mL only (*figure 2.1D*).

Regardless of the exact nature of the binding, the conclusion that biopharmaceuticals can adsorb to endothelium should not be surprising, as systematic reports on the binding of all kinds of proteins to cell membranes and components of the extracellular matrix date from the 1960s.[10,11] For example, binding of MABs to extracellular components cause them to be retained upon subcutaneous administration, glycosaminoglycans help regulate local levels of growth hormones and other signalling factors, and

the cellular glycocalyx was found to be a key component for certain protein-cell interactions.[12–14]

Electrostatic forces play an important role in the adsorption of proteins. Many contact surfaces in the body are negatively charged, including cell membranes and polysaccharides. In contrast, most MABs are basic and hence cationic at physiological pH.[15] What is interesting, however, is that one of the natural properties of the glycocalyx is preventing non-specific (protein) adsorption.[16] Biocompatibility research has elucidated some of the principal aspects underlying the interference caused by oligosaccharide (glycocalyx-like) polymers in the adsorption of proteins to negatively charged surfaces. This shows that the flexible hydrophilic chains offer steric hindrance preventing binding of proteins.[17,18] Such coatings greatly reduce but do not completely prevent adsorption.[19,20]

Thus, the local fraction of adsorbed protein is probably small in absolute terms, but with a total endothelium area of 4,000–7,000 m^2 in an adult,[21] even minor (local) adsorption to vessel walls can notably affect plasma concentration.

Our findings lend support to the hypothesis of endothelial adsorption. *Figure 2.4* displays (simplistically) how endothelial adsorption can cause a delay in t_{max}. Because of adsorption to the endothelium, the vascular compartment should not be regarded as a well-mixed container. Rather, a gradient exists between areas of high concentration, *e.g.* the tip of the IV cannula during administration, and areas of low concentration. Upon completion of infusion, the gradient gradually levels off and adsorbed drug product is released in areas where local concentration had previously been high. This increases the measured concentration at the sampling site (*figure 2.4D*).

Differences in perfusion between tissues may further delay the equilibration over the vascular compartment. Perhaps, the prerequisites for the phenomenon to occur are that the biopharmaceutical is administered continuously over a longer period of time (*e.g.* as a linear infusion) and that its plasma clearance is relatively slow. This would theoretically allow the build-up of a gradient, especially in lesser perfused tissues.

Staining of C1-inhibitor was unsuccessful, and therefore, adsorption to endothelium could not be ascertained. However, from a theoretical viewpoint, given the generical nature of protein-surface interactions, C1-inhibitor and the other proteins listed in *table 2.1* probably behave similarly to the tested MABs.

It should be noted, however, that our artificial vein is only an approximation of the *in vivo* situation and does not preclude other mechanisms to contribute to the delay in t_{max}. The human vascular compartment consists of many parallel microcirculations, each with specialised (endothelial) cells, which adds to the complexity of understanding and (pharmacokinetically) modelling the distribution of biopharmaceuticals. Moreover, the plasma concentration profiles over time of biopharmaceuticals also show increases *after* the (delayed) t_{max}.[22] Therefore, simple adsorption of biopharmaceuticals to endothelium may only be one of many factors involved in determining plasma concentration. We imagine that an experiment with radio-labelled therapeutical proteins in test animals can be useful to study the distribution over the body during and after intravenous infusion, and to validate our findings.

The complexity of the human vasculature is in contrast to the highly controlled experimental conditions of constant laminar flow, temperature, and the use of a single type of endothelial cells (HUVECs) in combination with a particular buffer that contained BSA. The effect of any of these covariates on the results was not studied.

With the exception of the relevance of the presented data to the clinical pharmacologist for determining and interpreting the pharmacokinetic profile of biopharmaceuticals, the clinical relevance is more speculative. This would depend on the exact adsorption site, the tissue where the biopharmaceutical accumulates, and whether it is pharmacologically active there. In addition, the relevance is determined by whether a biopharmaceutical exerts an effect on the endothelium or whether the adsorption to endothelium interferes with a physiological process.

From the wash-out profiles (*figure 2.3*), it is seen that the bulk delivery of drug through the IV line is governed by convection alone, *i.e.* transport by the flow of the medium, in this case laminar flow.[23] There may be a blunting effect on the net delivery caused by diffusion of the drug from the infusate (high concentration) into the flushing solution (low concentration), although with an estimated maximum diffusion coefficient derived from the Stokes-Einstein equation[24] of 7 10^{-5} mm^2 s^{-1} for a 105 kDa protein (C1-inhibitor) in water at room temperature,[25] this effect is negligible compared to the effective fluid velocity of 2.4–7.1 mm/s in the IV line.

Recovery of biopharmaceuticals from the IV line could be incomplete, measuring up to 15% in the experiments where the prefilled lines were only flushed, which was unrelated to the biopharmaceutical tested. The only factor that seemingly influenced the net delivery was concentration, with higher concentrations increasing the likelihood of incomplete recovery.

Adsorption to IV materials is a well-recognised problem for certain drugs.[26,27] Given existing evidence on biocompatibility, adsorption to the IV line can also explain our observations. An argument against adsorption as the cause is that the reduced recovery was not observed in all experiments (*figure 2.3C*). Aggregation of the biopharmaceutical within the IV line is another possibility, although the used method to determine drug concentration in the wash-out also detects drug (protein) aggregates and the drop in protein concentration, therefore, cannot be the result of aggregation.

If the line is flushed following perfusion, drug administration continues after the theoretical EOI for a short time as a result of laminar flow (*figure 2.3*). However, this only partly explains the 'delay' in t_{max}, as the fraction of the total dose infused during flushing is very small (*figure 2.3A*). Furthermore, increases in plasma concentration after EOI have also been observed when the line was not flushed, for example with the experimental IgG1 (data on file). Wash-out of any adsorbed or otherwise retained biopharmaceutical material in the IV line during prolonged flushing did not occur. Thus, flushing of the infusion lines cannot contribute to a delay in t_{max}.

Concluding, biopharmaceuticals can adsorb to endothelium and be subsequently released into the circulation, which may explain the observation that t_{max} occurs long after completion of an intravenous administration. Flushing of the infusion lines to complete administration of a biopharmaceutical does not seem to contribute to the delay in t_{max}.

A–D

FIGURE 2.4 Pharmacokinetic profile

Schematic representation of the gradient of biopharmaceuticals over the vascular tree during intravenous administration as a result of endothelial adsorption (A). For illustrational purposes, extravascular distribution and elimination are set to nil. The relative endothelial surface area exposed to the biopharmaceutical in the considered body compartments is indicated by the number of capillary beds. After completion of administration, the gradient slowly dissipates and the relative peak concentration moves along the vasculature to ultimately reach the sampling site (B).
In the traditional model, the maximum plasma concentration (C_{max}) coincides with the end of infusion (EOI) (C).
In D, the vascular tree is conceptualised as a single long vessel and the local situation is depicted at three distinct moments in time. During intravenous infusion, the local plasma concentration is high at the administration side of the vessel, favouring adsorption to the vessel wall, thereby reducing the distal plasma concentration (D1). After EOI, the high local concentration at the administration side drops sharply as a result of recirculation of the relatively low concentration from the sampling side of the vessel. This shifts the balance from adsorption to desorption (D2). As the biopharmaceutical is released from the vessel wall, the downstream concentration continues to rise and the relative peak concentration, where adsorption is in equilibrium with desorption, gradually moves alongside the vessel (D2&D3). Behind this equilibrium, desorption predominates and ahead adsorption, until finally the gradient has levelled off.

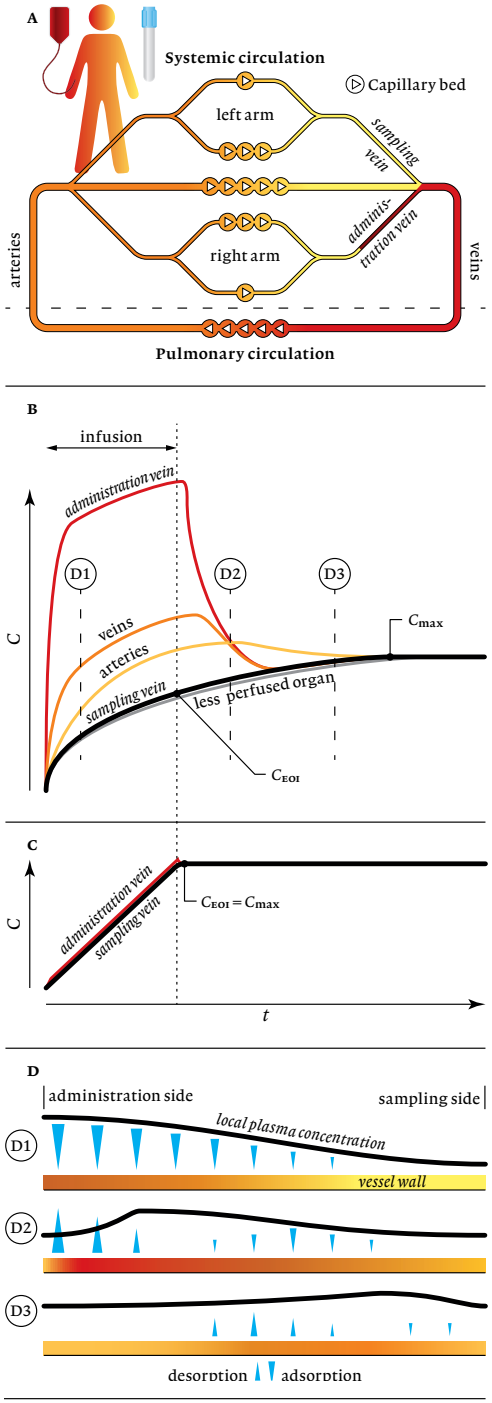

REFERENCES

1 Wang W. Protein aggregation and its inhibition in biopharmaceutics. *Int J Pharm* 2005; **289**: 1-30.
2 Wang W, Nema S, Teagarden D. Protein aggregation-pathways and influencing factors. *Int J Pharm* 2010; **390**: 89-99.
3 Lowe D, Dudgeon K, Rouet R, Schofield P, Jermutus L, Christ D. Aggregation, stability, and formulation of human antibody therapeutics. *Adv Protein Chem Struct Biol* 2011; **84**: 41-61.
4 Wang W, Wang EQ, Balthasar JP. Monoclonal antibody pharmacokinetics and pharmacodynamics. *Clin Pharmacol Ther* 2008; **84**: 548-58.
5 Suarez E, Paredes-Gamero E, Del Giglio A, Dos Santos Tersariol IL, Nader H, Pinhal MA. Heparan sulfate mediates trastuzumab effect in breast cancer cells. *BMC Cancer* 2013; **13**: 444.
6 Burgess AW, Cho HS, Eigenbrot C, *et al*. An open-and-shut case? Recent insights into the activation of EGF/ERBB receptors. *Mol Cell* 2003; **12**: 541-52.
7 Chen HX, Gore-Langton RE, Cheson BD. Clinical trials referral resource: current clinical trials of the anti-VEGF monoclonal antibody bevacizumab. *Oncology (Williston Park)* 2001; **15**: 1017, 1020, 1023-6.
8 Ilan N, Tucker A, Madri JA. Vascular endothelial growth factor expression, beta-catenin tyrosine phosphorylation, and endothelial proliferative behavior: a pathway for transformation? *Lab Invest* 2003; **83**: 1105-15.
9 Kim KJ, Li B, Houck K, Winer J, Ferrara N. The vascular endothelial growth factor proteins: identification of bio-

logically relevant regions by neutralizing monoclonal antibodies. *Growth factors* 1992; **7**: 53-64.
10 Ryser H, Aub JC, Caulfield JB. Studies on protein uptake by isolated tumor cells. II. Quantitative data on the adsorption and uptake of I-131-serum albumin by Ehrlich ascites tumor cells. *J Cell Biol* 1962; **15**: 437-49.
11 Curtis ASG. Cell adhesion. *Prog Biophys Mol Biol* 1973; **27**: 315-84.
12 Mach H, Gregory SM, Mackiewicz A, *et al*. Electrostatic interactions of monoclonal antibodies with subcutaneous tissue. *Ther Deliv* 2011; **2**: 727-36.
13 Häcker U, Nybakken K, Perrimon N. Heparan sulphate proteoglycans: the sweet side of development. *Nat Rev Mol Cell Biol* 2005; **6**: 530-41.
14 Reitsma S, Slaaf DW, Vink H, Van Zandvoort MAMJ, Oude Egbrink MGA. The endothelial glycocalyx: composition, functions, and visualization. *Pflügers Arch - Eur J Physiol* 2007; **454**: 345-59.
15 Boswell CA, Tesar DB, Mukhyala K, Theil FP, Fielder PJ, Khawli LA. Effects of charge on antibody tissue distribution and pharmacokinetics. *Bioconjug Chem* 2010; **21**: 2153-63.
16 Bell GI, Dembo M, Bongrand P. Cell adhesion. Competition between nonspecific repulsion and specific bonding. *Biophys J* 1984; **45**: 1051-64.
17 Torchilin VP, Trubetskoy VS. Which polymers can make nanoparticulate drug carriers long-circulating? *Adv Drug Deliv Rev* 1995; **16**: 141-55.
18 Satulovsky J, Carignano MA, Szleifer I. Kinetic and thermodynamic control of protein adsorption. *Proc Natl Acad Sci U S A* 2000; **97**: 9037-41.
19 Österberg E, Bergström K, Holmberg K, *et al*. Protein-rejecting ability of surface-bound dextran in end-on and side-on configurations: comparison to PEG. *J Biomed Mater Res* 1995; **29**: 741-7.
20 Holland NB, Qiu Y, Ruegsegger M, Marchant RE. Biomimetic engineering of non-adhesive glycocalyx-like surfaces using oligosaccharide surfactant polymers. *Nature* 1998; **392**: 799-801.
21 Aird WC. Spatial and temporal dynamics of the endothelium. *J Thromb Haemost* 2005; **3**: 1392-406.
22 Reijers JAA, Moerland M, Burggraaf J. Remarkable pharmacokinetics of monoclonal antibodies: a quest for an explanation. *Clin Pharmacokinet* 2017; **56**: 1081-9 (*chapter 3*).
23 Leonard EF, Grabowski EF, Turitto VT. The role of convection and diffusion on platelet adhesion and aggregation. *Ann N Y Acad Sci* 1972; **201**: 329-42.
24 Einstein A. Über die von der molekularkinetischen Theorie der Wärme geforderte Bewegung von in ruhenden Flüssigkeiten suspendierten Teilchen. *Ann Phys* 1905; **17**: 549-60.
25 Erickson HP. Size and shape of protein molecules at the nanometer level determined by sedimentation, gel filtration, and electron microscopy. *Biol Proced Online* 2009; **11**: 32-51.
26 Schildt B, Ahlgren T, Berghem L, Wendt Y. Adsorption of insulin by infusion materials. *Acta Anaesthesiol Scand* 1978; **22**: 556-62.
27 Smith JC, Davies MC, Melia CD, Denyer SP, Derrick MR. Uptake of drugs by catheters: the influence of the drug molecule on sorption by polyurethane catheters. *Biomaterials* 1996; **17**: 1469-72.
28 Stocks JM, Brantly M, Barker A, *et al*. Comparable pharmacokinetic properties of two alpha1-proteinase inhibitors after single therapeutic doses. *CHEST J* 2005; **128**: 2615.
29 Martinez-Saguer I, Rusicke E, Aygören-Pürsün E, Von Hentig N, Klingebiel T, Kreuz W. Pharmacokinetic analysis of human plasma-derived pasteurized C1-inhibitor concentrate in adults and children with hereditary angioedema: a prospective study. *Transfusion* 2010; **50**: 354-60.
30 Cocchio C, Marzella N. Cinryze, a human plasma-derived C1 esterase inhibitor for prophylaxis of hereditary angioedema. *P T* 2009; **34**: 293-328.
31 Doi T, Muro K, Yoshino T, *et al*. Phase 1 pharmacokinetic study of MK-0646 (dalotuzumab), an anti-insulin-like growth factor-1 receptor monoclonal antibody, in combination with cetuximab and irinotecan in Japanese patients with advanced colorectal cancer. *Cancer Chemother Pharmacol* 2013; **72**: 643-52.
32 Tabernero J, Ciardiello F, Rivera F, *et al*. Cetuximab administered once every second week to patients with metastatic colorectal cancer: a two-part pharmacokinetic/pharmacodynamic phase I dose-escalation study. *Ann Oncol* 2010; **21**: 1537-45.
33 Phillips M, Smith W, Balan G, Ward S. Pharmacokinetics of glucarpidase in subjects with normal and impaired renal function. *J Clin Pharmacol* 2008; **48**: 279-84.
34 Patnaik A, Kang SP, Rasco D, *et al*. Phase I study of pembrolizumab (MK-3475; anti-PD-1 monoclonal antibody) in patients with advanced solid tumors. *Clin cancer Res* 2015; **21**: 4286-93.
35 De Bono JS, Attard G, Bellmunt J, *et al*. Open-label phase II study evaluating the efficacy and safety of two doses of pertuzumab in castrate chemotherapy-naive patients with hormone-refractory prostate cancer. *J Clin Oncol* 2007; **25**: 257-62.
36 Felip E, Ranson M, Cedrés S, *et al*. A phase Ib, dose-finding study of erlotinib in combination with a fixed dose of pertuzumab in patients with advanced non-small-cell lung cancer. *Clin Lung Cancer* 2012; **13**: 432-41.
37 Albanell J, Montagut C, Jones ET, *et al*. A phase I study of the safety and pharmacokinetics of the combination of pertuzumab (RHUMAB 2C4) and capecitabine in patients with advanced solid tumors. *Clin Cancer Res* 2008; **14**: 2726-31.
38 Yoshino T, Yamazaki K, Gotoh M, *et al*. Safety and pharmacokinetics of second-line ramucirumab plus FOLFIRI in Japanese patients with metastatic colorectal carcinoma. *Anticancer Res* 2015; **35**: 4003-7.
39 Leyland-Jones B, Gelmon K, Ayoub JP, *et al*. Pharmacokinetics, safety, and efficacy of trastuzumab administered every three weeks in combination with paclitaxel. *J Clin Oncol* 2003; **21**: 3965-71.
40 Baselga J, Carbonell X, Castañeda-Soto N-J, et al. Phase II study of efficacy, safety, and pharmacokinetics of trastuzumab monotherapy administered on a 3-weekly schedule. *J Clin Oncol* 2005; **23**: 2162-71.
41 Wynne C, Harvey V, Schwabe C, Waaka D, McIntyre C, Bittner B. Comparison of subcutaneous and intravenous administration of trastuzumab: a phase I/Ib trial in healthy male volunteers and patients with HER2-positive breast cancer. *J Clin Pharmacol* 2013; **53**: 192-201.
42 Wisman LAB, De Cock EPM, Reijers JAA, et al. A phase I dose-escalation and bioequivalence study of a trastuzumab biosimilar in healthy male volunteers. *Clin Drug Investig* 2014; **34**: 887-94.

CHAPTER III

Remarkable pharmacokinetics of monoclonal antibodies: a quest for an explanation

J.A.A. Reijers, M. Moerland, J. Burggraaf

Monoclonal antibodies (MABs) usually display slow and limited distribution with combined linear and non-linear elimination mechanisms. While studying *individual* pharmacokinetic profiles, it was noticed that MAB plasma concentration can vary abruptly over time, with one or more increases after the time to maximum concentration, when theoretically the concentration should only decline. This chapter summarises the frequency of these additional peaks, and assesses whether normal intra-subject variability and assay variability can explain the observations. For this analysis, a benchmark was used which consisted of three registered (adalimumab, bevacizumab, and trastuzumab) and three unregistered IgG1 MABs.

At a selected 'normal' intra-subject variability of 12%, at least 70% of the study participants (approximately 90% for certain MABs) still had at least one additional peak, which decreased when the 'normal' variability was increased. There was no difference in occurrence between the high and low concentration ranges. Only high sample density seemed to be associated with increased likelihood of detecting additional peaks. Based on the analytical variability for the applied ligand-binding assays (5–10%, up to 15% at the lower limit of quantification), the number of observed increases was extremely improbable ($p < 0.01$) for most MABs, especially for the large excursions.

Therefore, the fluctuations are likely genuine. Possible explanations and the relevance for clinical practice are discussed.

Monoclonal antibodies (MABs) are widely used to treat diseases in almost all fields of medicine. They display highly similar pharmacokinetics with a relatively small volume of distribution and a long half-life. Many of the mechanisms responsible for these properties have been extensively studied and are excellently reviewed elsewhere.[1–5]

At Centre for Human Drug Disease (CHDR), multiple clinical trials with MABs are performed annually. When studying their pharmacokinetics, it was noticed that the plasma concentration of MABs in *individuals* can follow a remarkable, or even bizarre, time-course, characterised by (large) excursions (*figure 3.1*), which seems to be in disagreement with current understanding of drug distribution and/or elimination.

Initially, these findings were disregarded as normal intra-subject and assay variability, also because the mean (group) pharmacokinetic profile usually follows a predictable time-course of slow distribution combined with both linear and non-linear elimination. However, after observing fluctuating individual plasma concentrations for an increasing

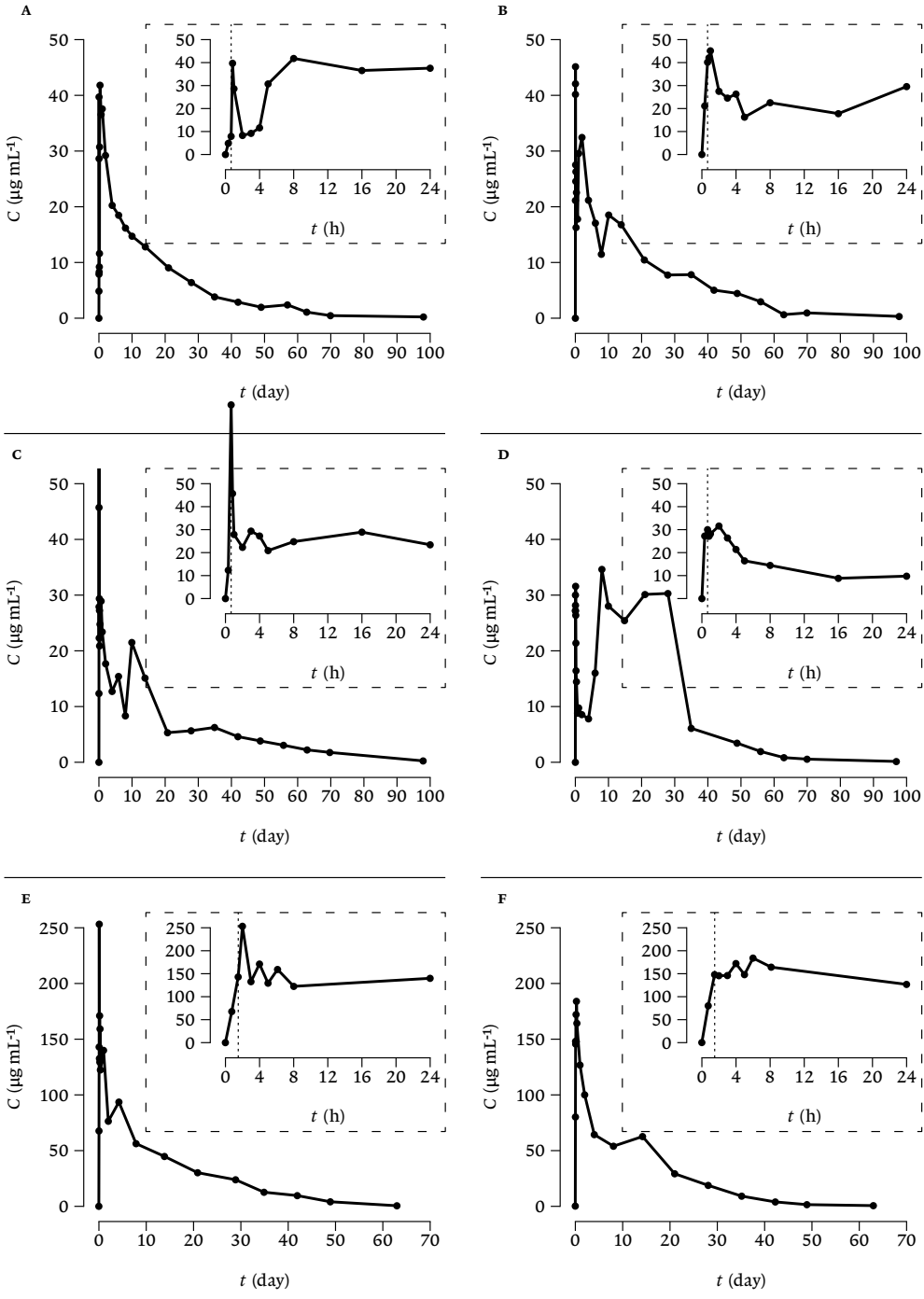
A
B
C
D
E
F
C (µg mL-1)
t (day)
t (h)

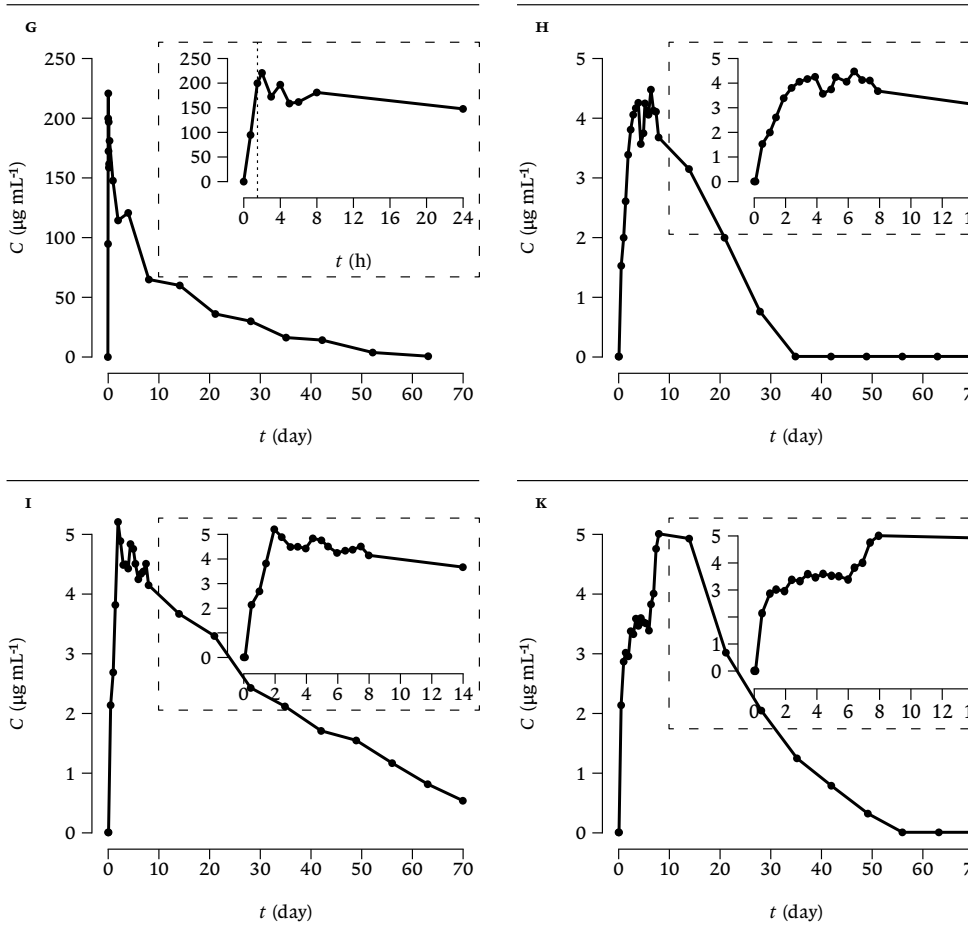

FIGURE 3.1 Individual pharmacokinetic profiles

Representative patterns in individual plasma drug concentrations over time for registered monoclonal antibodies: 2 mg/kg intravenous bevacizumab (A–D), 6 mg/kg intravenous trastuzumab (E–G), 40 mg subcutaneous adalimumab (H–K). The insets depict an enlarged section of the first part of the profile. The dashed lines mark the end of intravenous administration.

TABLE 3.1 Additional peak concentrations after intravenous administration

MAB / PERIOD	VARIABILITY											
	4%		8%		12%		16%		24%		50%	
Dose ≤3 mg/kg												
Bevacizumab ($n=90$)												
Total	88	(97.8%)	87	(96.7%)	83	(92.2%)	72	(80.0%)	65	(72.2%)	41	(45.6%)
<24 h	82	(91.1%)	79	(87.8%)	68	(75.6%)	54	(60.0%)	46	(51.1%)	25	(27.8%)
≥24 h	73	(81.1%)	70	(77.8%)	66	(73.3%)	61	(67.8%)	56	(62.2%)	30	(33.3%)
A ($n=18$)												
Total	18	(100%)	17	(94.4%)	16	(88.9%)	16	(88.9%)	12	(66.7%)	1	(5.6%)
<24 h	18	(100%)	17	(94.4%)	16	(88.9%)	16	(88.9%)	12	(66.7%)	1	(5.6%)
≥24 h	4	(22.2%)	4	(22.2%)	4	(22.2%)	4	(22.2%)	4	(22.2%)	0	
B ($n=33$)												
Total	12	(36.4%)	12	(36.4%)	7	(21.2%)	5	(15.2%)	3	(9.1%)	1	(3.0%)
<24 h	8	(24.2%)	8	(24.2%)	4	(12.1%)	2	(6.1%)	1	(3.0%)	0	
≥24 h	4	(12.1%)	4	(12.1%)	3	(9.1%)	3	(9.1%)	2	(6.1%)	1	(3.0%)
Dose >3 mg/kg												
Trastuzumab ($n=46$)												
Total	46	(100%)	44	(95.7%)	42	(91.3%)	37	(80.4%)	28	(60.9%)	8	(17.4%)
<24 h	45	(97.8%)	42	(91.3%)	39	(84.8%)	33	(71.7%)	22	(47.8%)	3	(6.5%)
≥24 h	21	(45.7%)	21	(45.7%)	20	(43.5%)	20	(43.5%)	16	(34.8%)	5	(10.9%)
C ($n=7$)												
Total	3	(42.9%)	3	(42.9%)	2	(28.6%)	1	(14.3%)	0		0	
<24 h	2	(28.6%)	2	(28.6%)	2	(28.6%)	1	(14.3%)	0		0	
≥24 h	1	(14.3%)	1	(14.3%)	0		0		0		0	

Number (percentage) of subjects with at least one peak concentration other than the maximum concentration (C_{max}) beyond 'normal' intra-subject variability, for which values between 4 and 50% were chosen. Values are displayed per monoclonal antibody (MAB). A separation is made between peaks occurring within the first 24 h from administration and thereafter. A, B, and C are unregistered IgG1 antibodies.

number of MABs, it was considered worthwhile to analyse individual profiles systematically, with the objective to determine whether the fluctuations are genuine. A benchmark was used to assess whether the result could indeed be explained by normal intra-subject and assay variability, or that other factors might be involved.

METHODS

Pharmacokinetic data were taken from clinical trials with MABs in healthy volunteers. Three registered MABs (adalimumab [Humira®], bevacizumab [Avastin®], and trastuzumab [Herceptin®]) were analysed, as well as three unregistered products (denoted A, B, and C). All drugs were IgG1 antibodies and were administered as a single intravenous dose, except for adalimumab, which was administered subcutaneously. The trial participants were healthy subjects, mainly males aged 18–50 years, but some trials included up to 50% females.

All trial procedures were performed in accordance with the different trial protocols. Samples were collected and handled following standard operating procedures. Within each clinical trial, MAB plasma concentration was determined in a single external laboratory, in a single analytical run per participant, using validated methods. Product C was quantitated in batches of samples across multiple subjects, resulting in more than one analytical run per participant.

To determine whether intra-subject variability for MAB plasma concentration would be related to, for example, changes in circulating plasma volume, the time-course of albumin plasma concentration and

erythrocyte counts were studied. As albumin and erythrocytes are produced at a relatively constant rate, and under normal circumstances do not leave the intravascular compartment, these analytes were considered suitable benchmarks.

Samples for albumin concentration and erythrocyte count were always collected concurrently with samples for MAB concentration, albeit at a lesser frequency. On the administration day, albumin and erythrocytes were quantitated 1–5 times, depending on the trial protocol. Thereafter, the ratio of the number of these samples to the number of pharmacokinetic samples ranged between 0.5 and 1. The mean of the individual coefficients of variation (CVs) of albumin concentration per clinical trial ($70 < n < 200$) varied between 3.6 and 4.4% with standard deviations (SDs) of 1.2–1.2 %-point. For erythrocyte count, the mean ranged between 2.7 and 3.7% and the SDs 0.75–1.2 %-point, irrespective if only samples collected on the same day (hours apart) or during the full length of the trial (days to weeks apart) were included in the calculation.

Hence, it appeared that a conservative reference CV (CV_r) of 4% for normal intra-subject variability (CV_i) was justified. It was subsequently investigated whether the observed fluctuations in MAB plasma concentration exceeded 1, 2, or 3 CVs_r, indicating increasing unlikeliness a change in the profile could be explained by 'normal (physiological) variability'. Additionally, we considered a less conservative CV_r of 8%, covering approximately two CVs of the observed variability for albumin and erythrocytes, and a very extreme variability of 50%. By applying this strategy to pharmacokinetic data for different MABs, the number of relative maxima in the concentration-time profile (other than the absolute maximum concentration, C_{max}) that could not be ascribed to the chosen intra-subject variability was counted.

Excursions beyond normal intra-subject variability were identified based on a deviation in the exponential growth constant (λ) outside the margins determined by 1–3 CVs_r (4, 8, and 12%) of the conservative variability estimate or of the less conservative CV_r (8, 16, and 24%). The margins for λ per observation were derived from the formula $A \pm CV_i = B \cdot e^{\lambda t}$, where A is the observed plasma concentration, CV_i the chosen intra-subject variability, B the plasma concentration of the previous sample, and t the difference in sample collection time between A and B. Next, the minimum number of unique λs was determined to describe the observations ($A \pm CV_i$) per individual. A deviation in λ beyond the chosen intra-subject variability was defined as the requirement of two or more unique λs to describe the rising leg of the plasma concentration curve before a relative (local) maximum was reached (see *figure 3S.1* for an example).

This approach assumes linear elimination kinetics, which is known not to be the case for MABs. However, the concentration-time profile of MABs usually approximates linearity at the observed (high) MAB plasma levels in healthy volunteers, where the non-linear elimination mechanism is saturated. Additionally, the non-linearity in elimination manifests as different *negative* λs, whereas the focus of this analysis was on deviations from the surrounding data points in the λ in the rising parts of the concentration profile. Therefore, this approach was considered fit for purpose.

A separation was made between peaks occurring within the first 24 h from intravenous administration – or 14 days from subcutaneous administration – and thereafter. Additionally, the results of the intravenously administered compounds were stratified based on dose.

To study the potential impact of assay variability, the total number of increases between relative

TABLE 3.2 Additional peak concentrations after subcutaneous administration

PERIOD	VARIABILITY					
	4%	8%	12%	16%	24%	50%
Total	128 (98.5%)	118 (90.8%)	90 (69.2%)	72 (55.4%)	54 (41.5%)	19 (14.6%)
<14 days	127 (97.7%)	116 (89.2%)	87 (66.9%)	70 (53.8%)	48 (36.9%)	15 (11.5%)
≥14 days	13 (10.0%)	13 (10.0%)	12 (9.2%)	11 (8.5%)	11 (8.5%)	8 (6.2%)

Number (percentage) of subjects with at least one peak concentration other than the maximum concentration (C_{max}) beyond 'normal' intra-subject variability after a single subcutaneous dose of 40 mg adalimumab ($n = 130$). Values for normal intra-subject variability were chosen between 4 and 50%. A separation is made between peaks occurring within the first 14 days from administration and thereafter.

TABLE 3.3 Probability of increases based on assay variability

MAB / FACTOR (k)		OBSERVED	CV_a 5%	10%	15%	20%	25%
Dose ⩽ 3 mg/kg							
Bevacizumab							
	1.12	228	$<10^{-93}$	$<10^{-5}$	0.86	1.00	1.00
	1.25	153	$<10^{-99}$	$<10^{-37}$	$<10^{-3}$	0.97	1.00
	1.5	78	$<10^{-99}$	$<10^{-99}$	$<10^{-20}$	0.01	0.99
	2	23	$<10^{-99}$	$<10^{-99}$	$<10^{-31}$	$<10^{-7}$	0.20
	3	8	$<10^{-99}$	$<10^{-97}$	$<10^{-37}$	$<10^{-16}$	$<10^{-6}$
	4	3	$<10^{-99}$	$<10^{-59}$	$<10^{-23}$	$<10^{-11}$	$<10^{-5}$
	5	2	$<10^{-99}$	$<10^{-53}$	$<10^{-22}$	$<10^{-11}$	$<10^{-5}$
A	1.12	34	$<10^{-18}$	$<10^{-3}$	0.10	0.39	0.62
	1.25	19	$<10^{-39}$	$<10^{-5}$	0.08	0.64	0.92
	1.5	10	$<10^{-70}$	$<10^{-14}$	$<10^{-3}$	0.16	0.73
	2	1	$<10^{-20}$	$<10^{-4}$	0.05	0.47	0.89
	3	0					
	4	0					
	5	0					
B	1.12	3	0.76	1.00	1.00	1.00	1.00
	1.25	1	0.06	0.99	1.00	1.00	1.00
	1.5	1	$<10^{-6}$	0.14	0.86	1.00	1.00
	2	1	$<10^{-20}$	$<10^{-4}$	0.04	0.38	0.82
	3	1	$<10^{-52}$	$<10^{-12}$	$<10^{-5}$	$<10^{-2}$	0.06
	4	0					
	5	0					
Dose > 3 mg/kg							
Trastuzumab							
	1.12	75	$<10^{-29}$	0.02	0.90	1.00	1.00
	1.25	26	$<10^{-43}$	0.01	1.00	1.00	1.00
	1.5	5	$<10^{-31}$	$<10^{-3}$	0.89	1.00	1.00
	2	1	$<10^{-19}$	$<10^{-3}$	0.14	0.85	1.00
	3	1	$<10^{-51}$	$<10^{-12}$	$<10^{-4}$	0.01	0.21
	4	1	$<10^{-82}$	$<10^{-19}$	$<10^{-8}$	$<10^{-3}$	$<10^{-2}$
	5	0					
C	1.12	3	0.07	0.76	0.94	0.97	0.99
	1.25	0					
	1.5	0					
	2	0					
	3	0					
	4	0					
	5	0					

Probability (p) of finding the observed number of increases ⩾ k in plasma concentration based on the assay's coefficient of variation (CV_a). Only increases after completion of intravenous administration are considered.

extremes ⩾ k in the individual plasma concentration-time profiles was compared to the expected number based on the CV of the used bioanalytical assays (CV_a). Here, k is a factor for which values were chosen as 1.12, 1.25, 1.5, 2, 3, 4, and 5, corresponding to increases between 12 and 400%. A one-tailed binomial test was performed to determine the probability (p) of finding at least the observed number of increases ⩾ k. Samples collected before or during infusion were excluded. This analysis could only be performed for intravenously administered MABs.

The expected number of increases ⩾ k between two consecutive extremes was calculated using the method by Reed *et al.*[6] This approach assumes that the plasma concentration between two samples remains constant, which results in an underestimation of the observed number of increases ⩾ k, as the plasma concentration theoretically declines after the completion of intravenous administration. Because the p-values of increases ⩾ k at any CV_a derived with the binomial tests are thereby overestimated, thus favouring the probability of increases being attributed to assay variability, this methodological shortcoming was accepted.

According to the regulatory guidelines for ligand-binding assays (the type usually applied when measuring MABs in plasma), the CV_a should not exceed 20%, except at the lower level of quantification (LLOQ), where it should not exceed 25%.[7,8] The actual CV_a for the bioanalyses applied in the clinical studies ranged between 5 and 10%, with higher levels (up to 15%) found at LLOQ. Therefore, p-values were obtained at different CVs_a from 5 to 25%.

Data analysis was performed with R (v2.15.2, R Foundation for Statistical Computing, Vienna, Austria, 2012).

RESULTS

Pharmacokinetic observations were available for 130 subjects receiving adalimumab (mean 26.1 observations per subject), 90 subjects receiving bevacizumab (mean 26.3), and 46 subjects receiving trastuzumab (mean 19.8). For products A, B, and C, data were available from respectively 18, 33, and 7 subjects, with a mean number of observations per subject of 18.9, 15.1, and

17.4, respectively. The samples collected during the first seven days after administration summed 16 for adalimumab, 15 for bevacizumab, 12 for trastuzumab, 12 for A, 10 for B, and 10 for C.

Tables 3.1 & 3.2 present the number of subjects with additional maxima beyond increasing CV_i. This shows that with a conservative CV_i of 4% virtually all subjects had an additional peak in their profile. Even if the variability considered normal is increased to 3 CV_r (12%), at least 70% of the study participants (approximately 90% for certain MABs) still had at least one additional peak, with the exception of products B and C. It should be noted, however, that for both products B and C, a sparse sampling scheme was used compared to the other MABs, with less than five samples collected during the first 24 h. This may have limited the chance to identify short-lasting concentration changes.

At a variability of 24%, 60–70% of the subjects who received bevacizumab, trastuzumab, or product A showed an unexplained additional relative maximum, a percentage which decreased further and became more dispersed among the MABs at a variability of 50%. For adalimumab, product B and C, the corresponding numbers were again lower, although the overall pattern observed with increasing intra-subject variability was similar for all investigated MABs. Even when considering an intra-subject variability of 24 or 50% as normal, which is well beyond the variability (CV_r) observed for albumin and erythrocytes, additional peaks remained.

The probability of finding a number of increases with a certain magnitude in plasma concentration rose with increasing assay variability (*table 3.3*). Conversely, the probability was lower for larger excursions. Within the actual CV range for the used ligand-binding assays (5–10%), the number of observed increases was extremely improbable based on assay variability, except for product C. Even at higher CVs_a, which are only accepted at LLOQ (up to 15% for the used assays), assay variability must be considered unlikely in causing the observed increases, especially for those with a large amplitude.

A relationship between standard demographical parameters (age, [lean] body weight, BMI) and the number or magnitude of additional peaks could not be detected, although it should be noted that, as a result of the trial protocols, the populations were highly homogeneous with regard to these parameters. Also, across the different trails, demographical variability was limited.

DISCUSSION

IN THIS CHAPTER, IT IS REPORTED THAT MABs may show unexpected and remarkable pharmacokinetic behaviour, with increases in plasma concentration at the time the compound is cleared. These increases, which are occasionally substantial and long-lasting, appear to be not explained by taking into account physiological or assay variability. There was no difference in occurrence between the high and low concentration ranges. Only high sample density seemed to be associated with an increased likelihood of detecting additional peaks.

When observing fluctuations – especially increases – in the concentration of a drug over time, that theoretically should decline steadily, there are a few explanations to consider. First, pre-analytical errors should be ruled out, such as not disconnecting and removing the infusion material upon stop of intravenous administration, sample switching, applying incorrect dilutions, or calculation errors, *etc.* Subsequently, the assay performance should be considered critically, including, among others, assay precision, within and between-run variability, limit of quantification, and effects of freeze-thaw cycles.

For multiple reasons, assay variability or interference was considered unlikely to explain our observations. First, a vast number of additional peaks was counted (*table 3.3*). Also, the finding that comparable fluctuations were observed for all investigated MABs, in each assay, both in the low and high concentration ranges, and at any moment in time after administration (*figure 3.1*) argues against an assay-related explanation. Furthermore, the data points before or after the peak often confirmed the relatively high concentration, or suggested a steady increase toward the maximum, respectively a decrease following the maximum. These observations are generally not compatible with the randomness one expects to arise from assay variability.

Another explanation to consider is physiological variability, as – for instance – changes in volume status over time may alter the concentration of the MAB in plasma, while the absolute quantity in the body remains unchanged. Fluid shifts were recently postulated by Van Iersel *et al.*[9] as the underlying mechanism for the postural changes in MAB concentration that they had observed. Similar day-to-day variability was seen in our study with adalimumab.

In that clinical trial, pharmacokinetic samples were collected 12 hours apart during the first week (*figure 3.1H–K*). Seemingly, the evening concentrations (0.5, 1.5, 2.5, ... days after administration) were higher than the morning concentrations (1, 2, 3, ... days after administration), with a mean difference of 13.3% (SD 10.5) per participant. It should be noted, however, that for the main part of the adalimumab trial, the participants were ambulatory, and travelled both in the morning and evening to the clinical unit, making postural changes unlikely.

Additionally, the magnitude of many of the remaining fluctuations in plasma concentration for the investigated MABs (*figure 3.1*) exceeded by far the reported increases by Van Iersel *et al.*[9] and what would be physiologically achievable as a result of contraction of the plasma volume. Furthermore, concurrent changes of equal magnitude in intravascularly distributed endogenous substances with a relatively constant production, such as albumin and erythrocytes, was not seen, which is not in keeping with the fluid shift hypothesis. In conclusion, we argue that the majority of the observed fluctuations in the profiles cannot be explained by physiological variability or assay variability and should be considered genuine.

Now that we have demonstrated that the observed fluctuations in MAB pharmacokinetic profiles are likely to be genuine, a few considerations are warranted. First, the occurrence of additional peaks immediately following administration (<24 h and <14 days for intravenous and subcutaneous administration, respectively) was usually higher than in the period thereafter, regardless of the chosen value for normal intra-subject variability. An explanation for this phenomenon may be that the sampling frequency is usually decreased over time, thereby reducing the chance to identify relative extremes. Additionally, some MABs had relatively short profiles, and thus a limited number of data points after 24 h, as was the case for products A and B.

Next, the question rises which physiological mechanism may be responsible for the phenomenon of fluctuating plasma concentration. One explanation comprises the capture and subsequent release of MABs by tissues or components, which would presumably be large quantities of MAB, given the observed magnitude of the excursions, with increases of 50% or more (*table 3.3*). Moreover, the MAB is presumably released quite rapidly, as the changes over time in certain cases approach the infusion rate of intravenous administration (*figure 3.1*). Earlier, we demonstrated the endothelium to be a potential candidate for dynamically binding biopharmaceuticals.[10] Nonetheless, there may be other locations where MABs can be stored temporally. For example, can MABs simply pool in the venous compartment or in less perfused organs? Does an extravascular reservoir exist? Which physiological or pathophysiological mechanisms underlie the release ('auto-injection') of the MAB into the circulation?

Considering daily life, the redistribution of blood flow to various organs during alimentation (gastrointestinal system), resting, and physical exercise (muscles) may either mask or expose sites for adsorption, absorption, and elimination, or, in contrast, flush out pooled or adsorbed MABs in these organs. Possibly, changes in the local milieu (*e.g.* pH), competition for adsorption sites by other substances, and modifications to structural components involved in binding or transport of MABs can mediate the release into the circulation. Without dedicated research on the distribution of MABs over the body, however, these options remain speculative at best.

MABs are designed to specifically bind a particular target, and the resulting complex is internalised and subsequently degraded by either immune cells or the target cell.[1,3] Therefore, this elimination process cannot contribute to increases in the plasma concentration of a MAB. However, it is conceivable that an abrupt decrease in the target-mediated elimination route – for example, because of down-regulation of the target following exposure to an abundance of circulating MABs – can acutely elevate plasma concentration, provided that there is continuous absorption of the MAB into the plasma compartment, as with subcutaneous administration. Other prerequisites for this possible explanation are a relative high absorption rate and a significant contribution of the target-mediated pathway to the total elimination of the MAB, which does not seem to be the case based on published values regarding absorption and elimination rates.[5,11] By analogy, although variations in the absorption rate over time after subcutaneous administration can theoretically change plasma concentrations of MABs, the absorption of MABs from a subcutaneous depot into the circulation is generally understood to be slow,[2] which is not in line with the observed rapid and large excursions.

The neonatal Fc-receptor (FcRn, or Brambell-receptor) requires special consideration. Binding of a mAb to this receptor does not result in lysosomal degradation, but returns the mAb-FcRn complex to the cell membrane.[1,4,5,12] Such recycling of mAbs to the vascular compartment may contribute to fluctuations in plasma concentration, as mAbs can be temporarily sequestered from the circulation.[13] However, research suggests the transportation of immunoglobulins by FcRn is quite rapid.[14] Another function of the FcRn is transcytosis of immunoglobulins, including mAbs. According to current understanding, distribution of mAbs to tissues is slow and limited,[1–3,5] which suggests this process cannot explain our observations. Furthermore, albumin is also a substrate of the FcRn,[12] and comparable fluctuations in its concentration have not been documented. Nonetheless, involvement of the FcRn cannot be ruled out, although it would be interesting to know which factors, in that case, can trigger abrupt changes in FcRn-mediated transcellular transport rate of mAbs.

An important question to be answered is what the clinical relevance of fluctuations in plasma concentration over time could be. Assuming that plasma concentration is a key determinant to achieve therapeutical concentrations at the site of action, measuring and understanding variations in plasma concentrations over time are probably pivotal. Therefore, we hope to initiate a broad discussion within the field on possible explanations for the observed phenomena, as well as how to increase more fundamental knowledge of the pharmacokinetics of mAbs.

In conclusion, the plasma concentration of mAbs can vary abruptly and to a great extent, which cannot be explained by normal physiological or assay variability. Future studies are required to elucidate this phenomenon and to determine its relevance for clinical practice.

REFERENCES

1 Keizer RJ, Huitema ADR, Schellens JHM, Beijnen JH. Clinical pharmacokinetics of therapeutic monoclonal antibodies. *Clin Pharmacokinet* 2010; **49**: 493–507.

2 Dostalek M, Gardner I, Gurbaxani BM, Rose RH, Chetty M. Pharmacokinetics, pharmacodynamics and physiologically-based pharmacokinetic modelling of monoclonal antibodies. *Clin Pharmacokinet* 2013; **52**: 83–124.

3 Shi S. Biologics: an update and challenge of their pharmacokinetics. *Curr Drug Metab* 2014; **15**: 271–90.

4 Wang W, Wang EQ, Balthasar JP. Monoclonal antibody pharmacokinetics and pharmacodynamics. *Clin Pharmacol Ther* 2008; **84**: 548–58.

5 Dirks NL, Meibohm B. Population pharmacokinetics of therapeutic monoclonal antibodies. *Clin Pharmacokinet* 2010; **49**: 633–59.

6 Reed GF, Lynn F, Meade BD. Use of coefficient of variation in assessing variability of quantitative assays. *Clin Diagn Lab Immunol* 2002; **9**: 1235–9.

7 Committee for Medicinal Products for Human Use (CHMP). Guideline on bioanalytical method validation. London: European Medicines Agency, 2012.

8 US Food and Drug Administration. Guidance for industry: bioanalytical method validation (draft). Washington, DC: US Department of Health and Human Services, 2013.

9 Van Iersel MP, Velinova M, Lutgerink R. A change in posture significantly affects plasma concentrations of Immunoglobulin G, such as monoclonal antibodies. *Clin Pharmacol Drug Dev* 2016; **5**: 6.

10 Reijers JAA, Dane MJC, van Zonneveld AJ, Burggraaf J, Moerland M. Potential influence of endothelial adsorption on the delayed time to maximum concentration of biopharmaceuticals. *Eur J Drug Metab Pharmacokinet* 2017; published online Aug 9 (*chapter 2*).

11 Ternant D, Bejan-Angoulvant T, Passot C, Mulleman D, Paintaud G. Clinical pharmacokinetics and pharmacodynamics of monoclonal antibodies approved to treat rheumatoid arthritis. *Clin Pharmacokinet* 2015; **54**: 1107–23.

12 Martins JP, Kennedy PJ, Santos HA, Barrias C, Sarmento B. A comprehensive review of the neonatal Fc receptor and its application in drug delivery. *Pharmacol Ther* 2016; **161**: 22–39.

13 Daugherty AL, Mrsny RJ. Formulation and delivery issues for monoclonal antibody therapeutics. *Adv Drug Deliv Rev* 2006; **58**: 686–706.

14 Tzaban S, Massol RH, Yen E, *et al.* The recycling and transcytotic pathways for IgG transport by FcRn are distinct and display an inherent polarity. *J Cell Biol* 2009; **185**: 673–84.

SUPPLEMENT

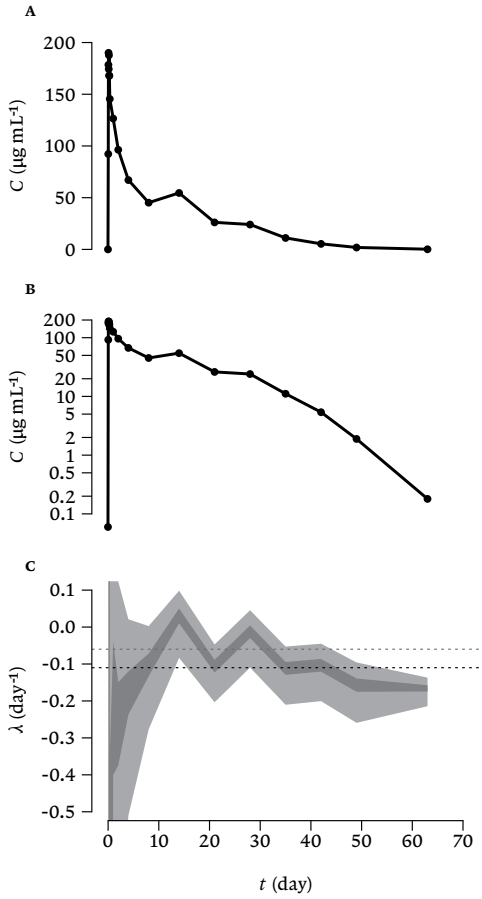

FIGURE 3.51 Example individual pharmacokinetic profile

Example individual pharmacokinetic profile on linear scale (A) and logarithmic scale (B). The margins of the exponential growth constant, λ, are displayed in C and are based on the formula $A \pm \mathrm{CV}_i = B \cdot e^{\lambda t}$, where A is the observed plasma concentration, CV_i the chosen intra-subject variability, B the plasma concentration of the previous sample, and t the difference in sample collection time between A and B. At a CV_i of 8% (dark grey area), no single λ can describe both the relative maximum at day 14 and the surrounding curve (black dashed line). However, at a CV_i of 50% (light grey area), a common λ can be found (grey dashed line). Hence, the additional peak is counted at a CV_i of 8% but not at a CV_i of 50%.

SECTION II

DIRTY PROTEINS

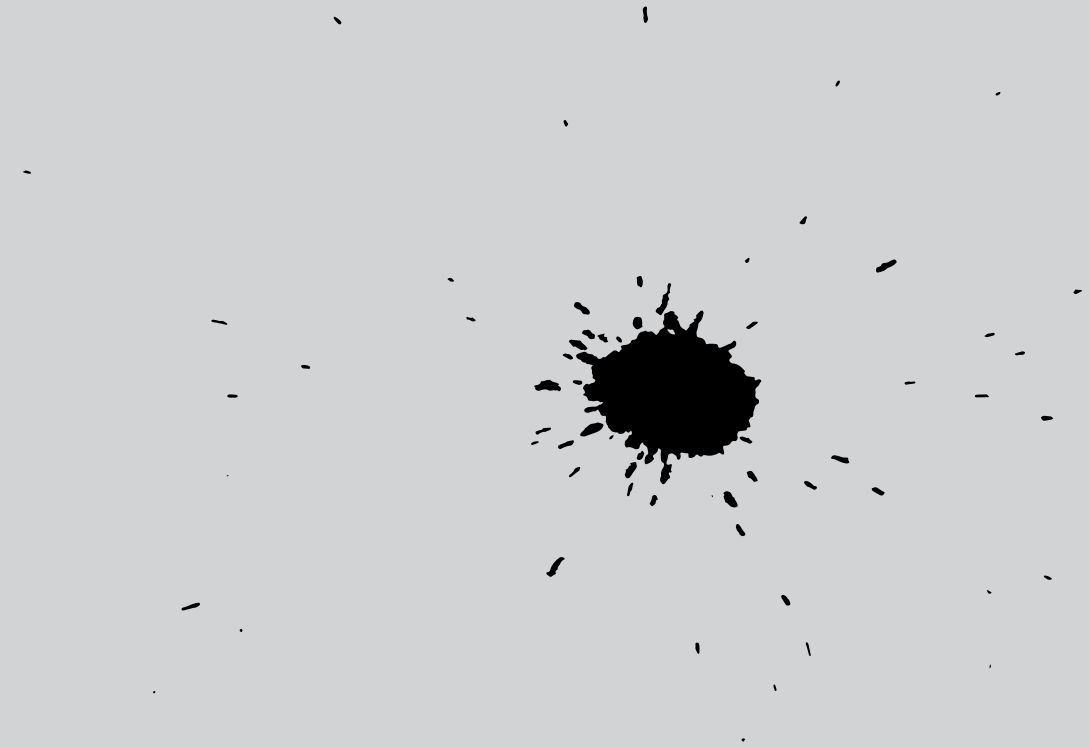

CHAPTER IV

Characterisation of immunostimulation by trastuzumab in responders and non-responders

J.A.A. Reijers, M.J.C. Dane, K.E. Malone, J. Burggraaf, M. Moerland

It is often difficult to predict the likelihood of immunostimulation by monoclonal antibodies and identify who is at risk based on preclinical results. We explored the feasibility of an *ex vivo* cytokine release assay to detect trastuzumab-induced immunostimulation by correlating *in vivo* and *ex vivo* results. Also, the effect of trastuzumab on human umbilical vein endothelial cells (HUVECs) was studied.

Healthy male volunteers were selected from a previous clinical trial in which they had been exposed to trastuzumab. Five donors had experienced fever (responders) and six had not (non-responders). Additionally, ten male donors were selected from a healthy, trastuzumab-naïve population. Heparinised whole blood samples were collected and incubated for 24 h with 0.2 mg/mL trastuzumab. HUVECs were grown under a constant laminar flow for 7 days, followed by incubation with 2 mg/mL trastuzumab alone or in combination with TNF-α.

Trastuzumab induced a very mild IL-6 response in the supernatant of the cell cultures, which was more pronounced in the responders. A correlation was detected between the *in vivo* maximum body temperature (T_{max}) and the IL-6 response with Pearson's $r = 0.83$ (95% confidence interval: 0.45–0.95), $p = 0.0017$. Virtually no TNF-α response was observed, although a linear relationship to T_{max} was suggested in responders: $r = 1.00$ (0.93–1.00), $p = 0.0004$. No increased conversion of C5 to C5a was observed. The trastuzumab-naïve population did not show any cytokine or complement response. Trastuzumab did not increase E-selectin expression in HUVECs.

Individuals who demonstrate clinical signs of trastuzumab-associated immunostimulation show a greater *ex vivo* IL-6 response to trastuzumab. Both IL-6 and TNF-α responses are correlated with T_{max}, yet do not explain the full clinical picture.

Some monoclonal antibodies (MABs) are known to induce an inflammatory response during or shortly after administration. The most common causative MABs include rituximab (incidence 77%), alemtuzumab (>80%), and trastuzumab (40%).[1] Frequently, the severity of the inflammatory reactions wanes with each subsequent infusion and the majority of patients experiences a reaction upon the first administration only. Although these events are usually only mildly discomforting to patients and easily manageable with anti-inflammatory agents, severe reactions occur in up to 1% of treated

patients, which can even be fatal as a result of uncontrolled activation of the immune system, similar to sepsis and anaphylaxis.[1]

It is often difficult to predict the likelihood of such reactions and identify who is at risk. Over recent years, especially after the disastrous TGN1412 case, progress has been made in developing *ex vivo* and *in vitro* models that have increased our knowledge on this topic.[2,3] These models typically utilise primary human immune cells or (human) cell lines transfected with innate immune-receptors that are thought to play a role. Some models incorporate other cell types, such as endothelial cells or the complement system.[3] An EMA workgroup[4] recognised cytokine release assays as a valuable tool, yet also identified numerous sources of variability, including donor selection, type of test matrix, and read-out parameters, adding to the complexity of designing and interpreting such assays.

For rituximab and alemtuzumab, which both target lymphocytes, *in vitro* test systems that mimic the clinical response are available.[5,6] Also, the T-cell stimulation by TGN1412 can be predicted by *ex vivo*

TABLE 4.1 Population characteristics

PARAMETER	PLACEBO ($n=8$)		TRASTUZUMAB					
			all ($n=46$)		non-responders ($n=37$)		responders ($n=9$)	
Age (year)	25.3	(3.6)	24.1	(5.8)	23.2	(5.0)	27.8	(7.8)
Height (cm)	182	(7)	182	(6)	182	(6)	182	(6)
Weight (kg)	76.3	(12.6)	77.1	(10.2)	77.3	(10.2)	76.5	(10.6)
BMI (kg m^{-2})	23.1	(3.3)	23.2	(2.7)	23.2	(2.8)	23.2	(2.8)
$t=0$ h								
Leucocytes (10^9 L^{-1})	6.0	(1.8)	5.4	(1.2)	5.4	(1.1)	5.6	(1.6)
Neutrophils	3.5	(1.3)	2.8	(0.8)	2.7	(0.6)	3.1	(1.3)
Lymphocytes	1.8	(0.5)	1.9	(0.6)	1.9	(0.6)	1.8	(0.3)
Monocytes	0.50	(0.17)	0.46	(0.14)	0.46	(0.14)	0.44	(0.13)
Eosinophils	0.17	(0.13)	0.24	(0.25)	0.26	(0.27)	0.17	(0.10)
Basophils	0.03	(0.03)	0.02	(0.01)	0.02	(0.01)	0.02	(0.01)
$t=24$ h								
Leucocytes (10^9 L^{-1})	6.0	(1.1)	7.3	(1.3)	7.1	(1.4)	8.2	(0.7)
Neutrophils	3.4	(0.8)	5.4	(1.4)	5.1	(1.4)	6.5	(0.8)
Lymphocytes	1.9	(0.4)	1.2	(0.4)	1.2	(0.4)	1.1	(0.2)
Monocytes	0.53	(0.12)	0.43	(0.16)	0.44	(0.16)	0.39	(0.17)
Eosinophils	0.16	(0.05)	0.27	(0.30)	0.29	(0.32)	0.17	(0.12)
Basophils	0.02	(0.01)	0.02	(0.01)	0.02	(0.01)	0.02	(0.01)
Ratio 0/24 h								
Leucocytes	0.99	(0.11)	1.39	(0.28)	1.36	(0.27)	1.54	(0.31)
Neutrophils	1.04	(0.17)	2.01	(0.57)	1.94	(0.55)	2.28	(0.60)
Lymphocytes	0.92	(0.09)	0.65	(0.14)	0.66	(0.15)	0.59	(0.06)
Monocytes	1.01	(0.16)	0.97	(0.29)	0.98	(0.28)	0.92	(0.36)
Eosinophils	1.04	(0.17)	1.17	(0.32)	1.21	(0.32)	1.00	(0.27)
Basophils	0.92	(0.57)	0.94	(0.45)	0.91	(0.45)	1.03	(0.48)
T_{max} (°C)	36.9	(0.2)	37.6	(0.7)	37.3	(0.4)	38.8	(0.4)
C_{max} (µg mL^{-1})	—		185	(34)	185	(33)	184	(39)
AUC_∞ (µg day mL^{-1})	—		1609	(224)	1635	(229)	1503	(174)

Data are presented as mean (standard deviation).

Leucocytes at 24 h post administration and corresponding ratio were not available for 3 placebo subjects.

AUC_∞: area under the (trastuzumab plasma) concentration-time curve extrapolated until infinity

C_{max}: maximum trastuzumab plasma concentration | T_{max}: maximum body temperature

models.[7,8] However, far less efforts have been devoted to trastuzumab, and some of the applied models fail in detecting a response to trastuzumab.[9]

We explored the feasibility of an *ex vivo* cytokine release assay in whole blood to detect trastuzumab-induced inflammatory responses in a group of healthy donors. The donor population was divided into a group of individuals who had demonstrated clinical signs of an inflammatory reaction induced by *in vivo* trastuzumab administration (responders) and a group of individuals who had not (non-responders). This allowed the correlation of the outcome of an *ex vivo* whole blood cytokine release with the observed clinical response following trastuzumab administration in the same person. Whereas the *ex vivo* cytokine release assay reflects the drug response of circulating immune cells, the *in vivo* inflammatory response is the result of the interaction between circulating immune cells and other immunological organs, such as the liver and endothelium. In cocultures, the combination of peripheral blood mononuclear cells (PBMCs) and endothelial cells has been shown to either be critical for the development of, or to enhance the *ex vivo* response towards an exogenous stimulus.[3,10] Therefore, we also tested direct endothelial activation by trastuzumab in an 'artificial vessel' with a quiescent monolayer of endothelial cells grown inside that closely resembles the physiological situation *in vivo*.

METHODS

Clinical results

Clinical data were collected in a randomised trial of parallel design, in which healthy male volunteers received a single intravenous dose of either placebo or trastuzumab.[11] For the purpose of this analysis, participants who received the registered form of trastuzumab (Herceptin®, $n = 46$) were compared with participants who received placebo ($n = 8$). The investigated dose of trastuzumab was 6 mg/kg (6.44 mg/kg based on actual protein content). A subgroup analysis was performed on responders and non-responders, *i.e.* subjects who experienced fever (body temperature ≥ 38°C) or not. Adverse events that were reported within the first 24 h after administration were analysed, as were vital signs and laboratory assessments (haematology and clinical chemistry) during the same period, and details on the exposure to trastuzumab (maximum plasma concentration and area under the curve [AUC]).

Ex vivo stimulation

For the *ex vivo* stimulation, healthy male volunteers were recruited from the cohort of 46 subjects who were previously exposed to trastuzumab (non-naïve population) and from the community (naïve population). Subjects were selected based on the severity of the inflammatory reaction upon *in vivo* exposure. This resulted in a group size of 11 for the non-naïve population, of whom 5 had experienced fever (responders), and 6 not (non-responders). The naïve population included 10 healthy male volunteers. The *ex vivo* stimulation was executed two years after the clinical trial was completed.

Heparinised whole blood samples (18 mL, BD Vacutainer, Becton Dickinson, Breda, The Netherlands) were collected and incubated for 24 h at 37°C in a humidified atmosphere with 5% CO_2, before flash-freezing the supernatant for subsequent analysis. Tested conditions were 0.2 mg/mL trastuzumab (Herceptin®), 2 ng/mL lipopolysaccharide (LPS) gel extracted from *E. coli* serotype O111:B4 (Sigma-Aldrich, St. Louis, Missouri, USA), and blank (unstimulated control). The trastuzumab concentration is similar to the maximum plasma concentration observed after an *in vivo* dose of 6 mg/kg. LPS concentration was based on the EC_{90} of maximum TNF-α release and served as a positive control. Conditions were made in RPMI with 25 mM HEPES and L-glutamine (Gibco products from Life Technologies Europe, Bleiswijk, the Netherlands). Final dilution of whole blood required to achieve the tested concentrations was 1%.

Inflammatory cytokines, IL-6 and TNF-α, were measured by multiplex electrochemiluminescence using a human ultrasensitive cytokine panel (Meso Scale Discovery, LLC, Rockville, Maryland, USA). C5a, a late product of complement activation, was measured by ELISA (eBioscience, Inc., San Diego, California, USA).

Endothelial stimulation

Human umbilical vein endothelial cells (HUVECs) were freshly isolated from umbilical cords by 0.25% trypsin treatment. HUVECs were cultured in EGM2 medium (Lonza, Basel, Switzerland) containing antibiotics and antimycotics (Life Technologies,

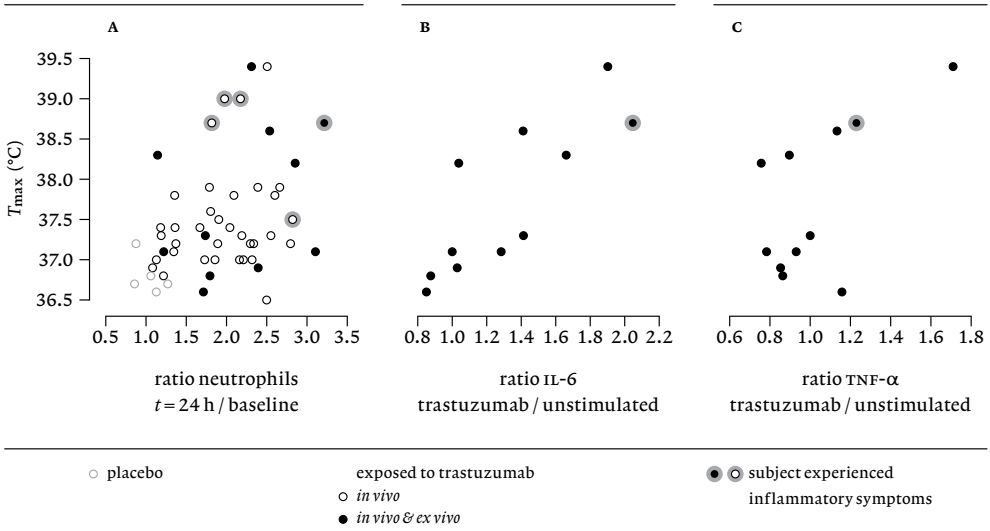

FIGURE 4.1 ***In vivo*** **and** ***ex vivo*** **response**
Maximum body temperature (T_{max}) is plotted against the ratio of neutrophil concentrations at 24 h post administration over pre-dose values for the total population exposed *in vivo* (A); and against the ratios of trastuzumab *ex vivo* stimulated IL-6 (B) and TNF-α (C) levels over background (unstimulated level) for a subset of responders ($T_{max} \geq 38°C$) and non-responders.

Carlsbad, California, USA) at 37°C and 5% CO_2, and used for experiments on passage 3–4. To obtain a confluent, quiescent, endothelial monolayer that closely resembles the physiological situation, HUVECs were grown under a constant laminar flow of 10 dyne cm^{-2} for 7 days using a closed perfusion Ibidi flow system (ibiTreat 0.4 µ-Slide VI Luer, Ibidi, Martinsried, Germany).

The endothelial monolayer was incubated for 5 h with TNF-α (R&D, Abingdon, UK) or trastuzumab in medium, or with medium only (blank control). Tested concentrations were 10, 1, 0.1 ng/mL for TNF-α and 2 mg/mL for trastuzumab (comparable to the concentration in the infusate).

After stimulation, HUVECs were fixed in 4% paraformaldehyde in HBSS for 10 min at room temperature, washed twice with 1% bovine serum albumin (BSA) in HBSS, and blocked with 5% normal goat serum (Dako, Carpinteria, California, USA) in HBSS for 30 min. Cells were permeabilised with TRITON X-100 (Merck, Darmstadt, Germany). Cultures were incubated for at least 60 min at 4°C with 10 µg/mL TRITC-labelled wheat germ agglutinin (WGA) (Sigma-Aldrich, 1:100), Hoechst 33258 (Sigma-Aldrich, 1:5,000), and a mouse anti-human E-selectin antibody (R&D, 1:100) diluted in HBSS + 1% BSA. Next, the cell-layer was washed three times with HBSS + 1% BSA, counterstained with an Alexa Fluor® 488-coupled anti-mouse-IgG (Thermo Fisher, Waltham, Massachusetts, USA, 1:500), washed again, and imaged using a Leica SP5 confocal microscope.

Confocal 12-bit greyscale axial image stacks (*xyz* dimensions, 0.08 × 0.08 × 0.13 µm) that covered 6,724 $µm^2$ of surface area per image and a height of 5 to 10 µm above the endothelial cell nuclear plane were recorded using LAS-AF image software (Leica). The image stacks were analysed with the public domain National Institutes of Health IMAGE program (http://rsb.info.nih.gov/nih-image). Cross-sections of the cell-layer were generated using this software.

Statistical analysis

Data are summarised as mean (standard deviation) or number (percentage), unless otherwise specified. Testing for linear relationships was done by calculating the Pearson product-moment correlation coefficient (r). P-values and 95% confidence intervals for the true population value (ρ) were obtained under the assumption of normal distribution. Because of the relatively small sample size, Spearman's rank correlation test was also performed. Fisher transformation was used to estimate the 95% confidence interval of the

corresponding coefficient (r_s). All analyses were performed with R (v2.15.2, R Foundation for Statistical Computing, Vienna, Austria, 2012).

RESULTS

Clinical response

Following trastuzumab administration, 9 (19.6%) subjects developed fever (responders, *table 4.1*). Maximum body temperature (T_{max}) was reached at 4.7 h (2.6) after the start of infusion. Seven subjects had a $T_{max} \geq 38.5°C$, and four $\geq 39.0°C$. Influenza-like symptoms (rigors, nausea, myalgia, fatigue) were reported by 5 subjects, of whom 1 without fever.

Leucocytes were observed to increase by 39% (28) at 24 h, predominantly neutrophils (increase 101% [57]), accompanied by a decrease in lymphocytes of 35% (14). These changes were more prominent in subjects with influenza-like symptoms or fever (*figure 4.1*). There were no differences between both subgroups in the maximum plasma concentration (C_{max}) and area under the curve (AUC) for trastuzumab.

Ex vivo response

Incubation of whole blood with 0.2 mg/mL trastuzumab induced a very mild IL-6 response, but virtually no TNF-α response (*table 4.2*). The increase in IL-6 was more pronounced in the responders than in the non-responders, whereas this difference was much smaller for TNF-α. The trastuzumab-naïve population did not show an IL-6 or a TNF-α response upon stimulation. No increased conversion of C5 to C5a was observed after trastuzumab treatment, compared to the unstimulated control in any (sub)population (*table 4.2*).

A–B

FIGURE 4.2 Endothelial stimulation
After 5 h incubation with medium alone, trastuzumab, or TNF-α, human umbilical vein endothelial cells (HUVECs) were stained with Hoechst 33258 (nucleus, *blue*), TRITC-labelled wheat germ agglutinin (WGA) binding the carbohydrate N-acetyl galactosamine on the cell surface (*red*), and a mouse anti-human E-selectin antibody (*green*) (A). Results after HUVECs were incubated with different concentrations of TNF-α for 5 h in the presence or absence of trastuzumab (trast.); only the green Alexa Fluor® 488 signal is displayed for clarity (B).

A strong positive and statistically significant correlation was detected between T_{max} and the IL-6 response (*figure 4.1*, correlation coefficient, $r = 0.83$ [0.45–0.95], $p = 0.0017$). Spearman's rank correlation test gave $r_s = 0.91$ (0.59–0.98), $p = 0.0001$. A similar linear relationship was suggested for TNF-α, though only in the responders (*figure 4.1*, $r = 1.00$ [0.93–1.00], $p = 0.0004$, $r_s = 1$); furthermore, it should be noted that the ratios of stimulated over unstimulated (background) levels ranged from ~0.8 to ~1.2 for the majority of subjects, which indicates no or minimal TNF-α release upon stimulation. A correlation was also observed between the *ex vivo* IL-6 and TNF-α responses: $r = 0.90$ (0.33–0.99), $p = 0.0146$; $r_s = 0.85$ (0.41–0.97), $p = 0.0341$. The changes in circulating leucocytes following *in vivo* trastuzumab exposure did not correlate with any of the *ex vivo* responses.

Endothelial stimulation

Trastuzumab did not increase E-selectin expression in HUVECs, whereas TNF-α dose-dependently increased E-selectin expression (*figure 4.2*). The combined stimulation (trastuzumab + TNF-α) did not reveal an additive or potentiating effect from trastuzumab.

TABLE 4.2 *Ex vivo* stimulation

RATIO	NAÏVE ($n = 10$)	NON-NAÏVE		
		all ($n = 11$)	non-responders ($n = 6$)	responders ($n = 5$)
IL-6	1.06 (1.40)	1.26 (1.36)	1.06 (1.23)	1.57 (1.31)
TNF-α	1.11 (1.30)	1.00 (1.27)	0.92 (1.15)	1.10 (1.37)
C5a	1.03 (1.13)	1.00 (1.06)	1.02 (1.08)	0.97 (1.03)

Geometric mean (standard deviation) of ratios of stimulated IL-6, TNF-α, and C5a levels over unstimulated (background) levels for the trastuzumab-naïve and non-naïve population.

A

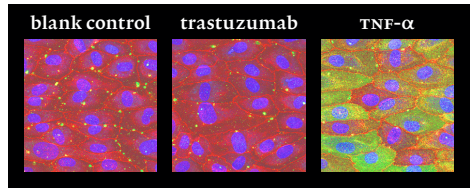

B

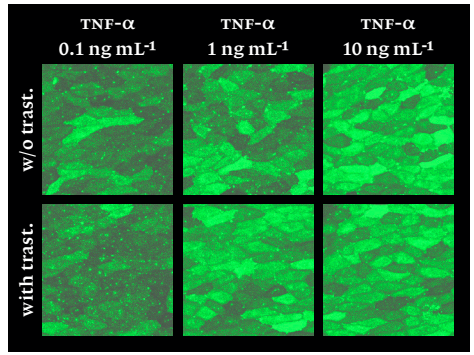

FIGURE 4.2

DISCUSSION

Following exposure to trastuzumab, approximately 20% of the healthy volunteers developed fever with or without accompanying influenza-like symptoms, which is half of that commonly reported in patients.[1] This may be the result of chance as another trial in healthy volunteers also found a lower incidence,[12] whereas a trial in healthy Japanese males reported an incidence of ~40%.[13] Batch differences could also have caused the disparity. Nonetheless, virtually all exposed participants showed an increase in neutrophils, parallelled by a decrease in lymphocytes, indicating that true non-responsiveness in terms of trastuzumab-induced immunostimulation is probably rare.

Although the occurrence of fever was associated with greater changes in neutrophil and lymphocyte counts, the opposite was not true. This suggests that more than one pathway is involved in the inflammatory reaction, which contributes to phenotypical variation. Therefore, the subgroups (with or without fever, termed responders and non-responders) were studied for differences that could explain the observed variability in response. In both groups, comparable exposure to trastuzumab, specifically maximum plasma concentration (C_{max}), was seen. Differences in any of the baseline laboratory and other parameters were not detected. Unfortunately, no additional material from the clinical trial was available to further characterise the subpopulations or further delineate their response with biomarkers that might provide mechanistic insight, *e.g.* (baseline) cytokine profiles.

Exposing a number of subjects from each subgroup to trastuzumab *ex vivo* revealed a difference in the responsiveness. The release of IL-6 was greater in responders than in the non-responders, which was also true for TNF-α, albeit the difference in TNF-α release was less pronounced. The IL-6 response upon *ex vivo* stimulation correlated with the maximum body temperature (T_{max}) seen clinically after trastuzumab administration, as did the TNF-α results, but only in the responders. This suggests both IL-6 and TNF-α release are involved in the production of fever. IL-6 correlated with T_{max} in the entire population exposed to trastuzumab *in vivo*, whereas TNF-α showed a linear relationship with T_{max} only within the responders. A relationship between changes in leucocytes and *ex vivo* IL-6 or TNF-α results could not be detected. Thus, the release of these two cytokines from circulating immune cells explains only certain aspects of the clinical picture.

Despite its almost perfect correlation, the role for TNF-α remains more controversial since the majority of individuals had ratios between 0.8 and 1.2, which is usually not considered a response to a stimulus. However, the 24 h duration of the incubation may have been suboptimal for detecting the peak values of this cytokine. We have data demonstrating that the measured TNF-α in the supernatant decreases with prolonged incubation, even after 4 h (data on file). Therefore, the presented TNF-α results could be a relative response rather than an absolute figure.

Because the *ex vivo* study was conducted *after* the *in vivo* study, carry-over effects cannot be excluded, but these are unlikely to have influenced the results. Based on available pharmacokinetic data, trastuzumab is completely cleared from the body two years after administration and thus could not have interfered with the *ex vivo* stimulation. The finding that most inflammatory reactions occur during the first infusion points toward the innate immune system in mediating the response. Furthermore, the *ex vivo* IL-6 response correlated well with the T_{max} observed two years earlier, which also suggests that an individual's responsiveness to trastuzumab does not change over time.

Complement activation was not observed by us upon *ex vivo* stimulation in any of the populations or subgroups. Additionally, trastuzumab did not activate endothelial cells, nor did trastuzumab potentiate TNF-α-mediated endothelial activation, which is in agreement with a report by Findlay *et al.*[14] However, these findings do not preclude the possibility of augmentation of the initially limited inflammatory (IL-6 and TNF-α) response when trastuzumab engages a particular target present on for example endothelium, or the activation of endothelial cells by the cytokines released from circulating immune cells.

Minor responses to trastuzumab were previously elicited in an *ex vivo* model using leucocytes and autologous platelet-poor plasma on top of a HUVEC layer,[8] but were not observed in a model that used peripheral blood mononuclear cells (PBMCs) in combination with autologous endothelial cells.[9] Similarly, trastuzumab immobilised onto a plastic surface induced cytokine release from PBMCs, whereas no reaction occurred when PBMCs were exposed to soluble trastuzumab.[14]

The method of culturing the endothelial cells in previous studies may also have influenced their results. Cultured endothelial cells are phenotypically different compared to *in vivo* endothelial cells. One of the key factors for this difference is the absence of flow in traditional endothelial cell culture. Since shear stress leads to a more quiescent, less inflammatory and less proliferative state,[15–17] it thereby better mimics the healthy *in vivo* situation. Culturing under flow, or perhaps even under flow in 3D cultured vessels, which are currently under development, may therefore improve these studies.

Remarkably, trastuzumab is sometimes used as a negative control in (*ex vivo*) immunostimulation experiments, which may be related to the small number of donors included in the published experiments. Our data suggest that trastuzumab is capable of eliciting an immune response in susceptible humans and therefore should not be used as a negative control in immunostimulation testing.

Main strength of our study is the correlation of known clinical responses with results from *ex vivo* whole blood stimulations within the same individual. Based on *in vivo* data, we were able to identify 'responders' and 'non-responders' and indeed observed differences in the reactivity of their circulating immune cells to *ex vivo* trastuzumab exposure. This in contrast to the naïve population ($n = 10$), where no response to trastuzumab could be found, which should not be surprising with a preselection incidence of ~20% for fever. Unfortunately, the difference between responders and non-responders in *ex vivo* IL-6 and TNF-α release was too small for this type of test to serve as a general screening assay.

For two MABs, alemtuzumab and rituximab, the pathogenesis of the inflammatory response has been elucidated. In both cases, different mechanism were involved in the immunostimulation; cytokine release (IL-6, TNF-α, and IFN-γ) following alemtuzumab was found to result from an interaction with natural killer (NK) cells via FCγ-receptors,[5,18] whereas rituximab induced complement activation and stimulated MIP-1β secretion from NK cells.[6,19] Lack of knowledge on the exact mechanism of trastuzumab-associated immunostimulation does not facilitate an easy interpretation of our results or the development of a discriminating (*ex vivo*) assay. Nonetheless, by simultaneously studying *in vivo* and *ex vivo* responses, the involved pathways may be unravelled.

In conclusion, individuals who demonstrate clinical signs of trastuzumab-associated immunostimulation show an elevated *ex vivo* IL-6 response to trastuzumab. Both IL-6 and TNF-α response are correlated with the observed *in vivo* maximum body temperature, yet do not explain the full clinical picture. It remains difficult to predict a clinical response in an individual or to separate responders from non-responders based on *ex vivo* results.

REFERENCES

1 Chung CH. Managing premedications and the risk for reactions to infusional monoclonal antibody therapy. *Oncologist* 2008; **13**: 725–32.

2 Stebbings R, Eastwood D, Poole S, Thorpe R. After TGN1412: recent developments in cytokine release assays. *J Immunotoxicol* 2013; **10**: 75–82.

3 Finco D, Grimaldi C, Fort M, *et al.* Cytokine release assays: current practices and future directions. *Cytokine* 2014; **66**: 143–55.

4 Vidal J-M, Kawabata TT, Thorpe R, *et al. In vitro* cytokine release assays for predicting cytokine release syndrome: the current state-of-the-science. Report of a European Medicines Agency Workshop. *Cytokine* 2010; **51**: 213–5.

5 Wing MG, Moreau T, Greenwood J, *et al.* Mechanism of first-dose cytokine-release syndrome by CAMPATH 1-H: involvement of CD16 (FCγRIII) and CD11a/CD18 (LFA-1) on NK cells. *J Clin Invest* 1996; **98**: 2819–26.

6 Kamburova EG, Van den Hoogen MWF, Koenen HJPM, Baas MC, Hilbrands LB, Joosten I. Cytokine release after treatment with rituximab in renal transplant recipients. *Transplantation* 2015; **99**: 1907–11.

7 Eastwood D, Findlay L, Poole S, *et al.* Monoclonal antibody TGN1412 trial failure explained by species differences in CD28 expression on CD4+ effector memory T-cells. *Br J Pharmacol* 2010; **161**: 512–26.

8 Bailey L, Moreno L, Manigold T, *et al.* A simple whole blood bioassay detects cytokine responses to anti-CD28SA and anti-CD52 antibodies. *J Pharmacol Toxicol Methods* 2013; **68**: 231–9.

9 Reed DM, Paschalaki KE, Starke RD, *et al.* An autologous endothelial cell:peripheral blood mononuclear cell assay that detects cytokine storm responses to biologics. *FASEB J* 2015; **29**: 2595.

10 Findlay L, Sharp G, Fox B, *et al.* Endothelial cells co-stimulate peripheral blood mononuclear cell responses to monoclonal

antibody TGN1412 in culture. *Cytokine* 2011; **55**: 141–51.
11 Wisman LAB, De Cock EPM, Reijers JAA, *et al.* A phase I dose-escalation and bioequivalence study of a trastuzumab biosimilar in healthy male volunteers. *Clin Drug Investig* 2014; **34**: 887–94.
12 Yin D, Barker KB, Li R, *et al.* A randomized phase 1 pharmacokinetic trial comparing the potential biosimilar PF-05280014 with trastuzumab in healthy volunteers (REFLECTIONS B327-01). *Br J Clin Pharmacol* 2014; **78**: 1281–90.
13 Morita J, Tanaka M, Nomoto M, *et al.* Pharmacokinetic bioequivalence, safety, and immunogenicity of DMB-3111, a trastuzumab biosimilar, and trastuzumab in healthy Japanese adult males: results of a randomized trial. *BioDrugs* 2016; **30**: 17–25.
14 Findlay L, Eastwood D, Ball C, *et al.* Comparison of novel methods for predicting the risk of pro-inflammatory clinical infusion reactions during monoclonal antibody therapy. *J Immunol Methods* 2011; **371**: 134–42.
15 Dekker RJ, Boon RA, Rondaij MG, *et al.* KLF2 provokes a gene expression pattern that establishes functional quiescent differentiation of the endothelium. *Blood* 2006; **107**: 4354–63.
16 Fledderus JO, Van Thienen JV, Boon RA, *et al.* Prolonged shear stress and KLF2 suppress constitutive proinflammatory transcription through inhibition of ATF2. *Blood* 2007; **109**: 4249–57.
17 Boon RA, Horrevoets AJG. Key transcriptional regulators of the vasoprotective effects of shear stress. *Hämostaseologie* 2009; **29**: 39–43.
18 Stauch D, Dernier A, Sarmiento Marchese E, *et al.* Targeting of natural killer cells by rabbit antithymocyte globulin and campath-1H: similar effects independent of specificity. *PLoS One* 2009; **4**: e4709.
19 Van Der Kolk LE, Grillo-López AJ, Baars JW, Hack CE, Van Oers MHJ. Complement activation plays a key role in the side-effects of rituximab treatment. *Br J Haematol* 2001; **115**: 807–11.

CHAPTER V

MDCO-216 does not induce adverse immunostimulation, in contrast to its predecessor ETC-216

J.A.A. Reijers, D.G. Kallend, K.E. Malone, J.W. Jukema, P.L.J. Wijngaard, J. Burggraaf, M. Moerland

Aim of this study was to demonstrate that MDCO-216 (human recombinant Apolipoprotein A-I Milano) does not induce adverse immunostimulation, in contrast to its predecessor, ETC-216, which was thought to contain host cell proteins (HCPs) that elicited an inflammatory reaction.

Data were taken from a clinical trial in which 24 healthy volunteers (HV) and 24 patients with proven stable coronary artery disease (sCAD) received a single intravenous dose of MDCO-216, ranging from 5 to 40 mg/kg. Additionally, whole blood from 35 HV, 35 sCAD patients, and 35 patients requiring acute coronary intervention (aCAD group) was stimulated *ex vivo* with MDCO-216 and ETC-216.

No inflammatory reaction was observed in HV and sCAD patients following MDCO-216 treatment, judging by body temperature, white cell counts, neutrophil counts, C-reactive protein, circulating cytokines (IL-6 and TNF-α), and adverse events. In the *ex vivo* experiment, the geometric means (standard deviation) of the ratio of MDCO-216 stimulated IL-6 over background levels were 0.8 (1.9), 0.7 (1.5), 1.0 (2.0) for respectively HV, sCAD, aCAD. The corresponding ETC-216 stimulated values were 15.8 (2.9), 9.5 (3.6), 3.8 (4.0). TNF-α results were comparable. Because many ETC-216 stimulated samples had cytokine concentrations > ULOQ, ratios were categorised and marginal homogeneity of the contingency table (MDCO-216 *vs.* ETC-216) was assessed with the Stuart-Maxwell test. *P*-values were ⩽0.0005 for all populations.

MDCO-216 did not induce adverse immunostimulation in HV and sCAD patients, in contrast to ETC-216. Results from the *ex vivo* stimulation suggest the same holds true for aCAD patients.

Over the past decades, high density lipoprotein (HDL) and Apolipoprotein A-I (ApoA-I) have been targeted in the pursuit of therapies that reduce the risk of cardiovascular events.[1] One of these therapies is ApoA-I Milano ($ApoA\text{-}I_M$), a naturally occurring mutant of ApoA-I, which was found to be associated with cardioprotective effects.[2,3]

Because of these effects, a human recombinant $ApoA\text{-}I_M$, codenamed ETC-216, was developed by Esperion Therapeutics in the nineties. *In vitro* results with recombinant $ApoA\text{-}I_M$ demonstrated enhanced reverse cholesterol transport, and, in animal models, regression of atherosclerotic plaques was observed.[4]

ETC-216 induced profound lipid changes in the initial phase I study (unpublished results), resulting in a lipid profile that closely resembled carriers of the $ApoA\text{-}I_M$ mutation. However, dose-dependent increases in neutrophils, parallelling decreases in lymphocytes were observed as well. This phenomenon

was first seen in males at a dose level of 50 mg/kg (neutrophil increase > 200%), and in females at a dose level of 15 mg/kg (increase ~80%).

After decreasing the infusion rate from 1.67 to 1.25 mg kg^{-1} min^{-1} for males and 0.83 mg kg^{-1} min^{-1} for females, a dose of 100 mg/kg in males and a dose of 50 mg/kg in females was required to induce equal changes in neutrophils and lymphocytes (*figure 5.1*). Maximum change from baseline in white blood cell counts was observed at 4 h after the start of the infusion, returning to baseline twenty hours later.

A similar dose-dependent pattern was seen for the adverse events reported within 24 h of administration. Following 15 mg/kg ETC-216 in healthy females, and following 50 mg/kg ETC-216 in healthy males, respectively 2/3 and 1/3 participants developed gastrointestinal symptoms (nausea, vomiting, diarrhoea). Lowering the infusion rate reduced the incidence of these events; however, at 100 mg/kg, 3/3 participants reported gastrointestinal symptoms. These events occurred approximately 2–4 h after infusion and were sometimes accompanied by systemic symptoms, such as diaphoresis and changes in body temperature.

In the subsequently executed phase II study in patients with an acute coronary syndrome (ACS),[5] it was shown that ETC-216 doses up to 45 mg/kg were associated with a significant regression of the atherosclerotic burden. Not many adverse events were reported, although in a single patient a possible hypersensitivity reaction was noted, consisting of gastrointestinal complaints, rash, chills, and diaphoresis.

Despite the overall promising results, clinical development was halted after a serious adverse reaction in one patient had occurred early during the third clinical trial. When administered intravenously within the hour after percutaneous coronary intervention (PCI), a patient developed a severe reaction during infusion, consisting of flushing, chills, and hypotension, ultimately leading to multi-organ failure.

Because the available data pointed to a systemic inflammatory reaction, contamination of the infused drug product was considered. Careful evaluation of the entire manufacturing process revealed that ETC-216 contained small quantities of residual host cell proteins (HCPs) that elicited an immune response (unpublished results). Importantly, these effects remained undetected during preclinical development, and became apparent only when the drug was administered to humans, even though all appropriate standards and guidelines had been followed.

A component of the HCPs in the ETC-216 drug product was demonstrated to be flagellin, using an assay

TABLE 5.1 Investigated populations

	HV	sCAD	aCAD
Inclusion criteria			
Age (years)	18–55	45–80	⩾18
Body weight (kg)	⩽110	⩽110	—
BMI (kg m^{-2})	18–25	⩽40	—
Coronary event	—	requiring a revascularisation procedure	requiring an acute revascularisation procedure
Latency between event and exposure	—	⩾1 year	immediately prior to the revascularisation procedure
Concomitant therapy	not allowed, except for oral contraceptives	standard of care, except for HDL-raising therapy	standard of care
Exposure details			
In vivo	single dose MDCO-216 5–40 mg/kg ($n = 16$) or placebo ($n = 8$) in 2 h	single dose MDCO-216 10–40 mg/kg ($n = 16$) or placebo ($n = 8$) in 2 h	—
Ex vivo	ETC-216 0.5 mg/mL MDCO-216 0.5 mg/mL	ETC-216 0.5 mg/mL MDCO-216 0.5 mg/mL	ETC-216 0.5 mg/mL MDCO-216 0.5 mg/mL

Inclusion criteria for the different populations and details of *in* and *ex vivo* exposure.
aCAD: patients with acute coronary artery disease (CAD) | HV: healthy volunteers | sCAD: patients with stable coronary artery disease (CAD)

based on the human toll-like receptor (TLR)5.[6] Other impurities included an oligopeptide-binding protein (OppA), a dipeptide-binding protein (DppA), and maltose-binding periplasmic protein (MalE).[7]

Due to the physical characteristics of ApoA-I_M, reducing these impurities proved difficult, and was ultimately achieved by selectively deleting the genes encoding some of the contaminating proteins and by other significant improvements to the downstream manufacturing process.[7–9] Hereafter, recombinant ApoA-I_M was reintroduced as MDCO-216 by the Medicines Company and was tested in healthy volunteers and in patients with stable coronary artery disease (CAD).[10]

This chapter describes the results of *ex vivo* stimulation of whole blood samples with ETC-216 and MDCO-216 in three populations (healthy volunteers, patients with stable CAD, and patients with acute CAD). The aim was to characterise the differences in cytokine releasing potential between both drug products. To confirm that the HCPs that induced an inflammatory response were indeed successfully eliminated, the *in vivo* experience with MDCO-216 was compared to the *ex vivo* results.

METHODS

Populations

Table 5.1 summarises the inclusion criteria of the investigated populations; these encompass both the *in vivo* and *ex vivo* exposed populations. Data on the *in vivo* experience with MDCO-216 came from a randomised, double-blind phase I clinical trial,[10] in which 24 healthy volunteers (HV) and 24 patients with stable CAD (sCAD) received a single intravenous dose of 5–40 mg/kg MDCO-216 or placebo.

All subjects enrolled in this trial were also challenged *ex vivo* with both ETC-216 and MDCO-216, together with those screened for participation and meeting the criteria as listed in *table 5.1*. All trial participants provided written informed consent.

Acute CAD (aCAD) patients were recruited from patients with an acute coronary syndrome (ACS) who presented to the department of cardiology of the Leiden University Medical Center (Leiden, The Netherlands) for a percutaneous coronary intervention (PCI). After verbal approval, the blood sample for *ex vivo* stimulation was collected alongside the routine clinical samples. Written consent was asked at a later stage; if not provided, the blood sample was destroyed and not analysed.

Approval was obtained from independent ethics committees for all trials and related procedures prior to the start of the respective studies, in accordance with pertaining legal requirements.

Ex vivo exposure

Ex vivo stimulations were performed at Good Biomarker Sciences (GBS, Leiden, The Netherlands). Heparinised whole blood samples (18 mL, BD Vacutainer, Becton Dickinson, Breda, The Netherlands) were collected and incubated for 4 h at 37°C in a humidified atmosphere with 5% CO_2, before flash-freezing the supernatant for subsequent analysis.

Tested conditions were 0.5 mg/mL ETC-216 or MDCO-216 (The Medicines Company, Zürich, Switzerland), 2 ng/mL lipopolysaccharide (LPS) gel extracted from *E. coli* serotype O111:B4 (Sigma-Aldrich, St. Louis, Missouri, USA), and blank (unstimulated control). The concentration of 0.5 mg/mL for ETC-216 and MDCO-216 correlates with the maximum plasma concentration achieved following an *in vivo* dose of 20–30 mg/kg. LPS concentration was based on the EC_{90} of maximum TNF-α release and served as a positive control. Conditions were made in RPMI with 25 mM HEPES and L-glutamine (Gibco products from Life Technologies Europe, Bleiswijk, the Netherlands). Final dilution of whole blood required to achieve the tested concentrations was 10%.

Ex vivo exposure of a subject to MDCO-216 always occurred prior to any *in vivo* exposure (HV and sCAD). Blood samples were kept at 37°C and processed within one hour after collection, with the exception of the aCAD population, where an interval of up to 12 h was allowed, to increase the number of evaluable samples. Additionally, these samples from aCAD patients were kept at room temperature, since this reduces cell death and subsequent lack in responsiveness upon stimulation (data on file).

Safety assessments

Safety assessments after *in vivo* exposure were performed at regular intervals during the follow up period. These consisted of vital signs, 12-lead electrocardiograms, physical examination, registration

of adverse events, and routine clinical chemistry and haematology evaluation. Safety blood samples were collected and analysed in accordance with local protocols.

Cytokines

TNF-α and IL-6 were quantitated in culture supernatants and in plasma samples by GBS. For supernatants, a R&D Quantikine ELISA assay (R&D Systems, Inc., Minneapolis, USA) was used, and for plasma samples, a R&D Quantikine HS ELISA assay. All samples from one subject were assayed in one run. LPS stimulated samples were initially measured after 20-fold and 50-fold dilution, for TNF-α and IL-6 respectively, in the manufacturer provided diluents. Other samples were initially measured undiluted. Samples were remeasured with higher dilution as needed.

TNF-α and IL-6 values in the supernatants were accepted if duplicates were <20% coefficient of variation for values within the calibration range: LLOQ (lower limit of quantification) 15.6 pg/mL and 3.1 pg/mL, and ULOQ (upper limit of quantification) 1,000 pg/mL and 300 pg/mL for TNF-α and IL-6, respectively. TNF-α and IL-6 values in the plasma samples were accepted if duplicates were <20% coefficient of variation for values within the calibration range: LLOQ 0.5 pg/mL and 0.16 pg/mL, and ULOQ 32 pg/mL and 10 pg/mL for TNF-α and IL-6, respectively.

Statistical analysis

All available data were included in the analyses unless otherwise indicated. Values <LLOQ or >ULOQ were replaced by respectively the LLOQ or ULOQ, as appropriate. Log-normally distributed parameters were ln-transformed prior to analysis.

Individual ratios of stimulated cytokine levels over unstimulated (background) levels were calculated and compared statistically. In case of background levels <LLOQ or stimulated levels >ULOQ, the corresponding ratio (respectively [stimulated]/LLOQ or ULOQ/[unstimulated]) was regarded as the lower margin of the interval (calculated ratio,∞] for the purpose of categorical data analysis.

Continuous data were primarily analysed using an analysis of variance, which could include a covariance analysis to correct for confounding factors. Contrasts

TABLE 5.2 Population characteristics

PARAMETER	EXPOSED *IN VIVO*				EXPOSED *EX VIVO*					
	HV ($n=24$)		sCAD ($n=24$)		HV ($n=35$)		sCAD ($n=35$)		aCAD ($n=35$)	
Age (year)	26.2	(8.6)	62.8	(7.0)	24.6	(7.5)	64.0	(7.8)	64.4	(12.9)
Height (cm)	175	(8.7)	177	(6.7)	176	(8.7)	177	(6.3)	176	(10.7)
Body weight (kg)	70.0	(11.3)	85.0	(12.8)	69.8	(10.8)	86.5	(13.3)	81.4	(19.2)
BMI (kg m^{-2})	22.5	(1.8)	27.0	(3.3)	22.3	(1.9)	27.4	(3.3)	26.1	(5.3)
Gender										
Female (*n*)	14	(58%)	1	(4%)	18	(51%)	1	(3%)	11	(31%)
Male (*n*)	10	(42%)	23	(96%)	17	(49%)	34	(97%)	24	(69%)
Revascularisation procedure										
CABG (*n*)	—		12	(50%)	—		14	(40%)	0	
PCI (*n*)	—		12	(50%)	—		21	(60%)	35	(100%)
Coronary involved										
Cx (*n*)	—		6	(25%)	—		10	(29%)	15	(43%)
LAD (*n*)	—		7	(29%)	—		8	(23%)	19	(54%)
RCA (*n*)	—		6	(25%)	—		12	(34%)	15	(43%)
Unknown (*n*)	—		10	(42%)	—		13	(37%)	12	(34%)

Mean (standard deviation) or number (percentage) for different populations, who were exposed *in vivo* to MDCO-216 or who were exposed *ex vivo* to both MDCO-216 and ETC-216.

aCAD: patients with acute coronary artery disease (CAD) | CABG: coronary artery bypass grafting | Cx: circumflex artery
HV: healthy volunteers | LAD: left anterior descending artery | PCI: percutaneous coronary intervention | RCA: right coronary artery
sCAD: patients with stable coronary artery disease (CAD)

TABLE 5.3 *Ex vivo* **results**

	HV (*n* = 35)		sCAD (*n* = 35)		aCAD (*n* = 35)	
IL-6						
LPS	797.7	(1.9)	933.5	(2.0)	62.1	(6.5)
ETC-216[a]	15.8	(2.9)	9.5	(3.6)	3.8	(4.0)
MDCO-216	0.8	(1.9)	0.7	(1.5)	1.0	(2.0)
TNF-α						
LPS	117.4	(1.9)	242.0	(1.8)	46.9	(4.0)
ETC-216[a]	9.0	(2.8)	6.0	(3.8)	3.5	(4.0)
MDCO-216	0.8	(1.8)	0.7	(1.9)	1.0	(2.0)

Geometric mean (standard deviation) of ratios of LPS, ETC-216, and MDCO-216 stimulated cytokine concentration over unstimulated (background) levels for IL-6 and TNF-α.

a. Ratios are underestimated as a result of stimulated samples being >ULOQ: for IL-6 in 26 (74.3%) HV, 19 (54.3%) sCAD, 16 (45.7%) aCAD; and for TNF-α in 20 (57.1%) HV, 24 (68.6%) sCAD, 6 (17.1%) aCAD.

aCAD: patients with acute coronary artery disease (CAD) | HV: healthy volunteers | LPS: lipopolysaccharide | sCAD: patients with stable coronary artery disease (CAD) | ULOQ: upper limit of quantification

and effects (with 95% confidence intervals) were calculated as relevant according to the Tukey method. If the assumption of equal variance was not met, multiple Welch's t-tests were performed to evaluate the validity of the statistical results. Categorical data were analysed in a logistic regression model, which could include a covariance analysis to correct for confounding factors. For contingency tables, marginal homogeneity was tested with the Stuart-Maxwell test.

Data analysis was performed with R (v2.15.2, R Foundation for Statistical Computing, Vienna, Austria, 2012). Results are presented as mean (standard deviation or 95% confidence interval) for continuous data, and as number (percentage) for categorical data, unless otherwise specified.

RESULTS

Ex vivo exposure

In total, 35 HV and 35 sCAD patients, who were screened for participation in the MDCO-216 phase I clinical trial, had evaluable results following *ex vivo* exposure and were included in the analysis. Additionally, 38 aCAD patients signed informed consent and provided a blood sample for *ex vivo* testing in the prespecified period (October 2013 to May 2014), of whom 35 had evaluable results and were included in the analysis. Baseline characteristics of the different populations are presented in *table 5.2*.

Table 5.3 presents the released IL-6 upon stimulation of whole blood samples with either ETC-216 or MDCO-216 in relation to background IL-6 levels. From this table, it is seen that ETC-216 clearly elicited a cytokine response, especially when compared to MDCO-216, which seemingly inhibited spontaneous (unstimulated) cytokine release, with a geometric mean ratio of 0.7–1.0, for respectively sCAD and aCAD. This was not caused by an interference of MDCO-216 in the measurement of IL-6, as was determined by measuring a sample with known cytokine levels with and without spiking of MDCO-216 just prior to analysis.

Because many ETC-216 stimulated samples had cytokine concentrations >ULOQ (*e.g.* HV: 26 [74.3%] for IL-6 and 20 [57.1%] for TNF-α), preventing the use of an analysis of variance, the ratios of ETC-216 and MDCO-216 stimulated over background levels were categorised and marginal homogeneity of the contingency table of MDCO-216 *vs.* ETC-216 was statistically tested with the Stuart-Maxwell test. Categories were chosen as <0.2, $[0.2,0.5)$, $[0.5,1)$, $[1,2)$, $[2,5)$, ≥ 5, based on the fact that virtually all >ULOQ values resulted in a ratio greater than 5. For IL-6, the thus obtained *p*-values under the null hypothesis of marginal homogeneity were $<10^{-5}$, $<10^{-5}$, and 0.0004 for HV, sCAD, and aCAD, respectively; the corresponding results for TNF-α were $<10^{-5}$, $<10^{-4}$, and 0.0005, indicating that ETC-216 and MDCO-216 yielded statistically significantly different cytokine responses.

When comparing the different populations, ETC-216 generally induced lower IL-6 release in the CAD patients than in healthy volunteers. Lower ratios in the CAD populations were also obtained for the MDCO-216 stimulated samples, but LPS exposure resulted in a lower ratio in the aCAD population only. These differences could not be related to age, weight, BMI, blood pressure, (differential) leucocyte count, the severity of the CAD based on total obstruction, the coronary involved, or the type of revascularisation procedure.

The *ex vivo* results in the aCAD population did not substantially differ from those obtained in the sCAD population. However, some acute CAD patients had considerably higher background (unstimulated) IL-6 levels, up to 2,664 pg/mL (median 37.3), compared to a maximum of 84.4 pg/mL (median 14.1) in sCAD.

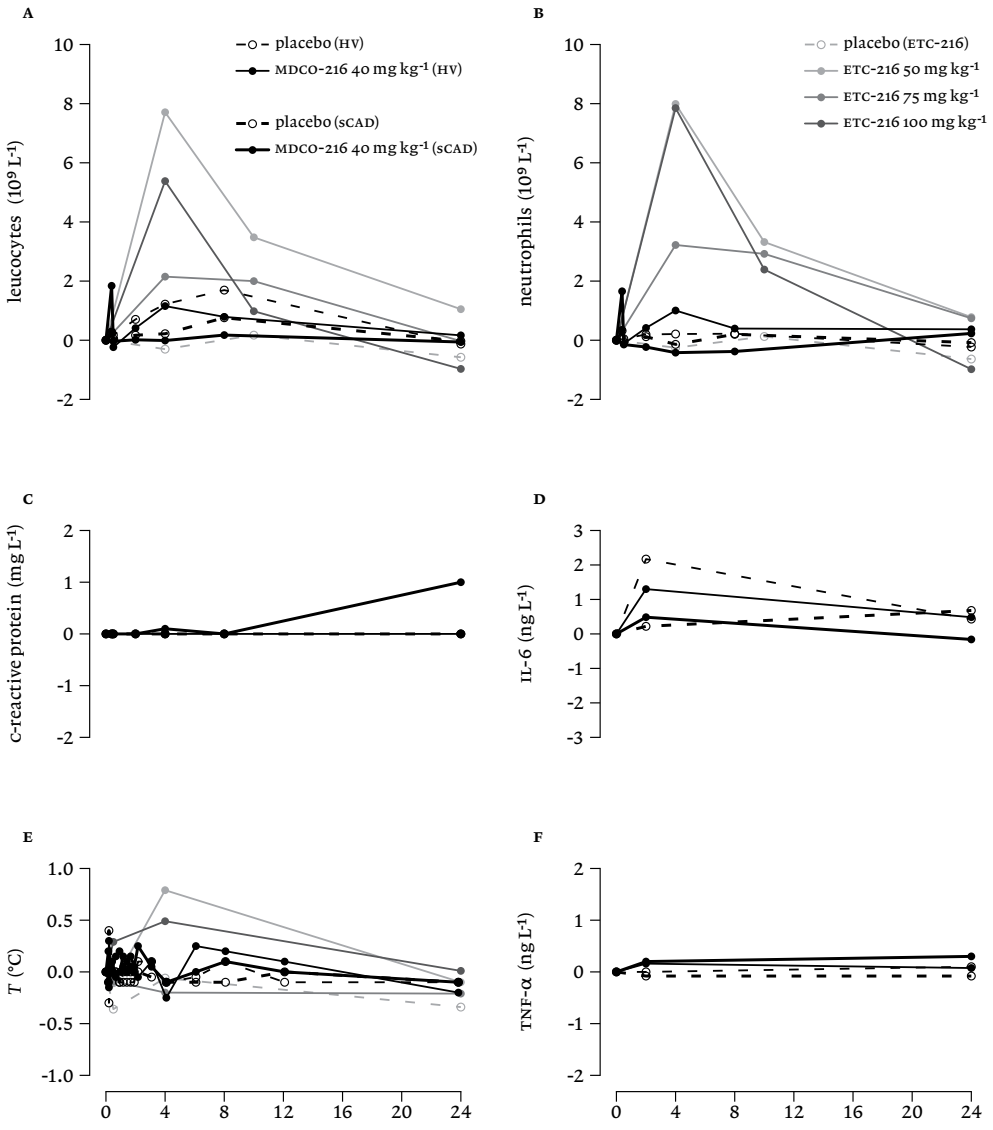

FIGURE 5.1 ***In vivo*** **results**

Absolute change (median) over time in clinical markers of inflammation is displayed for placebo and the highest dose (40 mg/kg) of MDCO-216 in healthy volunteers (HV) and in patients with stable coronary artery disease (sCAD): white cell counts (A), neutrophil counts (B), C-reactive protein (C), IL-6 levels (D), body temperature (E), and TNF-α levels (F). As a reference, the median profiles over time in males in the placebo and highest dose groups from the (unpublished) phase I ETC-216 trial are projected in the background. Of note, 75 mg/kg and 100 mg/kg of ETC-216 were administered at half the infusion rate as was 50 mg/kg of ETC-216 (see main body). Oral temperature served as body temperature in the ETC-216 phase I trial, whereas tympanic membrane temperature was used in the MDCO-216 phase I trial.

A relationship could not be detected between background levels and demographics or clinical parameters, such as severity of the coronary syndrome based on total coronary obstruction as estimated during acute angiography.

Bioanalytical causes for this phenomenon were not found, neither could the high background levels be related to the interval between sample collection and processing. Albeit true that a time-dependent decrease in cytokine response was observed, a prolonged interval was not associated with higher background levels, and judging from the ratios, the overall effects of ETC-216, MDCO-216, and LPS in these samples were consistent with the results obtained from samples that were processed immediately after collection (data not shown).

Statistical significance was reached for the population differences in MDCO-216 and LPS stimulated results, based on an analysis of variance of the ln-transformed ratios over background (unstimulated) cytokine levels, which included sex as covariate. For LPS, the difference in TNF-α ratios between the sCAD and HV population was 206% (95% confidence interval [CI]: 120–355, $p = 0.0057$), between aCAD and HV 40% (24–68, $p = 0.0002$), and between aCAD and sCAD 19% (11–33, $p < 10^{-9}$). For MDCO-216, only the difference between sCAD and aCAD populations was statistically significant (IL-6: ratio 69% [95% CI: 50–95], $p = 0.0170$; TNF-α: ratio 67% [48–94], $p = 0.0169$). Other covariates were not found to have a statistically significant effect, nor improved the model fit.

Population differences were difficult to test statistically for the ETC-216 stimulated condition and IL-6 results following LPS stimulation, due to many stimulated cytokine levels being >ULOQ. Analysing a reduced dataset which only included values <ULOQ resulted in underpowered comparisons. Attempts to fit a multinomial regression model after categorising the data failed for the same reason.

In vivo exposure

Table 5.2 lists the baseline characteristics of the populations exposed to MDCO-216 *in vivo*. The most commonly used medication by stable CAD patients was an antithrombotic agent (96%), mainly acetylsalicylic acid (83%). Statins were used by 92%, β-blockers by 58%, and ACE-inhibitors by 38% of the patients.

In the HV population exposed to MDCO-216, two subjects complained of abdominal pain or distension, one (50%) in the 10 mg/kg group and one (25%) in the 20 mg/kg group, which started 9 h after administration. Stable CAD patients receiving MDCO-216, reported nausea once (4 h post-dose, 20 mg/kg group) and diarrhoea once (13 h post-dose, 40 mg/kg). The latter case was a patient who had undergone a cholecystectomy and since then regularly developed diarrhoea after ingesting high-fat meals.

No inflammatory reaction was observed in HV and sCAD patients, judging by body temperature, white cell counts, neutrophil counts, C-reactive protein, and circulating cytokines (*figure 5.1*).

DISCUSSION

Recombinant proteins represent a powerful class of drugs that is employed to supplement absent or insufficient quantities of essential enzymes, hormones, and coagulation factors. Additionally, peptides can be designed to specifically interact with cells or receptors and thus interfere in the pathophysiology of certain diseases.[11–13]

However, since these proteins or peptides are invariably expressed in allogeneic, often non-human, cell systems, foreign material is released into the medium together with the protein of interest. Countless impurities can trigger the immune system; especially bacterial based platforms, such as those using *Escherichia coli*, are notorious suppliers of immunostimulatory impurities like endotoxin (lipopolysaccharide or LPS).[14] Also, the remaining proteins in a pharmaceutical, collectively referred to as host cell proteins (HCPs), can potentially elicit an inflammatory reaction.[15]

ETC-216, expressed in *E. coli*, was approved for intravenous administration to humans in accordance with all pertaining regulatory guidelines. Specifically, the limulus amoebocyte lysate (LAL) test was negative, HCP levels were ⩽10 ppm, and each dose contained <10 ng of residual DNA.

Nevertheless, administration of ETC-216 to healthy volunteers induced dose-dependent neutrophilic leucocytosis, increases in body temperature, and gastrointestinal side effects. In CAD patients, hypersensitivity-like reactions were observed as well as gastrointestinal side effects. In retrospect, these findings are easily recognised as signs and symptoms of an inflammatory response caused by the HCP impurities.

After several modifications were made to the manufacturing process to reduce the HCP levels, the recombinant APOA-I_M was reintroduced as MDCO-216. Because it was deemed unethical to expose a human population to a product with a known immunostimulatory propensity (ETC-216), an *ex vivo* whole blood incubation assay was applied to compare differences in cytokine response to MDCO-216 and ETC-216.

Results demonstrated that ETC-216 clearly induced cytokine release, in contrast to MDCO-216. In HV and SCAD patients, MDCO-216 even slightly inhibited (spontaneous) release. This difference was statistically significant for all populations, with p-values $\leqslant 0.0005$. The observed inhibition of approximately 30% by MDCO-216 is in accordance with previous studies that have reported that HDL or HDL-like particles display many anti-inflammatory properties.[16]

The absence of an inflammatory reaction was confirmed in a clinical trial with MDCO-216. No increases in neutrophils were observed following MDCO-216 infusion in HV and SCAD patients. Also, the more sensitive biomarkers (C-reactive protein and circulating cytokines) did not suggest immune stimulation by MDCO-216. Additionally, the observed gastrointestinal side effects did not display a dose-relationship as was seen for ETC-216, although it should be noted that MDCO-216 was infused at a lower rate compared to ETC-216.

An interesting question to be asked is whether an *ex vivo* incubation assay can be implemented to detect adverse immune stimulation. Certainly, a whole blood stimulation test can detect a myriad of pyrogenic substances, such as LPS, porins, lipoteichoic acid (LTA) and peptidoglycan.[17–22] Nonetheless, many uncertainties still surround the interpretation of its result.[23] Our results revealed differences in reactivity between the three tested populations, not only with regard to the HCP impurities in ETC-216, but also to LPS, which highlights some of the uncertainties. For example, LPS stimulation resulted in higher cytokine responses in SCAD patients compared to HV, and ETC-216 induced lower levels in SCAD patients compared to HV. After correction for the differences in monocyte count, the statistically significant differences remained. Other factors, such as age, BMI, and blood pressure, could not explain any of the found effects.

Comorbidities may have influenced the response, as – for example – hypertension was previously found by Dörffel *et al.*[24] to increase TNF-α and IL-1β secretion from peripheral blood monocytes after *in vitro* LPS stimulation by >50%, although these patients were untreated. The antihypertensives losartan, captopril, and amlodipine dose-dependently reduced IL-1β release induced by LPS, but not below LPS stimulated levels in normotensive subjects.[25]

Other cardiovascular medications are also known to influence the (innate) immune response. For example, certain calcium channel blockers were observed to interfere with both flagellin and LPS signalling.[26,27] Statins and aspirin demonstrate similar anti-inflammatory properties.[28–30] Interestingly however, whereas many cardiovascular drugs inhibit TLR4-mediated responses, with β-blockers being a notable exception,[31,32] *ex vivo* LPS stimulation induced higher cytokine levels in SCAD patients than in HV. Although effects of certain cardiovascular medications and conditions on toll-like receptor signalling have not been examined as extensively for TLR5 (flagellin) as for TLR4 (LPS), our results suggest that the response to flagellin and other HCP impurities can be modified by these factors as well.

Notwithstanding the aforementioned effects, compared to stable CAD patients, acute CAD patients displayed higher background cytokine levels, as well as an overall diminished responsiveness to both LPS and ETC-216. Severity of the coronary disease, based on total obstruction, or the coronary involved, was not related to background cytokine levels, or any of the observed effects after *ex vivo* stimulation with LPS, ETC-216, or MDCO-216.

ACS is associated with elevated plasma levels of pro-inflammatory cytokines, chemokines, and leucocytes, which are governed at least partly by TLR4 stimulation.[33,34] Conversely, stress hormones, such as catecholamines and hydrocortisone, that have a general immune-inhibiting mode of action, are increased in parallel.[35–37] This combination might explain both the high background cytokine levels and the reduced response to ETC-216 observed in the aCAD patients. TLR4-mediated cytokine release in ACS can also account for the observation that a subsequent (experimental) LPS challenge did only modestly increase IL-6 and TNF-α concentrations *ex vivo*.

It should be stressed, however, that although (the consequences of) an inflammatory response can be influenced by external factors, a reduced response is not synonymous with an improved outcome, especially in critically ill patients. This warrants a cautious approach when exposing (vulnerable) humans to an

experimental biopharmaceutical. Furthermore, it underlines the current limitations of an *ex vivo* stimulation test in reliably predicting inflammatory reactions upon *in vivo* administration in the target population, although it can be used to highlight differences between two pharmacological products within a population.

Concluding, MDCO-216 does not elicit an acute immune response in healthy volunteers nor in patients with stable coronary artery disease, in contrast to what was previously observed with ETC-216. Results from an *ex vivo* stimulation with both products suggest the same holds true for patients with an acute coronary syndrome.

REFERENCES

1 Boekholdt SM, Arsenault BJ, Hovingh GK, *et al.* Levels and changes of HDL cholesterol and apolipoprotein A-I in relation to risk of cardiovascular events among statin-treated patients: a meta-analysis. *Circulation* 2013; **128**: 1504–12.

2 Franceschini G, Sirtori CR, Capurso A, Weisgraber KH, Mahley RW. A-IMilano apoprotein. Decreased high density lipoprotein cholesterol levels with significant lipoprotein modifications and without clinical atherosclerosis in an Italian family. *J Clin Invest* 1980; **66**: 892–900.

3 Franceschini G, Sirtori CR, Bosisio E, *et al.* Relationship of the phenotypic expression of the A-IMilano apoprotein with plasma lipid and lipoprotein patterns. *Atherosclerosis* 1985; **58**: 159–74.

4 Nicholls SJ, Uno K, Kataoka Y, Nissen SE. ETC-216 for coronary artery disease. *Expert Opin Biol Ther* 2011; **11**: 387–94.

5 Nissen SE, Tsunoda T, Tuzcu EM, *et al.* Effect of recombinant ApoA-I Milano on coronary atherosclerosis in patients with acute coronary syndromes: a randomized controlled trial. *JAMA* 2003; **290**: 2292–300.

6 Huang L-Y, Dumontelle JL, Zolodz M, Deora A, Mozier NM, Golding B. Use of toll-like receptor assays to detect and identify microbial contaminants in biological products. *J Clin Microbiol* 2009; **47**: 3427–34.

7 Caparon MH, Rust KJ, Hunter AK, *et al.* Integrated solution to purification challenges in the manufacture of a soluble recombinant protein in *E. coli*. *Biotechnol Bioeng* 2010; **105**: 239–49.

8 Hunter AK, Suda EJ, Herberg JT, *et al.* Separation of recombinant apolipoprotein A-IMilano modified forms and aggregates in an industrial ion-exchange chromatography unit operation. *J Chromatogr A* 2008; **1204**: 42–7.

9 Hunter AK, Wang X, Suda EJ, *et al.* Separation of product associating *E. coli* host cell proteins OppA and DppA from recombinant apolipoprotein A-I milano in an industrial HIC unit operation. *Biotechnol Prog* 2009; **25**: 446–53.

10 Kallend DG, Reijers JAA, Bellibas SE, *et al.* A single infusion of MDCO-216 (ApoA-1 Milano/POPC) increases ABCA1-mediated cholesterol efflux and pre-beta 1 HDL in healthy volunteers and patients with stable coronary artery disease. *Eur Hear journal Cardiovasc Pharmacother* 2016; **2**: 23–9.

11 Buckel P. Recombinant proteins for therapy. *Trends Pharmacol Sci* 1996; **17**: 450–6.

12 Walsh G. Biopharmaceutical benchmarks 2014. *Nat Biotechnol* 2014; **32**: 992–1000.

13 Sanchez-Garcia L, Martín L, Mangues R, Ferrer-Miralles N, Vázquez E, Villaverde A. Recombinant pharmaceuticals from microbial cells: a 2015 update. *Microb Cell Fact* 2016; **15**: 33.

14 Terpe K. Overview of bacterial expression systems for heterologous protein production: from molecular and biochemical fundamentals to commercial systems. *Appl Microbiol Biotechnol* 2006; **72**: 211–22.

15 Wang X, Hunter AK, Mozier NM. Host cell proteins in biologics development: identification, quantitation and risk assessment. *Biotechnol Bioeng* 2009; **103**: 446–58.

16 Vuilleumier N, Dayer J-M, Von Eckardstein A, Roux-Lombard P. Pro- or anti-inflammatory role of apolipoprotein A-1 in high-density lipoproteins? *Swiss Med Wkly* 2013; **143**: w13781.

17 Cusumano V, Tufano MA, Mancuso G, *et al.* Porins of Pseudomonas aeruginosa induce release of tumor necrosis factor alpha and interleukin-6 by human leukocytes. *Infect Immun* 1997; **65**: 1683–7.

18 Nakagawa Y, Maeda H, Murai T. Evaluation of the *in vitro* pyrogen test system based on proinflammatory cytokine release from human monocytes: comparison with a human whole blood culture test system and with the rabbit pyrogen test. *Clin Diagn Lab Immunol* 2002; **9**: 588–97.

19 Hermann C, Von Aulock S, Graf K, Hartung T. A model of human whole blood lymphokine release for in vitro and ex vivo use. *J Immunol Methods* 2003; **275**: 69–79.

20 Popa C, Netea MG, Barrera P, *et al.* Cytokine production of stimulated whole blood cultures in rheumatoid arthritis patients receiving short-term infliximab therapy. *Cytokine* 2005; **30**: 72–7.

21 Draing C, Pfitzenmaier M, Zummo S, *et al.* Comparison of lipoteichoic acid from different serotypes of *Streptococcus pneumoniae*. *J Biol Chem* 2006; **281**: 33849–59.

22 Meron-Sudai S, Matityahou A, Keisari Y, Cox KH, Hasty DL, Ofek I. Lipoteichoic acid synergizes with glycosphingolipids to potently stimulate secretion of interleukin-6 from human blood cells. *Clin Vaccine Immunol* 2008; **15**: 1309–15.

23 Vidal J-M, Kawabata TT, Thorpe R, *et al. In vitro* cytokine release assays for predicting cytokine release syndrome: the current state-of-the-science. Report of a European Medicines Agency Workshop. *Cytokine* 2010; **51**: 213–5.

24 Dörffel Y, Latsch C, Stuhlmuller B, *et al.* Preactivated peripheral blood monocytes in patients with essential hypertension. *Hypertension* 1999; **34**: 113–7.

25 Nemati F, Rahbar-Roshandel N, Hosseini F, Mahmoudian M, Shafiei M. Anti-inflammatory effects of anti-hypertensive agents: influence on interleukin-1β secretion by peripheral blood polymorphonuclear leukocytes from patients with essential hypertension. *Clin Exp Hypertens* 2011; **33**: 66–76.
26 Li G, Qi XP, Wu XY, *et al.* Verapamil modulates LPS-induced cytokine production via inhibition of NF-kappa B activation in the liver. *Inflamm Res* 2006; **55**: 108–13.
27 Chen Y-L, Chen Y-S, Lin H-H, Chan C-W, Chen S-C, Chen C-H. Immunostimulatory flagellin from *Burkholderia pseudomallei* effects on an increase in the intracellular calcium concentration and up-regulation of TNF-alpha by mononuclear cells. *Microbiol Immunol* 2007; **51**: 81–6.
28 Sadowitz B, Maier KG, Gahtan V. Statin therapy—part I: the pleiotropic effects of statins in cardiovascular disease. *Vasc Endovascular Surg* 2010; **44**: 241–51.
29 Akinosoglou K, Alexopoulos D. Use of antiplatelet agents in sepsis: a glimpse into the future. *Thromb Res* 2014; **133**: 131–8.
30 Ruggieri A, Gambardella L, Maselli A, *et al.* Statin-induced impairment of monocyte migration is gender-related. *J Cell Physiol* 2014; **229**: 1990–8.
31 Yurinskaya MM, Vinokurov MG, Grazhdankin EB, Grachev SV. The effect of propranolol on LPS-induced activation of human neutrophils. *Dokl Biochem Biophys* 2010; **435**: 330-3.
32 Stanojević S, Dimitrijević M, Kuštrimović N, Mitić K, Vujić V, Leposavić G. Adrenal hormone deprivation affects macrophage catecholamine metabolism and β2-adrenoceptor density, but not propranolol stimulation of tumour necrosis factor-α production. *Exp Physiol* 2013; **98**: 665–78.
33 Fang L, Moore X-L, Dart AM, Wang L-M. Systemic inflammatory response following acute myocardial infarction. *J Geriatr Cardiol* 2015; **12**: 305–12.
34 Liebetrau C, Hoffmann J, Dörr O, *et al.* Release kinetics of inflammatory biomarkers in a clinical model of acute myocardial infarction. *Circ Res* 2015; **116**: 867–75.
35 Logan RW, Murdoch WR. Blood-levels of hydrocortisone, transaminases, and cholesterol after myocardial infarction. *Lancet* 1966; **2**: 521–4.
36 Hansen B, Beck-Nielsen J, Juul J, Nielsen BL, Nielsen FU. Plasma-hydrocortisone values in heart disease. Results after acute myocardial infarction (with and without cardiogenic shock) and in patients with congestive heart failure. *Acta Med Scand* 1969; **186**: 411–6.
37 Sigurdsson A, Held P, Swedberg K. Short- and long-term neurohormonal activation following acute myocardial infarction. *Am Heart J* 1993; **126**: 1068–76.

CHAPTER VI

Adverse immunostimulation caused by impurities: the dark side of biopharmaceuticals

J.A.A. Reijers, K.E. Malone, J.J. Bajramovic, R. Verbeek, J. Burggraaf, M. Moerland

Drug safety is an important issue, especially in the experimental phases of development. Adverse immunostimulation (AI) is sometimes encountered following treatment with biopharmaceuticals, which can be life-threatening if it results in a severe systemic inflammatory reaction. Biopharmaceuticals that unexpectedly induce an inflammatory response still enter the clinic, even while meeting all regulatory requirements. Impurities (of microbial origin) in biopharmaceuticals are an often-overlooked cause of AI. This demonstrates that the current guidelines for quality control and safety pharmacology testing are not flawless.

Based on two case examples, several shortcomings of the guidelines are discussed. The most important of these are lack of sensitivity for impurities, lack of testing for other pyrogens than endotoxin, and the use of insensitive animal species and biomarkers in preclinical investigations. Moreover, testing for immunotoxicity of biopharmaceuticals is explicitly *not* recommended by the international guidelines. Publication of cases of AI is pivotal, both to increase awareness and to facilitate scientifical discussions on how to prevent AI in the future.

Whenever a new pharmaceutical enters the clinic, it is subjected to rigorous testing to ensure the safety of patients. Guidelines and regulations are designed to maintain the high standard expected by the public. Agencies and inspectors oversee the correct implementation of these regulations and guidelines by manufacturers and researchers.

This is especially important when humans are exposed for the first time to a new drug product. Recent history has seen two cases where life-threatening events occurred unexpectedly in a clinical trial. The first is TGN1412, a T-cell superagonistic anti-CD28 monoclonal antibody, administered to six healthy volunteers in 2006. Following drug administration, the trial participants developed multi-organ failure resulting from what was later termed a cytokine storm.[1] The second case is a fatality following treatment with BIA 10-2474, a FAAH-inhibitor, and although it is now more than a year after the trial was suspended, many questions into the cause remain to be answered.[2–4] Both drugs differ greatly, not only in structure and molecular size, but also in formulation, route of administration, intended target, and type of associated adverse event.

The TGN1412 case underlined once more the potentially lethal consequences of a systemic inflammatory reaction induced by a pharmaceutical and thus the importance of studying a pharmaceutical's immunostimulatory propensity during preclinical development. One therefore would expect that part of the current preclinical testing strategy is directed toward detecting activation of the immune system. However, we know from personal experience that unregistered drug products, mostly biopharmaceuticals, can unexpectedly cause adverse immunostimulation (AI, see

TABLE 6.1 Product specifications

	X	Y
Sterility (membrane filtration)	Sterile	Sterile
Endotoxin[a] (LAL-assay) (IU kg^{-1} h^{-1})	<2.3	<0.4
rDNA[a] (ng)	3[b]	0.3[c]
HCP (ppm)	⩽10	⩽50
Aggregates (SE-HPLC) (%)	<0.6	Not detected

a. Results are based on the highest (single) dose administered to humans.
b. Threshold technique
c. Quantitative polymerase chain reaction (q-PCR)
HCP: host cell protein | LAL: limulus amoebocyte lysate
SE-HPLC: size exclusion high-performance liquid chromatography (HPLC).

box 6.1) when administered to human volunteers, even while meeting all criteria set forth by the applicable guidelines (see *box 6.2*).

In this opinion, we will share our experience with two such investigational medicinal products (IMPs), illustrating how the currently employed testing strategy failed in detecting AI. Despite strict adherence to the pertaining guidelines as well as careful scientific and ethical review, AI was only first detected when these IMPs were administered to humans. These cases are not, or only partly, in the public domain and will be denoted X and Y, respectively.

CASE X

X IS A RECOMBINANT HUMAN APOLIPOPROTEIN A-I MILANO, WITH A MOLECULAR WEIGHT OF ROUGHLY 55 kDa AND DEVELOPED UNDER THE CODE NAME ETC-216.[5] It is expressed in the periplasmic space of *E. coli*, and was manufactured at fully certified and accredited facilities in the US and Western Europe. Only compendial (pharmacopoeia grade) materials were used, and in case these were not available, the used materials had to adhere to predefined internal standards. Sterility was confirmed by the membrane filtration method (*European Pharmacopoeia*, Ph.Eur.,[6] paragraph 2.6.1; *US Pharmacopoeia*, USP,[7] general chapter ‹71›) and all release criteria were met in terms of physical appearance, concentration, and desired activity. Details on the impurity content and endotoxin levels are presented in *table 6.1*.

Single dose toxicity of the drug substance was studied in rats and cynomolgus monkeys up to a dose more than tenfold the highest dose ever administered to humans (allometrically scaled). Repeated dose toxicity studies were performed with the same dose levels in rats for up to 2 weeks, and in monkeys for up to 6 weeks. Only effects that could be attributed to exaggerated pharmacology were observed and those were completely reversible. Changes in behaviour, haematology, and clinical chemistry did not occur. No relevant findings at autopsy were made.

Additionally, pharmacodynamic activity of the drug, albeit a different lot, had been studied in rabbits and in a mouse model of atherosclerosis. In this research, multiple animals died after repeated doses.

BOX 6.1 Adverse immunostimulation

Immunotoxicity caused by pharmaceuticals has been classified by the FDA in five groups,[28] which partly overlap the pathophysiologically orientated categories α–γ of immune-related adverse effects by Pichler[45] (*table 6.2*). Pichler proposed a classification specifically for biopharmaceuticals, which also categorised non-immunotoxic adverse reactions (types δ and ε). Regarding immunopathological phenomena, type α reactions (termed ‘adverse immunostimulation’ by the FDA) and hypersensitivity (type β), particularly anaphylaxis, are the most dangerous, for they can quickly become lethal. Anaphylaxis and type α reactions have in common that unbalanced propagation of an immune reaction occurs with systemic release of various mediators, which ultimately leads to widespread organ dysfunction.[46–49] In type α reactions, these mediators are cytokines,[45] resulting in a so-called cytokine storm.[48,49] The source of these cytokines is the administration of (high doses of) cytokines or the release of cytokines following treatment with a biopharmaceutical.[45] This last category includes TGN1412 and other monoclonal antibodies.[50–52] Another, often overlooked, cause for cytokine release is the presence of impurities or contaminants within pharmaceuticals, typically of microbial origin, triggering an immune response.

It should be noted that a subtle difference exists between the original definition of type α reactions and adverse immunostimulation (AI): in AI high cytokine levels are not necessarily part of the pathogenesis, and AI can also include chronic inflammation.[28] Later modifications to Pichler’s classification[52,53] broadened the definition of type α reactions toward a general pro-inflammatory concept, thus becoming more or less synonymous with the FDA’s definition of adverse immunostimulation. To further complicate uniformity, other terms appear in literature, *e.g.* (acute) infusion reactions and flu-like syndromes, which may refer to type α or type β reactions, or to both.[52–55] For the sake of simplicity, the term adverse immunostimulation (AI) will be used throughout this chapter to describe acute, systemic, inflammatory reactions. It can be a matter of discussion whether these reactions may be classified as classical type α reactions.

TABLE 6.2 Classification of immunopathological phenomena caused by biopharmaceuticals

PATHOPHYSIOLOGICAL CLASSIFICATION[45]	IMMUNOTOXICITY CLASSIFICATION[28]
Type α	Adverse immunostimulation
High cytokines	
Cytokine administration (augmented primary pharmacology)	
Cytokine release	
Type β	
Immunogenicity (immune response against pharmaceutical)	
Hypersensitivity (drug allergy), including type IV (T-cell-mediated)	Hypersensitivity
Neutralising or non-neutralising anti-drug antibodies	Immunogenicity
Type γ	
Immune deviation (by pharmaceutical)	
Immunosuppression, immunodeficiency	Immunosuppression
Immune imbalance or enhancement	
Autoimmunity	Autoimmunity
Exacerbation of existing atopy	
Induction of atopy	

The pathophysiological classification[45] includes non-immunotoxic adverse reactions, namely type δ (cross-reactivity) and type ε (non-immunological effects). Type α reactions are considered adverse immunostimulation by the FDA,[28] but the terms are not synonymous, as adverse immunostimulation can also include chronic inflammation and the underlying mechanism does not require high cytokine levels (see *box 6.1*).

The cause of these fatalities in mice was judged to be the induced disease. In rabbits, anaphylaxis developed, which was considered to be a response to repetitive exposure to a foreign protein.

In an unpublished phase I single dose study in healthy volunteers ($n = 28$, 5 dose levels), X induced dose-dependent increases in neutrophils, with a maximum at 4 h post administration. Also, the incidence of gastrointestinal symptoms – occurring 2–4 h after infusion – rose with each dose escalation, as did the incidence of diaphoresis and fever. In the next phase, in patients with an acute coronary syndrome,[8] one patient out of a group of 22 receiving the highest dose level experienced what was described as a hypersensitivity reaction. A second (unpublished) patient trial was quickly suspended after one patient on active treatment developed a severe reaction during infusion leading to multi-organ failure.

Later investigations demonstrated elevations in circulating IL-6 and TNF-α levels following administration of X in humans, which were traced back to several host cell proteins (HCPs) within X, one of which was flagellin.[9,10] The manufacturer required more than a decade to reduce or eliminate these HCPs, but in the end X could be successfully reintroduced. Clinical studies with the new drug product confirmed the absence of any cytokine response in both healthy volunteers and patients.[11,12]

CASE Y

Y IS A MUTANT FORM OF A HUMAN PLASMA protein, approximately 45 kDa in size. Years earlier, the wild type protein had been manufactured via recombinant DNA techniques and tested extensively in dozens of clinical trials. Its track record was spotless in terms of safety, other than the risks associated with its intended pharmacological action. Especially, no indication of AI was noticed in any of the performed trials, nor was AI anticipated based on the mode of action. The missense mutation (Y) was produced to increase the stability of the protein and this product had been tested in many animal models (rats, dogs, rhesus monkeys) before clinical development commenced. None of the animals ever demonstrated signs or symptoms of an inflammatory reaction, even at toxic doses.

E. coli was used to produce pharmacological grade material of Y at a fully certified and accredited facility in Western Europe. All raw materials conformed to US or EU pharmacopoeias, or were controlled by internal specifications. Sterility was confirmed by the membrane filtration method (Ph.Eur.[6] 2.6.1, USP[7] ‹71›) and all release criteria were met in terms of physical appearance, concentration, and desired activity. Details on the impurity content and endotoxin levels are presented in *table 6.1*.

TABLE 6.3 Overview of current testing strategy

CATEGORY / PARAMETER	METHOD	ACCEPTANCE CRITERION	GUIDELINES[i]
Quality control	Laboratory assessments		Q5D
Sterility (bioburden)	Culture	no growth	Ph.Eur. 2.6.1, USP ‹71›
Endotoxin (LPS)	LAL-test	<5.0 IU kg^{-1} h^{-1} (body weight)[f]	Ph.Eur. 2.6.14, USP ‹85›
	(Rabbit) pyrogen test	<0.5°C increase in 3 h[g]	Ph.Eur. 2.6.8, USP ‹151›
	Monocyte activation test (MAT)	Reaction less than the reaction induced by the allowed endotoxin contamination[f]	Ph.Eur. 2.6.30
Host cell impurities[b]	Identified and quantitated		
Residual DNA (rDNA)	PCR / hybridisation	<10 ng/dose[h] / (strict) upper limits, as appropriate	57, Ph.Eur. 01/2008:0784, USP ‹1045›
Proteins (HCP)	Immunoassay (ELISA), Western blot	(strict) upper limits, as appropriate	57, Ph.Eur. 01/2008:0784, USP ‹1045›
Virus[e]		Maximal clearance	Q5A, Ph.Eur. 01/2008:0784, USP ‹1045›
Safety pharmacology[a]	Animal toxicology	Evaluation and interpretation	S6
Safety battery			
Central nervous system toxicity	Body temperature		S7A
Cardiovascular toxicity	Heart rate		
Respiratory toxicity	Respiratory rate		
Immunotoxicity[c]			S8, 28
Standard	(Differential) leucocyte count		
	Globulin levels		
Additional[d]	Immune function (*e.g.* T-cell-dependent antibody response, natural killer cell activity, host resistance, cell-mediated immunity)		
Clinical pharmacology[a]	Human toxicology		

a. Only required for marketing authorisation, not for control of different batches (release specification)
b. Only recommended for biopharmaceuticals
c. Only recommended for chemically derived pharmaceuticals
d. Optional
e. Viral inactivation or removal is usually only tested on the cell line, not on the drug substance.
f. Notwithstanding pharmacopoeia monographs, a margin of 5.0 IU (or endotoxin unit, EU) per kg body weight per hour, or a dosing equivalent, is usually considered acceptable for parenterally administered products, with the exception of radiopharmaceuticals and intrathecally administered products, for which a lower limit is set.
g. Respective European and US pharmacopoeias are not harmonised, they differ in the number of animals included in a retest, whether maximal individual temperature responses or summed responses are used, and the exact acceptance criteria.
h A limit of 10 ng per dose is commonly suggested,[58] though it is not absolute.[25,57]
i. Guidelines include *ICH Harmonised Tripartite Guidelines* (Q5A,[59] Q5D,[60] S6,[20] S7A,[24] S8[27]), *European Pharmacopoeia*[6] general texts and monographs (Ph.Eur.), *US Pharmacopoeia*[7] general chapters (USP), and other guidelines or directives (denoted by their reference number).

HCP: host cell protein | LAL: limulus amoebocyte lysate | LPS: lipopolysaccharide (endotoxin) | PCR: polymerase chain reaction

Toxicity was examined in rats and cynomolgus monkeys at a dose more than tenfold the highest dose ever administered to humans (allometrically scaled). Only single dose toxicity studies were performed because the product was being developed as a one-dose treatment. No effects other than those expected to result from exaggerated pharmacology were detected.

In humans, dose-dependent increases in the incidence of gastrointestinal complaints and fever were observed following treatment with Y (single dose, $n \approx 10$). The severity of the reaction correlated with the peak value of C-reactive protein and plasma cytokine levels (IL-6 and TNF-α). Subsequent analyses into the cause of the events revealed that Y caused toll-like receptor (TLR)4-mediated activation despite a negative LAL-test (see *table 6.3*). Also, using a different method, > 10% protein aggregates were detected in Y. More than three years were necessary to produce a new pharmacological grade product with reduced levels of endotoxin, protein aggregates, residual DNA (rDNA) and host cell proteins. When this product was administered to healthy volunteers, no AI occurred at much higher plasma levels than were previously reached.

THE WEAKEST LINK

THESE TWO CASES RAISE THE QUESTION of how the causative impurities remained undetected or why their immunostimulatory propensity was not recognised at an earlier stage, especially since the developmental histories were not marked by carelessness. On the contrary, the products were being manufactured by renowned companies, and studied and tested by dedicated scientists. The guidelines were meticulously followed and more stringent than necessary acceptance criteria were applied (*table 6.1 & 6.3*). Yet, despite all this, unforeseen AI occurred in the clinical studies. In the following paragraphs, the most important shortcomings of the current testing strategy are identified, which allowed the culprits of AI in X and Y to escape detection in the preclinical phases of development.

It's all in the number: test sensitivity

Quality control is essentially based on using specific, validated methods of detecting unwanted components in pharmaceuticals. However, all laboratory tests have their limitations and particularly the insufficient sensitivity can be problematical. For example, Y met the endotoxin specification when tested with the LAL-assay (*table 6.1 & 6.3*); yet, subsequent investigations demonstrated TLR4-mediated activation and a specific endotoxin ELISA indicated actual levels were 10–20-fold higher than previously measured.

Although the definitive cause of the negative result in the LAL-assay remains to be elucidated, it is known from literature that the LAL-assay cannot detect certain endotoxins, such as low-molecular weight endotoxin.[13] The tests for other impurities can also give spuriously low results. Most commercially available assays for rDNA utilise an amplification technique which allows detection of only a selection of rDNA.[14] Likewise, assays for HCP quantification, typically ELISAs, only measure proteins against which antibodies were raised during the development of the assay and do not capture other sources of contamination.[15,16] The latter was the case with X, in which a process specific ELISA measured a HCP concentration that was a factor 3–4 higher than the initial result using a commercial, generical *E. coli* HCP ELISA.

Number and species: animal toxicology

AI resulting from impurities can remain undetected in safety pharmacology studies as the relevant immunological pathway may not exist in the particular animal species or is different from humans. Also, the sensitivity for bacterial products, such as endotoxin, can differ.[17] Especially, the relative incomparability of the human and murine immune system is noteworthy.[18,19] However, the guidelines also call for short-term toxicity studies in a non-rodent species in case two pharmacologically relevant species are available.[20] Commonly, a primate or dog is used for such studies with biopharmaceuticals.[21]

Although the aforementioned factors may contribute to the failure to recognise AI, a subsequent investigation with X demonstrated that it elicited a cytokine response in cynomolgus monkeys similar to humans with all the associated clinical features, such as fever, tachycardia, and increase in white blood cells. The real issue in this case therefore seems to be that either appropriately sensitive measures of AI (*e.g.* circulating cytokines) had initially not been selected or that measurements had been done too infrequently to detect AI (*e.g.* vital parameters, haematology results).

BOX 6.2 Testing for adverse immunostimulation

Before a new drug product can be studied clinically, sufficient evidence needs to be supplied regarding its safety. Tests performed to substantiate these claims fall into two main categories: quality control and safety pharmacology. Quality control encompasses laboratory assessments to verify the compound's identity by structure, amino-acid sequence, physical and chemical properties, receptor affinity and potency, and includes assessments for (product-related) impurities and contaminants. Preclinical pharmacology studies are directed toward identifying safety issues as a result of exaggerated intended pharmacodynamics (primary pharmacology) or unintended toxic effects. These studies are usually a mixture of *in vitro* (animal/human cell lines) and *in vivo* (animal) experiments. Clinical experiments with IMPs are executed once sufficient evidence has been gathered during the preclinical phases of development that the product is safe. A summary of the commonly applied tests to detect AI by IMPs is provided in *table 6.3*.

FIRST STEP: QUALITY CONTROL

All parenterally administered pharmaceuticals have to conform to the requirements regarding sterility and endotoxin content, which are captured in the national yet harmonised pharmacopoeias. Sterility is considered proven by a negative culture result of a predefined fraction of the produced batch, usually after 14 days in a suitable medium. For endotoxin, a margin of 5.0 IU per kg body weight per hour is internationally accepted (*table 6.3*). The limulus amoebocyte lysate (LAL) assay is the preferred method for measuring endotoxin levels and has largely replaced the rabbit pyrogen test. Biopharmaceuticals, such as X and Y, should be specifically tested for the presence of impurities. Residual cellular components of the manufacturing platform are recognised as potential triggers of the immune system, usually rDNA and/or HCPs. Regulatory guidelines do not prescribe specific assays and acceptance criteria, but introduce a general concept of using validated, appropriate methods and setting (strict) upper limits, which need to be justified.[25] The exact battery of tests and criteria are reviewed and approved on a case-by-case basis by the regulatory authorities. Upon approval, these quality control measures are applied as release specification for individual batches of the drug product.

SECOND STEP: SAFETY PHARMACOLOGY

For chemically derived compounds, an initial screen for potential immunotoxicity is mandatory, but not for biopharmaceuticals, because they are target-specific by design.[20,27] Indications for potential immunotoxicity are derived from animal experiments. Relevant *in vivo* signs to detect AI include changes in (differential) leucocyte counts and globulin levels. Other useful parameters in assessing immune stimulation are part of the standard safety battery and include body temperature, heart rate and respiratory rate (*table 6.3*).

THIRD STEP: CLINICAL PHARMACOLOGY

Specific tests for immunotoxicity in humans are not required, unless there is an indication that the drug candidate is potentially immunotoxic. Testing for immunogenicity by biopharmaceuticals is usually included, because it is a known problem of this drug class.[56] Standard safety markers, such as haematology, clinical biochemistry, vital signs, as well as reports of adverse events can be an indication of AI, provided these are measured sufficiently frequent.

Behind the number: potency

Specific, quantitative tests are routinely applied in quality control settings, as clear limits of acceptance can be defined. While assays for tested impurities and contaminants *seemingly* provide black and white cut-offs, they are limited in predicting *in vivo* toxicity. For example, the LAL-assay yields no information on the biological potency of a given endotoxin, which can differ between bacterial strains by a factor of 10,000.[22,23] Additionally, a strict cut-off for one impurity does not take into account the potentially synergistical effects of multiple impurities. This is an important limitation since it is conceivable that multiple impurities are copurified at any given time during the production process. Both in X[10] and Y, it was not a single HCP or other bacterial product that could be identified as cause for the AI; it was the reduction of the total load of non-human material other than the pharmacologically active substance which resulted in the absence of AI in trial volunteers upon reintroduction into the clinic.

Blind spot

Surprisingly, testing for immunopathological effects is not included in the 'Safety Pharmacology Core Battery' and also 'routine testing' is explicitly *not* recommended by the ICH guidelines for biopharmaceuticals,[20,24] even though biopharmaceuticals have an inherent risk of AI caused by impurities, especially if manufactured in bacterial cell systems. Testing for toxicities is not required if those are not reasonably expected to occur.[25] For biopharmaceuticals, for example, when there is extensive knowledge and data on receptor distribution and function, and the biopharmaceutical under investigation has a selectively high affinity for that receptor, dedicated safety pharmacology studies may be eliminated entirely or in part. For biopharmaceuticals intended for end-stage cancer treatment, even further exceptions to the requirements are possible.[24,26] This guidance may result in minimal safety testing of a compound before entering the clinic.

Even when dedicated immunotoxicity studies are performed, the emphasis seems to be on long-term immunosuppression or enhancement by evaluating macroscopical pathology, organ weights, and histology.[27,28] This is at odds with the observation that undesired inflammatory reactions are commonly transient and do rarely manifest themselves in histological changes. Case X highlights how the AI can

be overlooked in safety pharmacology experiments as well as during clinical trials. AI in clinical trials may be easily misinterpreted as hypersensitivity or be grouped under a non-specific term like 'infusion reaction'.

LESSONS FROM X AND Y

In the aftermath of the TGN1412 tragedy, an Expert Scientific Group made 22 recommendations to increase the safety of participants in (first-in-human) clinical trials.[29,30] Many of these were reiterated following the more recent BIA 10-2474 trial.[31,32] The proposed risk assessments[29,31,33] focus on establishing the likelihood of unanticipated adverse effects of new drug substances entering the clinic, especially for those with complex and novel mechanisms. When applying this strategy to compounds X and Y, and specifically to (the novelty of) the mode of action and knowledge on human exposure to similar substances, it must be concluded that both X and Y were correctly labelled safe.

The true unsafety was caused by the uncharacterised components in X and Y, by impurities, the presence of which was not disputed (*table 6.1*), but the potential risk involved was underestimated. This line of reasoning is common, as is also apparent from the importance placed on dedicated immune toxicity studies in the international guidelines. They are explicitly *not* recommended for biopharmaceuticals.[20] Furthermore, the immune system is regarded 'of less immediate investigative concern' because it is an organ system, 'the functions of which can be transiently disrupted by adverse pharmacodynamic effects without causing irreversible harm'.[24]

The outcome of the risk assessment of the uncharacterised components should immediately raise several red flags. Little knowledge usually exists on the effect of impurities in humans or animals, and safe levels are often not available. Multiple signalling pathways may be triggered and the impurity can act via the immune system. All these factors should have placed trials with X and Y in a high-risk category,[31] and considering the bacterial origin of the impurities an immune-mediated effect could have been anticipated. The lack of emphasis on immunotoxicity caused by biopharmaceuticals is therefore striking.

Investigating and reducing the adverse immune stimulatory propensity of biopharmaceuticals is not only important for the safety of trial volunteers and future patients, but identifying and possibly eliminating such characteristics in an early stage of development is also favourable from a business' perspective. Each step forward increases the expenses of going back to the drawing board, as well as the financial loss associated with ultimate failure and drug withdrawal. Discovering severe AI during clinical studies usually results in delays of many years, case X and Y being no exception. It may even lead to termination of the development pipeline, no matter how promising a compound.

Case X and Y did not make the news, neither did they lead to a public outcry, making the need for changes less pressing, even though details of the clinical trials with X and Y are known to regulatory agencies and health authorities around the globe. The lack of publicly available data on unexpected adverse reactions following administration of an IMP is at odds with the Expert Scientific Group recommendations to expedite the collection and to improve the sharing of safety information.[29] Once more, the call by the scientifical community for public release of the study results was heard in the days after the BIA 10-2474 trial,[4,31] yet remains to be fully answered.

Unanticipated immunostimulation caused by parenterally administered pharmaceuticals is not limited to the experimental setting, though only a few reports exist on recalls of drug products as a result of microbial contamination.[34,35] However, AI may be underreported, because AI can be misdiagnosed as hypersensitivity, as occurred in a phase II trial with X.[8] Financial and other company interests can also guide decisions which ultimately hide cases of AI from public knowledge.

Although these published examples of AI differ from case X and Y in type of product and the fact the cause was a contamination instead of an impurity, they have in common with each other that conventional quality control did not generate a safety signal. For example, peptidoglycan, the culprit in cases of aseptic peritonitis,[34] is not assayed in the standard approach (*table 6.3*).

Alternative assays have been implemented to predict AI with certain pharmaceuticals. Cytokine release assays utilising human immune cells and other cell types are most commonly used, which have demonstrated pro-inflammatory responses upon

stimulation with several monoclonal antibodies, including TGN1412, rituximab, and alemtuzumab.[36-40] Host cell impurities or microbial contamination have also been detected with cytokine release assays.[15,34] The same was true for product X, which elicited an IL-6 and TNF-α response that was completely absent after the production process was modified. In contrast, product Y induced no IL-6 or TNF-α release in any of the assays. Because many variables can influence the read-out in these assays and controversy surrounds the interpretation of the results, cytokine release assays are currently not standardised.[37,41]

Another strategy which has proven its usefulness in detecting immunostimulation employs cell lines transfected with reporter genes for specific components of the innate immune system. Existing cell reporter assays include libraries of human cell lines that are transfected with pathogen pattern recognition receptors (*e.g.* TLR and NOD-like receptors) that are also engineered to express a reporter enzyme (*e.g.* luciferase, or alkaline phosphatase) in response to signal transduction.[9,42–44] These assays revealed TLR5-mediated activation with product X and TLR4-mediated activation with product Y. Nevertheless, potential synergistical effects of multiple host cell impurities cannot be detected with this test system. The use of reporter cell lines that endogenously express multiple pattern recognition receptors (such as THP1 cells) might prove to be useful for this aspect.

Despite the promising developments, no definitive answer to the best preclinical testing strategy can be given, as a fail-safe one probably does not exist. Every laboratory test has its limitations, can suffer from interference, or produce false-negative results and with it a false sense of safety. These limitations should however not be used as an argument to maintain the *status quo*. Undisputedly, the newer assays described above can detect far more causes of immunostimulation than the currently advised ones (*table 6.3*). Given the potential outcome of missing AI during early drug development, specific testing for AI should be part of performed toxicity studies for biopharmaceuticals, which is in sharp contrast with current guidelines.

It may be considered reassuring that, in retrospect, safety pharmacology studies in cynomolgus monkeys could have detected the immunostimulating propensity of X, provided the right biomarkers were included. Likewise, signals of AI were observed early in the clinical trials with X and Y. Therefore, investigators should be on the alert for AI when studying biopharmaceuticals in animals and humans, especially if preclinical studies indicated that an IMP may elicit an inflammatory response. As always, a sentinel approach and a cautious dose escalation scheme with a prudently low starting dose should be applied in first-in-human trials. These measures will decrease the likelihood of (severe) AI in later stages, although such reactions can probably never be completely prevented.

Moreover, AIs should not be treated lightly as rare idiosyncratic reactions that may be caused by a few biopharmaceuticals. They can severely disrupt vital organ systems and in many cases indicating marks of AI were left for the appreciating eye at some point during development. Awareness is thus probably the most important lesson to be learnt from case X and case Y. Equally important is the publication of cases of AI to facilitate scientifical discussion and to improve drug safety.

REFERENCES

1 Suntharalingam G, Perry MR, Ward S, *et al.* Cytokine storm in a phase 1 trial of the anti-CD28 monoclonal antibody TGN1412. *N Engl J Med* 2006; **355**: 1018–28.

2 Butler D, Callaway E. Scientists in the dark after French clinical trial proves fatal. *Nature* 2016; **529**: 263–4.

3 Kerbrat A, Ferré J-C, Fillatre P, *et al.* Acute neurologic disorder from an inhibitor of fatty acid amide hydrolase. *N Engl J Med* 2016; **375**: 1717–25.

4 Brøsen K, Funck-Brentano C, Kroemer HK, Pirmohamed M, Schwab M. Open letter on access to the BIA 10-2474 clinical trial data. *Lancet* 2017; **389**: 156.

5 Nicholls SJ, Uno K, Kataoka Y, Nissen SE. ETC-216 for coronary artery disease. *Expert Opin Biol Ther* 2011; **11**: 387–94.

6 European Pharmacopoeia Commission. European Pharmacopoeia 2014, 8th edn. Straßburg: Council Of Europe: European Directorate for the Quality of Medicines and Healthcare, 2013.

7 United States Pharmacopeial Convention. 2016 USP 39 NF 34 US Pharmacopeia National Formulary Volumes 1-4. Rockville, MD: United States Pharmacopeial Convention, 2015.

8 Nissen SE, Tsunoda T, Tuzcu EM, *et al.* Effect of recombinant APOA-I Milano on coronary atherosclerosis in patients with acute coronary syndromes: a randomized controlled trial. *JAMA* 2003; **290**: 2292–300.

9 Huang L-Y, Dumontelle JL, Zolodz M, Deora A, Mozier NM, Golding B. Use of toll-like receptor assays to detect and

identify microbial contaminants in biological products. *J Clin Microbiol* 2009; **47**: 3427–34.
10 Caparon MH, Rust KJ, Hunter AK, *et al.* Integrated solution to purification challenges in the manufacture of a soluble recombinant protein in *E. coli*. *Biotechnol Bioeng* 2010; **105**: 239–49.
11 Kallend DG, Reijers JAA, Bellibas SE, *et al.* A single infusion of MDCO-216 (ApoA-1 Milano/POPC) increases ABCA1-mediated cholesterol efflux and pre-beta 1 HDL in healthy volunteers and patients with stable coronary artery disease. *Eur Hear journal Cardiovasc Pharmacother* 2016; **2**: 23–9.
12 Nicholls S. Impact of infusion of an ApoA-IMilano HDL mimetic on regression of coronary atherosclerosis in acute coronary syndrome patients: the MILANO-PILOT study. *Am Hear Assoc Sci Sess* 2016.
13 Laude-Sharp M, Haeffner-Cavaillon N, Caroff M, Lantreibecq F, Pusineri C, Kazatchkine MD. Dissociation between the interleukin 1-inducing capacity and Limulus reactivity of lipopolysaccharides from gram-negative bacteria. *Cytokine* 1990; **2**: 253–8.
14 Wang X, Morgan DM, Wang G, Mozier NM. Residual DNA analysis in biologics development: review of measurement and quantitation technologies and future directions. *Biotechnol Bioeng* 2012; **109**: 307–17.
15 Wang X, Hunter AK, Mozier NM. Host cell proteins in biologics development: identification, quantitation and risk assessment. *Biotechnol Bioeng* 2009; **103**: 446–58.
16 Hogwood CEM, Bracewell DG, Smales CM. Measurement and control of host cell proteins (HCPs) in CHO cell bioprocesses. *Curr Opin Biotechnol* 2014; **30**: 153–60.
17 Copeland S, Warren HS, Lowry SF, Calvano SE, Remick D, Inflammation and the Host Response to Injury Investigators. Acute inflammatory response to endotoxin in mice and humans. *Clin Diagn Lab Immunol* 2005; **12**: 60–7.
18 Mestas J, Hughes CCW. Of mice and not men: differences between mouse and human immunology. *J Immunol* 2004; **172**: 2731–8.
19 Seok J, Warren HS, Cuenca AG, *et al.* Genomic responses in mouse models poorly mimic human inflammatory diseases. *Proc Natl Acad Sci U S A* 2013; **110**: 3507–12.
20 International Conference on Harmonisation of technical requirements for registration of pharmaceuticals for human use. S6(R1)—Preclinical safety evaluation of biotechnology-derived pharmaceuticals. Genève: International Council for Harmonisation (ICH), 2011.
21 Brennan FR, Shaw L, Wing MG, Robinson C. Preclinical safety testing of biotechnology-derived pharmaceuticals: understanding the issues and addressing the challenges. *Mol Biotechnol* 2004; **27**: 59–74.
22 Dehus O, Hartung T, Hermann C. Endotoxin evaluation of eleven lipopolysaccharides by whole blood assay does not always correlate with Limulus amebocyte lysate assay. *J Endotoxin Res* 2006; **12**: 171–80.
23 Brandenburg K, Howe J, Gutsman T, Garidel P. The expression of endotoxic activity in the Limulus test as compared to cytokine production in immune cells. *Curr Med Chem* 2009; **16**: 2653–60.
24 International Conference on Harmonisation of technical requirements for registration of pharmaceuticals for human use. S7A—Safety pharmacology studies for human pharmaceuticals. Genève: International Council for Harmonisation (ICH), 2000.
25 International Conference on Harmonisation of technical requirements for registration of pharmaceuticals for human use. Q6B—Specifications: test procedures and acceptance criteria for biotechnological/biological products. Genève: International Council for Harmonisation (ICH), 1999.
26 International Conference on Harmonisation of technical requirements for registration of pharmaceuticals for human use. S9—Nonclinical evaluation for anticancer pharmaceuticals. Genève: International Council for Harmonisation (ICH), 2009.
27 International Conference on Harmonisation of technical requirements for registration of pharmaceuticals for human use. S8—Immunotoxicity studies for human pharmaceuticals. Genève: International Council for Harmonisation (ICH), 2005.
28 US Food and Drug Administration. Immunotoxicology evaluation of investigational new drugs. Washington, DC: US Department of Health and Human Services, 2002.
29 Dowsing T, Kendall MJ. The Northwick Park tragedy – protecting healthy volunteers in future first-in-man trials. *J Clin Pharm Ther* 2007; **32**: 203–7.
30 St Clair EW. The calm after the cytokine storm: lessons from the TGN1412 trial. *J Clin Invest* 2008; **118**: 1344–7.
31 Eddleston M, Cohen AF, Webb DJ. Implications of the BIA-102474-101 study for review of first-into-human clinical trials. *Br J Clin Pharmacol* 2016; **81**: 582–6.
32 Mullard A. EMA rewrites phase I guidelines in aftermath of FAAH tragedy. *Nat Rev Drug Discov* 2016; **15**: 595–595.
33 Kenter M, Cohen A. Establishing risk of human experimentation with drugs: lessons from TGN1412. *Lancet* 2006; **368**: 1387–91.
34 Martis L, Patel M, Giertych J, *et al.* Aseptic peritonitis due to peptidoglycan contamination of pharmacopoeia standard dialysis solution. *Lancet* 2005; **365**: 588–94.
35 Smith RM, Tipple M, Chaudry MN, Schaefer MK, Park BJ. Relapse of fungal meningitis associated with contaminated methylprednisolone. *N Engl J Med* 2013; **368**: 2535–6.
36 Stebbings R, Eastwood D, Poole S, Thorpe R. After TGN1412: recent developments in cytokine release assays. *J Immunotoxicol* 2013; **10**: 75–82.
37 Finco D, Grimaldi C, Fort M, *et al.* Cytokine release assays: current practices and future directions. *Cytokine* 2014; **66**: 143–55.
38 Wing MG, Moreau T, Greenwood J, *et al.* Mechanism of first-dose cytokine-release syndrome by CAMPATH 1-H: involvement of CD16 (FcγRIII) and CD11a/CD18 (LFA-1) on NK cells. *J Clin Invest* 1996; **98**: 2819–26.
39 Kamburova EG, Van den Hoogen MWF, Koenen HJPM, Baas MC, Hilbrands LB, Joosten I. Cytokine release after treatment with rituximab in renal transplant recipients. *Transplantation* 2015; **99**: 1907–11.
40 Findlay L, Eastwood D, Ball C, *et al.* Comparison of novel methods for predicting the risk of pro-inflammatory clinical infusion reactions during monoclonal antibody therapy. *J Immunol Methods* 2011; **371**: 134–42.

41 Vidal J-M, Kawabata TT, Thorpe R, *et al*. *In vitro* cytokine release assays for predicting cytokine release syndrome: the current state-of-the-science. Report of a European Medicines Agency Workshop. *Cytokine* 2010; **51**: 213–5.
42 Bsibsi M, Bajramovic JJ, Vogt MHJ, *et al*. The microtubule regulator stathmin is an endogenous protein agonist for TLR3. *J Immunol* 2010; **184**: 6929–37.
43 Jagessar SA, Kap YS, Heijmans N, *et al*. Induction of progressive demyelinating autoimmune encephalomyelitis in common marmoset monkeys using MOG34-56 peptide in incomplete freund adjuvant. *J Neuropathol Exp Neurol* 2010; **69**: 372–85.
44 Haanstra KG, Jagessar SA, Bauchet A-L, *et al*. Induction of experimental autoimmune encephalomyelitis with recombinant human myelin oligodendrocyte glycoprotein in incomplete Freund's adjuvant in three non-human primate species. *J Neuroimmune Pharmacol* 2013; **8**: 1251–64.
45 Pichler WJ. Adverse side-effects to biological agents. *Allergy* 2006; **61**: 912–20.
46 Palm NW, Rosenstein RK, Medzhitov R. Allergic host defences. *Nature* 2012; **484**: 465–72.
47 Lieberman P, Garvey LH. Mast cells and anaphylaxis. *Curr Allergy Asthma Rep* 2016; **16**: 20.
48 Chousterman BG, Swirski FK, Weber GF. Cytokine storm and sepsis disease pathogenesis. *Semin Immunopathol* 2017; **39**: 517-28.
49 Behrens EM, Koretzky GA. Cytokine storm syndrome: looking toward the precision medicine era. *Arthritis Rheumatol* 2017; **69**: 1135–43.
50 Chung CH. Managing premedications and the risk for reactions to infusional monoclonal antibody therapy. *Oncologist* 2008; **13**: 725–32.
51 Descotes J. Immunotoxicity of monoclonal antibodies. *MAbs* 2009; **1**: 104–11.
52 Scherer K, Spoerl D, Bircher AJ. Adverse drug reactions to biologics. *J DDG J der Dtsch Dermatologischen Gesellschaft* 2010; **8**: 411–26.
53 Borchers AT, Leibushor N, Cheema GS, Naguwa SM, Gershwin ME. Immune-mediated adverse effects of biologicals used in the treatment of rheumatic diseases. *J Autoimmun* 2011; **37**: 273–88.
54 Maggi E, Vultaggio A, Matucci A. Acute infusion reactions induced by monoclonal antibody therapy. *Expert Rev Clin Immunol* 2011; **7**: 55–63.
55 Boyman O, Comte D, Spertini F. Adverse reactions to biologic agents and their medical management. *Nat Rev Rheumatol* 2014; **10**: 612–27.
56 Gunn GR, Sealey DCF, Jamali F, Meibohm B, Ghosh S, Shankar G. From the bench to clinical practice: understanding the challenges and uncertainties in immunogenicity testing for biopharmaceuticals. *Clin Exp Immunol* 2016; **184**: 137–46.
57 Committee for Medicinal Products for Human Use (CHMP). Production and quality control of medicinal products derived by recombinant DNA technology. London: European Medicines Agency, 1994.
58 WHO Expert Committee on Biological Standardization. Sixty-first Report (WHO Technical Report Series). Genève: World Health Organization, 2013.
59 International Conference on Harmonisation of technical requirements for registration of pharmaceuticals for human use. Q5A(R1)—Viral safety evaluation of biotechnology products derived from cell lines of human or animal origin. Genève: International Council for Harmonisation (ICH), 1999.
60 International Conference on Harmonisation of technical requirements for registration of pharmaceuticals for human use. Q5D—Derivation and characterisation of cell substrates used for production of biotechnological/biological products. Genève: International Council for Harmonisation (ICH), 1997.

DISCUSSION

Insulin was the first therapeutical protein manufactured via recombinant DNA techniques that became commercially available in 1982.[1] It marked the start of the biopharmaceutical era, which saw ever increasing market values and expanding developmental budgets.[1–5] More than 30 years have passed, yet many of the applied pharmacological concepts have changed little over time. An excellent example hereof is the field of bioequivalence research, even though only slightly older than recombinant human insulin.[6]

Bioequivalence is a regulatory concept which entails that a generical drug product ('test product') is therapeutically equivalent to the originator ('reference product') and can be used interchangeably.[6,7] Equivalence generally has to be demonstrated statistically on four endpoints: pharmacokinetic, pharmacodynamic, clinical, and *in vitro* endpoints.[6] Maximum plasma concentration (C_{max}) and area under the plasma concentration-time profile (AUC) are historically used to establish pharmacokinetic bioequivalence. Although various reports have criticised the use of these parameters to compare 'exposure' between two drugs,[8,9] C_{max} and AUC, determined in a non-compartmental analysis (NCA),[10] remain the required parameters by regulatory agencies to allow market authorisation.

With regard to biopharmaceuticals, the term biosimilarity is used, as it understood that the biotechnological manufacturing process cannot create an *exact* copy of the reference product. Instead of equivalence, a high degree of similarity has to be demonstrated on the aforementioned endpoints, and any remaining difference should be clinically insignificant.[11–13] Biopharmaceuticals are more complex than small molecules; their concentration-time profiles being no exception.[14–16] Even though a NCA is inadvertently ill-suited to cover the non-linear elimination pathways of monoclonal antibodies (MABs) and other large biopharmaceuticals, it still remains the gold standard in biosimilarity research.

In ***chapter 1***, two methods are described of how a population pharmacokinetics approach can be used to support the pharmacokinetic biosimilarity claim, and which can perhaps in the future even replace the NCA. Although such a method is not new,[17–19] it has never before been applied before to a MAB. Benefits of a modelled approach over a NCA are that a pharmacokinetic model can accurately describe the non-linear elimination pathways of MABs. Also, a model is not concerned with differences in administered doses. This is especially important for biopharmaceuticals with non-linear pharmacokinetics, since the NCA assumes linearity in its correction. Furthermore, a population pharmacokinetics approach can correct for covariates, and is relatively little affected by missing samples or deviations in sample collection times and administration time or dose.

More importantly, use of a population pharmacokinetic model allows for statistical testing of differences between test and reference products via covariate analysis. This can be done for all model parameters. Because these parameters are related to pharmacokinetic properties, such as absorption and elimination rates, the methods described in *chapter 1* may circumvent the problems[8,9] identified with the NCA in establishing pharmacokinetic biosimilarity. The chapter also discusses how model-based simulations can be used to proof that a therapeutical concentration is reached at the site of action with the test product, which further supports a biosimilarity claim.

However, a prerequisite for applying any modelling approach to pharmacokinetic data is a correct understanding of the mechanisms governing the distribution of a pharmaceutical over the body, which is still incomplete, as demonstrated in the *chapters 2 & 3*. The developed model in *chapter 1* (*figure 1.1*) has a so-called central compartment, to which drug product is added during administration and from which drug product is cleared via a linear and a non-linear process. After completion of intravenous infusion, the addition of drug to the central compartment terminates immediately. Since elimination continues, the maximum concentration in this compartment is theoretically reached at the end of infusion (EOI), assuming a constant volume. In other words, the time to C_{max} (t_{max}) equals the infusion duration, which is not the case for many MABs, including trastuzumab (*table 2.1*).

The fact that t_{max} can occur after EOI seems to have been ignored since the first introduction of large biopharmaceuticals. At best, the 'delayed' t_{max} is reported without further explanation (see *table 2.1*), but more frequently, this parameter is lacking from publications and one has to guess when C_{max} occurred. As an example, in at least five publications[20–24] on bevacizumab, a C_{max} is reported without a t_{max}. In other cases, a too sparse sampling design is chosen to allow the phenomenon to be observed; possibly, because C_{max} is expected at EOI and the slow elimination of many biopharmaceuticals does not necessitate dense sampling in the first hours after EOI. Yet, the finding of an increase in plasma concentration after intravenous administration has ceased is a strong indication that biopharmaceuticals do not always follow current pharmacokinetic theory, which is to a large extent still based on experience with small molecules.

Chapter 2 investigated two closely related, plausible theories to explain the 'delayed' t_{max}. The first hypothesis is that the biopharmaceutical is bound to and released from the vessel wall or taken up and released by endothelial cells, particularly in the presence of a high local concentration at the infusion site. After EOI, the concentration drops, and drug substance is released from the wall or by the cells, causing a rise in plasma concentration and hence a delayed t_{max}. The second hypothesis only applies to cases where infusion lines are flushed (*e.g.* with normal saline) in order to also administer the line content. If biopharmaceuticals can adsorb to the infusion line and desorb when the infusion line is flushed, drug administration actually continues after the anticipated EOI; thus, causing an *apparent* delay in t_{max}.

The performed studies found evidence for binding to endothelial cells. In an artificial vessel covered with endothelial cells, the MABs trastuzumab and bevacizumab were observed to adsorb to the luminal surface, though the pattern differed (*figure 2.1*). This adsorption seemed to be concentration-dependent and easily reversible upon washing the cell-layer with a lower concentration. Binding of tested MABs to the extracellular matrix was also noted. Together with existing knowledge on interaction between proteins and body surfaces,[25,26] these observations point to non-specific binding. Adsorption to endothelial cells and subsequent desorption can therefore theoretically explain a delayed t_{max}.

A lower recovery than expected was sometimes observed in experiments where administration procedures were mimicked with a standard infusion lines. However, the wash-out from the infusion line during flushing did not contain any quantifiable biopharmaceutical, other than what can be predicted based on laminar flow. Thus, flushing of the infusion lines cannot contribute to a delay in t_{max}.

Both the finding of adsorption to endothelium and the possibility of drug loss during infusion are relevant to the clinical pharmacologist. The concept of dose-response requires knowledge of the drug exposure at the site of action at a certain moment in time, and thus knowledge of the *exact* dose administered. Adsorption of biopharmaceuticals to endothelium, of which the delayed t_{max} is only one symptom, results in an uneven distribution over the vascular compartment (*figure 2.4*). In that respect, predicting the exposure at the site of action becomes even more difficult based on a limited number of plasma samples collected from a single vein.

Although the performed studies do not preclude alternative mechanisms to be involved in causing an increase in plasma concentration after EOI, these yet unidentified mechanisms pose the same challenge for the clinical pharmacologist, namely how relevant the measured quantity at the sampling site is in studying drug effects and the relationship between the two (pharmacokinetic-pharmacodynamical model). In any case, the observation that $C_{max} > C_{EOI}$ implies the biopharmaceutical is not evenly distributed over the vascular compartment.

Chapter 3 further adds to the complexity of the pharmacokinetics of some biopharmaceuticals. MABs, and perhaps biopharmaceuticals in general, demonstrate highly variable plasma concentrations over time within the same individual (*figure 3.1*), as opposed to the stability one expects from current theory.[14–16,27,28] This feature may have gone undetected because the collection of multiple samples within an hour is uncustomary for supposedly slowly distributing and eliminated drugs like MABs. A simple solution would be to ascribe the fluctuations to normal (assay) variability. However, for various reasons, such an explanation must be considered unlikely, as argued in this chapter.

Adsorption to the endothelium may not only account for the delay in t_{max}, it may also account for the observed fluctuations in the plasma concentration, if one includes the dynamical state of the endothelium and circulation in the equation. For example, numerous physiological and pathological stimuli have

been identified that can influence the endothelium, including the glycocalyx.[29–33] Such changes to the endothelium may affect the local balance between adsorption and desorption with rises or falls in plasma concentration as manifestations. Additionally, blood flow can be increased or diminished to certain organs, depending on overall body activity, and, in tissues, capillary beds can be opened or closed, depending on local metabolic demands.[34] Thus, the endothelial surface area available for adsorption varies, as do the haemodynamical characteristics and with it the wash-out of adsorbed biopharmaceutical. These and other possible explanations – as discussed in *chapter 3* – are still speculative without support from dedicated studies. Moreover, it remains to be established whether the observation for certain MABs can be extended to all large therapeutical proteins.

If one cannot accurately predict drug concentration at the (desired) site of action in a particular patient at any moment, one cannot instigate rational (effective) pharmacotherapy. This notion undermines the current quest for personalised medicine. For many rheumatological biopharmaceuticals, it remains challenging to accurately predict efficacy and toxicity from animal or *ex vivo* models, or to correlate clinical effects and pharmacokinetic parameters.[35,36] In patient trials, usually, only a few plasma samples are collected for determination of drug concentration and the investigated pharmacokinetic-pharmacodynamic relationship is based on a single parameter, such as through or steady-state concentration. Considering that the presented data indicate that the plasma concentration of MABs can fluctuate significantly within short times, a lack of correlation between clinical effects and standardised pharmacokinetic parameters may be explained.

On the other hand, if one understands the basic factors that together determine local drug concentration, one can fully individualise treatments to maximise efficacy, or at least ensure adequate drug exposure at the site of action. As a hypothetical case, it may – for example – be considered that eating can be beneficial to patients with an intestinal neoplasm, who are being treated with a particular MAB, as alimentation directs blood flow – and hence a therapeutical protein – to the digestive tract. However, the *in vivo* situation is usually far more complicated than predicted by current theory and models, a recurrent theme in this thesis. Therefore, influencing a single factor will probably not revolutionise pharmacotherapy.

EVEN IF WE WERE TO FULLY UNDERSTAND the pharmacokinetics of biopharmaceuticals, clinical effects following biopharmaceutical treatment would sometimes be difficult to predict upfront, especially unwanted, toxic effects.[37–41] For example, certain MABs are also associated with inflammatory reactions, typically upon first administration, which can be severe.[42–44] These reactions are classified as 'adverse immunostimulation' or type α reaction, although the terms are not necessarily interchangeable (see *box 6.1*). The occurrence of a severe, unopposed, systemic inflammatory reaction following administration of a drug is particularly troublesome as these syndromes are life-threatening, similar to sepsis and anaphylaxis.[45–48]

For some MABs, the underlying mechanism of the adverse immunostimulation (AI) has been unravelled,[49–51] but for others, it remains to be elucidated. This lack of insight, combined with the fact that involved immune pathways in the pathogenesis of the AI differ between biopharmaceuticals, does not facilitate the development of a standardised platform which can be used to screen compounds for AI.

Chapter 4 sheds light on one of the lesser understood cases of AI, by employing an *ex vivo* whole blood incubation assay. This study compared individuals who had shown clinical signs of an inflammatory reaction following trastuzumab administration with those who had not. Higher *ex vivo* IL-6 release was observed in the clinical 'responders' compared to 'non-responders', which correlated to maximum body temperature (*figure 4.1*). A similar linear correlation was found between the *ex vivo* TNF-α response and maximum body temperature, but only within the 'responders'. Nonetheless, the magnitude of the differences was too small to serve as a screening tool for (trastuzumab-associated) immunostimulation.

A factor complicating the implementation of novel screening methods for AI is that results vary in different cytokine release assays utilising living human tissues, depending on the exact test conditions and donors included.[52–54] Together with the fact that it is often unknown how *in vitro* cytokine release translates into clinical effects, this makes the interpretation of many assay results difficult, as was also acknowledged by an EMA workgroup.[55]

Not only can inflammatory reactions be induced by the drug substance, they can also arise as a result of (microbial) impurities or contaminants in the drug product. Biopharmaceuticals are usually produced in

cell based platforms, frequently of microbial origin.[56] This process inevitably introduces foreign (non-human) substances in the drug product, substances that can elicit an immune response. Nonetheless, standard toxicological studies are not directed at capturing immune responses toward a pharmaceutical. Surprisingly, even for biopharmaceuticals, despite their inherent risk, dedicated immunotoxicological studies are not required by the regulatory guidelines.[57] Yet, by following the guidelines, potentially dangerous immunostimulation induced by (microbial) impurities in biopharmaceuticals can be missed, as detailed in *chapters 5 & 6*.

The first case (described in *chapter 5*) is that of a recombinant human Apolipoprotein A-I Milano, with code name ETC-216.[58] After it had been administered to healthy volunteers and patients with coronary artery disease, ETC-216 was found to induce AI in the third clinical trial. During subsequent analyses, it was discovered that ETC-216 contained several immunostimulatory host cell proteins (HCPs), one of which was flagellin.[59,60] In the second case (described in *chapter 6*), the AI was already observed in the first clinical trial with a recombinant human plasma protein. Here, the cause was also traced back to HCPs, one of which stimulated toll-like receptor (TLR)4.

In ***chapter 5***, a study is described where an *ex vivo* cytokine release assay was used once more to test ETC-216. The results indicated a strong IL-6 and TNF-α response elicited by ETC-216, but not by the remanufactured product (MDCO-216). The difference was statistically significant in all examined donor populations: healthy volunteers, and patients with stable and acute coronary artery disease. *In vivo* administration of MDCO-216 to healthy volunteers and patients with stable coronary artery disease confirmed the result that the immunostimulatory HCPs were successfully removed.[61]

However, the conclusion that the AI could have been prevented by using this assay is premature. *Table 5.3* clearly shows that the response to a stimulus varies between different populations, and also within populations. Comorbidities and medication use, as well as other patient characteristics, may explain some of the found differences. Because such factors can either increase or decrease an individual's susceptibility to AI, translation of *ex vivo* results to *in vivo* effects is less than straightforward, increasing the complexity of predicting AI during the preclinical phase of development.

An important question to be answered is why the preclinical safety testing had not revealed the immunostimulatory propensity of ETC-216. Can other tests than those commonly applied or required by international guidelines predict AI, especially if caused by impurities of microbial origin? ***Chapter 6*** illustrates the main shortcomings of current practice on the basis of two case histories.

The first shortcoming relates to the sensitivity of the used assays during quality control of the drug substance. Endotoxin is a recognised impurity or contaminant within biopharmaceuticals, yet the commonly employed limulus amoebocyte lysate (LAL) assay failed to detect its presence in one of the cases. Assays for other HCPs only detect a selection of all host cell proteins. Because the identity of the found HCPs remains hidden, these tests generate results of unknown significance. Nonetheless, even if all HCPs are characterised, for many impurities, the clinical effect and hence a safe level is unclear, least of all when dealing with combinations of impurities. This is the second shortcoming: the quantification instead of the qualification of impurities.

More sophisticated test platforms are available, which utilise human immune cells or cells transfected which immune receptors and try to mimic the *in vivo* situation. These platforms can detect a number of untoward reactions that would previously not have been discovered, such as those caused by endotoxin, flagellin, peptidoglycan, and others. However, no laboratory test is fail-safe, as also discussed above. Furthermore, many of the developed test platforms, including the applied *ex vivo* cytokine release assay in *chapters 4 & 5*, are back-translations, starting from an unanticipated clinical finding and trying to reproduce it *in vitro*. They are validated only against known examples of biopharmaceuticals causing AI. Thus, their claims to accurately predict AI still need to be substantiated by new test cases.

Toxicological studies in animals may overcome the first two shortcomings, provided the chosen species' immune system reacts similarly to the impurities as does the human one. Indeed, ETC-216 induced AI in cynomolgus monkeys, but this was missed because sensitive biomarkers (*e.g.* circulating cytokines) were not included and the safety measurements that could have suggested AI (*e.g.* vital parameters, haematology results) were done too infrequently. Moreover, immunotoxicity is neither routinely investigated, nor is it required by the guidelines. Even if dedicated

immunotoxicological studies are performed, the focus is on long-term immunosuppression or enhancement and not on rapidly occurring, transient reactions that characterise most cases of AI.

Awareness of the possibility of AI is another important aspect for early detection and prevention of similar cases in the future. This calls for more openness and the sharing of safety information. Proposals to be implemented in the guidelines – aiming to increase drug safety – can only occur after proper scientifical debate.

DESPITE DECADES OF EXPERIENCE WITH biopharmaceuticals, our understanding of many *in vivo* pharmacokinetic and adverse effects is still limited, although this observation should not deter from continuing to perform dedicated studies with this class of drugs. On the contrary, it should inspire to investigate these poorly understood aspects. Clinical trials remain essential, for only such trials allow integration of all complex mechanisms occurring simultaneously in different, complex tissues and thus proof-of-concept. Where it comes to potentially hazardous effects of biopharmaceuticals, such as adverse immunostimulation, all reasonable efforts must be focussed on detecting these before administering the product to humans. Even then, however, human *in vivo* data are required to guide or validate preclinical research.

Sticky proteins, *i.e.* the dynamical binding ('stickiness') of proteins to various (bodily) surfaces, is a concept that can theoretically explain some of the ill-understood pharmacokinetic characteristics of biopharmaceuticals, most notably, the delay in t_{max} after intravenous infusion and the highly variable plasma concentration over time. *Dirty proteins* denotes a concept where therapeutical proteins induce an inflammatory reaction ('adverse immunostimulation') in humans, whose immune system perceives the biopharmaceutical a hostile ('dirtiness'). The active ingredient can serve as the stimulus, as can the co-administered contaminants or impurities.

Although these issues with biopharmaceuticals remain difficult to predict, because the underlying mechanisms are not completely elucidated, knowledge of these concepts – *sticky & dirty proteins* – appears to be indispensable for clinical pharmacologists and physicians primarily involved in patient care.

REFERENCES

1 Nagle T, Berg C, Nassr R, Pang K. The further evolution of biotech. *Nat Rev Drug Discov* 2003; **2**: 75–9.
2 Gene Techno Science. Overview of global pharmaceutical market. 2015. http://www.g-gts.com/en/business/market/ (accessed Aug 1, 2017).
3 IMS Institute for Healthcare Informatics. A growing share of all medicines are biologic, with biosimilars and non-original biologic (NOB) products now taking a small share of the total market. 2013. https://www.imshealth.com/files/web/IMSH Institute/Reports/The_Global_Use_of_Medicines_2017/ global use of med 2017 right6 Biologics_Market.pdf (accessed Aug 1, 2017).
4 McNamee LM, Ledley FD. Patterns of technological innovation in biotech. *Nat Biotechnol* 2012; **30**: 937–43.
5 Lawrence S, Lahteenmaki R. Public biotech 2013—the numbers. *Nat Biotechnol* 2014; **32**: 626–32.
6 Midha KK, McKay G. Bioequivalence; its history, practice, and future. *AAPS J* 2009; **11**: 664–70.
7 Carpenter D, Tobbell DA. Bioequivalence: the regulatory career of a pharmaceutical concept. *Bull Hist Med* 2011; **85**: 93–131.
8 Bate R, Mathur A, Lever HM, *et al*. Generics substitution, bioequivalence standards, and international oversight: complex issues facing the FDA. *Trends Pharmacol Sci* 2016; **37**: 184–91.
9 Rescigno A, Powers J, Herderick EE. Bioequivalent or nonbioequivalent? *Pharmacol Res* 2001; **43**: 543–7.
10 Gabrielsson J, Weiner D. Non-compartmental analysis. In: Reisfeld B, Mayeno AN, eds. Computational Toxicology: Volume I. New York City, NY: Humana Press, 2012: 377–89.
11 WHO Expert Committee on Biological Standardization. Guidelines on evaluation of similar biotherapeutic products (SBPs). Genève, 2009.
12 US Food and Drug Administration. Scientific considerations in demonstrating biosimilarity to a reference product. Silver Spring: US Department of Health and Human Services, 2015.
13 Committee for Medicinal Products for Human Use (CHMP). Guideline on similar biological medicinal products. London: European Medicines Agency, 2015.
14 Keizer RJ, Huitema ADR, Schellens JHM, Beijnen JH. Clinical pharmacokinetics of therapeutic monoclonal antibodies. *Clin Pharmacokinet* 2010; **49**: 493–507.
15 Shi S. Biologics: an update and challenge of their pharmacokinetics. *Curr Drug Metab* 2014; **15**: 271–90.
16 Wang W, Wang EQ, Balthasar JP. Monoclonal antibody pharmacokinetics and pharmacodynamics. *Clin Pharmacol Ther* 2008; **84**: 548–58.
17 Panhard X, Mentré F. Evaluation by simulation of tests based on non-linear mixed-effects models in pharmacokinetic

interaction and bioequivalence cross-over trials. *Stat Med* 2005; **24**: 1509–24.
18 Dubois A, Gsteiger S, Pigeolet E, Mentré F. Bioequivalence tests based on individual estimates using non-compartmental or model-based analyses: evaluation of estimates of sample means and type I error for different designs. *Pharm Res* 2010; **27**: 92–104.
19 Dubois A, Gsteiger S, Balser S, *et al.* Pharmacokinetic similarity of biologics: analysis using nonlinear mixed-effects modeling. *Clin Pharmacol Ther* 2012; **91**: 234–42.
20 Gordon MS, Margolin K, Talpaz M, *et al.* Phase I safety and pharmacokinetic study of recombinant human anti-vascular endothelial growth factor in patients with advanced cancer. *J Clin Oncol* 2001; **19**: 843–50.
21 Garnier-Viougeat N, Rixe O, Paintaud G, *et al.* Pharmacokinetics of bevacizumab in haemodialysis. *Nephrol Dial Transplant* 2007; **22**: 975.
22 Wu JY, Wu XN, Ding L, *et al.* Phase I safety and pharmacokinetic study of bevacizumab in chinese patients with advanced cancer. *Chin Med J (Engl)* 2010; **123**: 901–6.
23 Zhi J, Chen E, Major P, *et al.* A multicenter, randomized, open-label study to assess the steady-state pharmacokinetics of bevacizumab given with either XELOX or FOLFOX-4 in patients with metastatic colorectal cancer. *Cancer Chemother Pharmacol* 2011; **68**: 1199–206.
24 Knight B, Rassam D, Liao S, Ewesuedo R. A phase I pharmacokinetics study comparing PF-06439535 (a potential biosimilar) with bevacizumab in healthy male volunteers. *Cancer Chemother Pharmacol* 2016; **77**: 839–46.
25 Ryser H, Aub JC, Caulfield JB. Studies on protein uptake by isolated tumor cells. II. Quantitative data on the adsorption and uptake of I-131-serum albumin by Ehrlich ascites tumor cells. *J Cell Biol* 1962; **15**: 437–49.
26 Curtis ASG. Cell adhesion. *Prog Biophys Mol Biol* 1973; **27**: 315–84.
27 Dostalek M, Gardner I, Gurbaxani BM, Rose RH, Chetty M. Pharmacokinetics, pharmacodynamics and physiologically-based pharmacokinetic modelling of monoclonal antibodies. *Clin Pharmacokinet* 2013; **52**: 83–124.
28 Dirks NL, Meibohm B. Population pharmacokinetics of therapeutic monoclonal antibodies. *Clin Pharmacokinet* 2010; **49**: 633-59.
29 Alphonsus CS, Rodseth RN. The endothelial glycocalyx: a review of the vascular barrier. *Anaesthesia* 2014; **69**: 777–84.
30 Rabelink TJ, De Zeeuw D. The glycocalyx—linking albuminuria with renal and cardiovascular disease. *Nat Rev Nephrol* 2015; **11**: 667–76.
31 Tarbell JM, Cancel LM. The glycocalyx and its significance in human medicine. *J Intern Med* 2016; **280**: 97–113.
32 Boulanger CM. Endothelium. *Arterioscler Thromb Vasc Biol* 2016; **36**: e26–31.
33 Potente M, Mäkinen T. Vascular heterogeneity and specialization in development and disease. *Nat Rev Mol Cell Biol* 2017; **18**: 477–94.
34 Boulpaep EL. Integrated control of the cardiovascular system. In: Boron WF, Boulpaep EL, eds. Medical Physiology, 3rd edn. Philadelphia: Elsevier, 2016: 572–89.
35 Strand V, Kimberly R, Isaacs JD. Biologic therapies in rheumatology: lessons learned, future directions. *Nat Rev Drug Discov* 2007; **6**: 75–92.
36 Rothe A, Rubbert A. Recombinant proteins in rheumatology – recent advances. *N Biotechnol* 2011; **28**: 502–10.
37 Cohen A. Should we tolerate tolerability as an objective in early drug development? *Br J Clin Pharmacol* 2007; **64**: 249–52.
38 Tralau T, Luch A. Drug-mediated toxicity: illuminating the 'bad' in the test tube by means of cellular assays? *Trends Pharmacol Sci* 2012; **33**: 353–64.
39 Hornberg JJ, Laursen M, Brenden N, *et al.* Exploratory toxicology as an integrated part of drug discovery. Part I: why and how. *Drug Discov Today* 2014; **19**: 1131–6.
40 Hornberg JJ, Laursen M, Brenden N, *et al.* Exploratory toxicology as an integrated part of drug discovery. Part II: screening strategies. *Drug Discov Today* 2014; **19**: 1137–44.
41 Patlewicz G, Fitzpatrick JM. Current and future perspectives on the development, evaluation, and application of in silico approaches for predicting toxicity. *Chem Res Toxicol* 2016; **29**: 438–51.
42 Chung CH. Managing premedications and the risk for reactions to infusional monoclonal antibody therapy. *Oncologist* 2008; **13**: 725–32.
43 Maggi E, Vultaggio A, Matucci A. Acute infusion reactions induced by monoclonal antibody therapy. *Expert Rev Clin Immunol* 2011; **7**: 55–63.
44 Bugelski PJ, Achuthanandam R, Capocasale RJ, Treacy G, Bouman-Thio E. Monoclonal antibody-induced cytokine-release syndrome. *Expert Rev Clin Immunol* 2009; **5**: 499–521.
45 Palm NW, Rosenstein RK, Medzhitov R. Allergic host defences. *Nature* 2012; **484**: 465–72.
46 Lieberman P, Garvey LH. Mast cells and anaphylaxis. *Curr Allergy Asthma Rep* 2016; **16**: 20.
47 Chousterman BG, Swirski FK, Weber GF. Cytokine storm and sepsis disease pathogenesis. *Semin Immunopathol* 2017; **39**: 517–28.
48 Behrens EM, Koretzky GA. Cytokine storm syndrome: looking toward the precision medicine era. *Arthritis Rheumatol* 2017; **69**: 1135–43.
49 Wing MG, Moreau T, Greenwood J, *et al.* Mechanism of first-dose cytokine-release syndrome by CAMPATH 1-H: involvement of CD16 (FcγRIII) and CD11a/CD18 (LFA-1) on NK cells. *J Clin Invest* 1996; **98**: 2819–26.
50 Kamburova EG, Van den Hoogen MWF, Koenen HJPM, Baas MC, Hilbrands LB, Joosten I. Cytokine release after treatment with rituximab in renal transplant recipients. *Transplantation* 2015; **99**: 1907–11.
51 Eastwood D, Findlay L, Poole S, *et al.* Monoclonal antibody TGN1412 trial failure explained by species differences in CD28 expression on CD4+ effector memory T-cells. *Br J Pharmacol* 2010; **161**: 512–26.
52 Bailey L, Moreno L, Manigold T, *et al.* A simple whole blood bioassay detects cytokine responses to anti-CD28SA and anti-CD52 antibodies. *J Pharmacol Toxicol Methods* 2013; **68**: 231–9.
53 Reed DM, Paschalaki KE, Starke RD, *et al.* An autologous endothelial cell:peripheral blood mononuclear cell assay that detects cytokine storm responses to biologics. *FASEB J* 2015; **29**: 2595.
54 Findlay L, Sharp G, Fox B, *et al.* Endothelial cells co-stimulate peripheral blood mononuclear cell responses to monoclonal antibody TGN1412 in culture. *Cytokine* 2011; **55**: 141–51.

55 Vidal J-M, Kawabata TT, Thorpe R, *et al. In vitro* cytokine release assays for predicting cytokine release syndrome: the current state-of-the-science. Report of a European Medicines Agency Workshop. *Cytokine* 2010; **51**: 213–5.
56 Sanchez-Garcia L, Martín L, Mangues R, Ferrer-Miralles N, Vázquez E, Villaverde A. Recombinant pharmaceuticals from microbial cells: a 2015 update. *Microb Cell Fact* 2016; **15**: 33.
57 International Conference on Harmonisation of technical requirements for registration of pharmaceuticals for human use. S6(R1)—Preclinical safety evaluation of biotechnology-derived pharmaceuticals. Genève: International Council for Harmonisation (ICH), 2011.
58 Nicholls SJ, Uno K, Kataoka Y, Nissen SE. ETC-216 for coronary artery disease. *Expert Opin Biol Ther* 2011; **11**: 387–94.
59 Huang L-Y, Dumontelle JL, Zolodz M, Deora A, Mozier NM, Golding B. Use of toll-like receptor assays to detect and identify microbial contaminants in biological products. *J Clin Microbiol* 2009; **47**: 3427–34.
60 Caparon MH, Rust KJ, Hunter AK, *et al.* Integrated solution to purification challenges in the manufacture of a soluble recombinant protein in *E. coli*. *Biotechnol Bioeng* 2010; **105**: 239–49.
61 Kallend DG, Reijers JAA, Bellibas SE, *et al.* A single infusion of MDCO-216 (APOA-1 Milano/POPC) increases ABCA1-mediated cholesterol efflux and pre-beta 1 HDL in healthy volunteers and patients with stable coronary artery disease. *Eur Hear journal Cardiovasc Pharmacother* 2016; **2**: 23–9.

SAMENVATTING

De klinische farmacologie is het vakgebied dat in brede zin de werking van medicatie bestudeert en daarmee tevens de rationaliteit van behandelingen. In dat kader zijn twee vragen belangrijk, namelijk 'Hoe bereikt een geneesmiddel in voldoende hoeveelheden de werkzame plaats?' (farmacokinetiek) en 'Hoe werkt een geneesmiddel?' (farmacodynamiek).

Hoewel van onderzoek met medicatie, in het bijzonder onderzoek in mensen, al voorbeelden uit de oudheid bekend zijn, stamt de klinische farmacologie als discipline uit medio twintigste eeuw. Destijds bestond het farmaceutische arsenaal vooral uit relatief eenvoudige stoffen, die vrijwel altijd door een reeks chemische reacties tot stand (kunnen) komen, de zogenaamde 'kleine moleculen', zoals paracetamol. Vanaf 1980 zijn zogenaamde biofarmaceutica in opkomst. Deze geneesmiddelen worden geproduceerd door levende organismen, meestal door aanpassing van het genetische materiaal (recombinant DNA). Dankzij deze techniek kunnen menselijke eiwitten worden nagemaakt en dienen als behandeling voor patiënten met een gebrek aan bepaalde, (vaak) essentiële eiwitten. Ook kunnen eiwitten speciaal worden ontworpen om heel doelgericht te binden aan cellen of signaalstoffen en zodoende te interfereren in het ziekteproces. Deze laatste groep eiwitten bestaat veelal uit monoklonale antilichamen (MAb's).

Juist de specificiteit van biofarmaceutica maakt deze categorie geneesmiddelen gevierd, zij het tegen hoge gezondheidszorgkosten, die zijn terug te voeren op de grotere complexiteit van het productie- en ontwikkelingsproces van therapeutische eiwitten ten opzichte van 'conventionele' geneesmiddelen. De complexere structuur van biofarmaceutica leidt ook tot andere farmacokinetische eigenschappen dan veel van de gangbare modellen, die waren ontwikkeld op basis van het gedrag van kleine moleculen, voorspellen. In het *eerste deel* van deze thesis (*sticky proteins*, 'kleverige eiwitten') worden enkele bijzondere, farmacokinetische eigenschappen van biofarmaceutica verkend; eigenschappen die momenteel onvoldoende worden gedekt of begrepen door huidige theorieën.

Hoofdstuk 1 richt zich op bioequivalentieonderzoek, biosimilariteitsonderzoek geheten als het de vergelijking tussen biofarmaceutica betreft. Kern van zulk onderzoek is de vergelijkbaarheid van een generiek product (het 'testproduct') aan te tonen ten opzichte van het originele product (het 'referentieproduct') op diverse vlakken, waaronder vergelijkbare farmacokinetiek. Van oudsher wordt farmacokinetische bioequivalentie of biosimilariteit gebaseerd op twee parameters, namelijk de maximale plasmaconcentratie (C_{max}) van een geneesmiddel en het oppervlakte onder de plasmaconcentratie-tijd-curve ('area under the curve', AUC). Deze twee parameters worden bepaald in een non-compartimentele analyse (NCA), zoals vereist door de registratieautoriteiten, die uiteindelijk beslissen of het testproduct tot de (geneesmiddelen)markt wordt toegelaten.

Een NCA gaat uit van lineaire kinetiek en lineaire eliminatie van een medicament en is daarmee inherent ongeschikt voor de correcte beschrijving van het farmacokinetische profiel van veel biofarmaceutica, die vrijwel zonder uitzondering (eveneens) worden geëlimineerd via een non-lineair proces. Eerder is een populatie-farmacokinetische benadering (PPK) toegepast op de vergelijking tussen een test- en referentiebiofarmaceuticum. In tegenstelling tot een NCA kan een PPK non-lineaire processen beschrijven.

In *hoofdstuk 1* wordt voor het eerst de bruikbaarheid van een PPK onderzocht voor het aantonen van farmacokinetische biosimilariteit van de grootste, therapeutische eiwitten, de MAb's. In het eerste deel van het onderzoek werd een model ontwikkeld waarin alle plasmaconcentraties van zowel het test- als het referentieproduct waren opgenomen. Uit de covariatenanalyse bleek dat geen statisch significante verschillen bestonden tussen beide producten. Een voordeel van deze methode is dat alle parameters in een PPK-model kunnen worden getest, en daarmee diverse (primaire) farmacokinetische eigenschappen van test- en referentieproduct, zoals absorptie, distributie en eliminatie. Daarentegen wordt momenteel als standaard alleen de vergelijkbaarheid op twee afgeleide (secundaire) parameters, C_{max} en AUC, onderzocht.

Het tweede deel bestond uit de ontwikkeling van twee afzonderlijke modellen, één voor het testproduct en één voor het referentieproduct. Anders dan bij het gecombineerde model uit het eerste deel is de aanname hierbij niet dat het test- en referentieproduct dezelfde (werkzame) stof bevatten. Hoewel de twee afzonderlijk ontwikkelde modellen in grote mate overeenkomst vertoonden en daarmee vóór biosimilariteit pleitten, is een statische vergelijking met deze methode lastig. Nochtans kunnen met beide modellen simulaties worden uitgevoerd, die bijvoorbeeld aantonen dat ook het testproduct therapeutische concentraties bereikt, vergelijkbaar met het referentieproduct, en die derhalve de biosimilariteitshypothese ondersteunen.

Een belangrijke voorwaarde voor een adequaat farmacokinetisch model is een juist begrip van de onderliggende mechanismen. Ofschoon de modellen in *hoofdstuk 1* de non-lineaire eliminatie van een MAB konden beschrijven, kunnen deze modellen niet verklaren waarom de plasmaconcentratie blijft stijgen nadat de (intraveneuze) toediening van een geneesmiddel is geëindigd, waarna theoretisch alleen nog eliminatie plaatsheeft. Voor meerdere biofarmaceutica is dit fenomeen beschreven (*tabel 2.1*), waarbij de tijd tot C_{max} (t_{max}) niet – zoals verwacht – gelijk is aan de infusieduur (t_{EOI}), maar enige tijd tot vele uren later optreedt. Afgezien van het rapporteren van de 'verlate' t_{max} is tot op heden geen onderzoek verricht naar mogelijke oorzaken. Vaker nog ontbreekt in publicaties de t_{max} van biofarmaceutica die intraveneus worden toegediend.

Hoofdstuk 2 onderzoekt twee hypotheses die de verlate t_{max} kunnen verklaren. Volgens de eerste hypothese binden biofarmaceutica reversibel aan vaatwanden of worden tijdelijk door endotheelcellen opgenomen, afhankelijk van de lokale concentratie. Doordat op de toedieningslocatie de geneesmiddelconcentratie relatief hoog is, treedt aanvankelijk binding of opname op. Nadat de infusie is voltooid, daalt de lokale concentratie abrupt, waardoor desorptie of exocytose van respectievelijk geadsorbeerd of opgenomen biofarmaceuticum plaatsvindt. Dit heeft tot gevolg dat de plasmaconcentratie antegraad van de toedieningslocatie stijgt, totdat in alle vaten een evenwicht is bereikt tussen adsorptie en pino- of endocytose enerzijds en desorptie en exocytose anderzijds (*figuur 2.4*).

In een reeks experimenten werden endotheelcellen blootgesteld aan wisselende concentraties van trastuzumab of bevacizumab. Concentratieafhankelijke adsorptie van deze MAB's aan de luminale zijde van endotheelcellen werd inderdaad waargenomen, terwijl opname door de cellen niet leek op te treden. Ook bonden de onderzochte MAB's aan de extracellulaire matrix. Samen met bestaand bewijs over de interactie tussen eiwitten en uiteenlopende biologische structuren, wijzen deze bevindingen op een aspecifieke vorm van adsorptie, die de eerste hypothese ondersteunen.

De tweede, onderzochte hypothese is dat biofarmaceutica kunnen adsorberen aan infuuslijnen tijdens toediening. In sommige gevallen worden de infuuslijnen nagespoeld met een fysiologischezoutoplossing; indien in die gevallen geadsorbeerd eiwit oplost in de spoelvloeistof, duurt de infusie van geneesmiddel voort ná de verwachte t_{EOI} en veroorzaakt zo *schijnbaar* een verlate t_{max}. Bij het nabootsen van zulke toedieningsprocedures met diverse biofarmaceutica onder verschillende omstandigheden (infusieconcentratie en -snelheid) in het laboratorium werd wel een afname van de toegediende dosis geneesmiddel gedurende de verwachte infusieduur gezien, maar in geen geval bevatte de spoelvloeistof een meetbare eiwitconcentratie (*figuur 2.3*). Derhalve werd voor de tweede hypothese geen bewijs gevonden.

Naast een verlate t_{max} blijkt het farmacokinetische profiel van sommige biofarmaceutica meerdere pieken te vertonen dan uitsluitend één C_{max} (*figuur 3.1*), een fenomeen dat in ***hoofdstuk 3*** nader wordt beschreven. Theoretisch daalt de plasmaconcentratie uitsluitend na de t_{max} als gevolg van eliminatie, hetgeen in tegenspraak schijnt met de waargenomen fluctuerende concentraties over tijd van meerdere MAB's. Onder andere door deze fluctuaties te vergelijken met de (slechts minimale) tijdsafhankelijke variabiliteit van de bloedconcentraties van albumine en erythrocyten – van nature voorkomende bestanddelen die in belangrijke mate overeenkomsten vertonen met MAB's qua distributie – wordt onaannemelijk dat de geobserveerde fluctuaties kunnen worden toegeschreven aan 'normale' variabiliteit. Tevens zijn de analysemethodes voor de bepaling van plasmaconcentraties van MAB's dermate nauwkeurig dat de kans zeer klein is dat de (vrij grote) schommelingen in de plasmaconcentraties het gevolg van variabiliteit in de analysemethode zijn.

Ofschoon op de voornoemde gronden de fluctuerende MAB-concentratie over tijd als reëel moet worden beschouwd, blijft iedere verklaring voor het fenomeen vooralsnog speculatief. De in *hoofdstuk 2*

beschreven adsorptie aan endotheel zou ook de fluctuaties na t_{max} kunnen veroorzaken als men in ogenschouw neemt dat het endotheel dynamisch is, evenals het aan de circulatie blootgestelde endotheeloppervlakte. Indien deze dynamiek gepaard gaat met wijziging van de bindingskarakteristieken, zouden op deze wijze grote hoeveelheden van een MAB kunnen vrijkomen of juist worden gebonden met abrupte stijgingen en dalingen in de plasmaconcentratie tot gevolg.

Kennis van de exacte verdeling van geneesmiddelen over het lichaam is essentieel voor de klinisch farmacoloog. Rationele farmacotherapie met biofarmaceutica kan niet worden ingesteld zonder wetenschap van de individuele farmacokinetiek. Zoals uit de *eerste sectie* van deze thesis blijkt, is de *in vivo* kinetiek van biofarmaceutica doorgaans vele malen complexer dan wordt voorspeld door de huidige theorieën, zeker als deze uitsluitend zijn gebaseerd op kleine moleculen. In hoeverre deze afwijkingen in de *aangenomen* farmacokinetiek van een biofarmaceuticum leiden tot het falen van een behandeling, of tot meer of onverwachte neveneffecten, hangt af van de concentratieafhankelijke effecten van het geneesmiddel en de werkelijke distributie over het lichaam.

Zelfs al ware de farmacokinetiek van biofarmaceutica volledig bekend, blijken neveneffecten van deze klasse geneesmiddelen geregeld lastig te voorspellen op basis van preklinisch onderzoek. Bepaalde biofarmaceutica zijn bijvoorbeeld geassocieerd met inflammatoire reacties, die meestal bij de eerste toediening optreden en ernstig kunnen verlopen. De overkoepelende term voor zulke reacties is 'ongewenste immunostimulatie' (in dit proefschrift afgekort als AI). Deze bijzondere eigenschap van biofarmaceutica staat centraal in het *tweede deel* van deze thesis (*dirty proteins*, 'vuile eiwitten').

Trastuzumab is één van de MAB's die AI kan induceren, maar waarvan het pathofysiologische mechanisme niet is opgehelderd. In ***hoofdstuk 4*** worden de resultaten van gezonde proefpersonen die koorts (*i.c.* AI) ontwikkelden na *in vivo* toediening van trastuzumab vergeleken met de resultaten van proefpersonen die geen koorts kregen. De 'respondenten' vertoonden in een *ex vivo* volbloedincubatietest met trastuzumab hogere IL-6-waarden dan de 'non-respondenten', en deze waarde correleerde met de bereikte maximale lichaamstemperatuur (*figuur 4.1*). Een lineaire correlatie werd ook gevonden tussen de *ex vivo* TNF-α-waarde en de maximale lichaamstemperatuur, maar uitsluitend in de respondenten.

Niettemin waren de verschillen in de uitslagen tussen beide groepen klein, waardoor de gebruikte incubatiemethode vooralsnog ongeschikt is als screeningtest voor (trastuzumab-geassocieerde) AI. Anderzijds is dit één van de weinige onderzoeken waarin een relatie wordt gelegd tussen *in* en *ex vivo* resultaten.

Niet alleen de actieve stof in het geneesmiddel, maar ook verontreinigingen en onzuiverheden kunnen tot een immuunrespons leiden, zeker als de verontreinigingen of onzuiverheden van microbiële origine zijn. Aangezien biofarmaceutica doorgaans in niet-humane cellijnen, zoals bacteriën, worden geproduceerd, eindigen celresten onvermijdelijk in het eindproduct, resten die AI kunnen veroorzaken. Wegens het potentieel levensbedreigende karakter van AI zou men verwachten dat hiernaar specifiek onderzoek wordt gedaan tijdens de preklinische fase van ontwikkeling. Echter, zelfs voor biofarmaceutica, ondanks het inherent verhoogde risico op AI, vereisen de richtlijnen zulke onderzoekingen niet. Dat hierdoor AI als gevolg van (microbiële) onzuiverheden kan worden gemist, blijkt uit twee casus.

Hoofdstuk 5 beschrijft de eerste casus over een recombinant, humaan apolipoproteine A-I Milano met de codenaam ETC-216, waarvan eerst in het derde klinische onderzoek men zich realiseerde dat het middel AI induceerde, al bleken in retrospectie de eerdere onderzoeken meerdere aanwijzingen te tonen. Tijdens latere analyses werd duidelijk dat ETC-216 diverse bacteriële (rest)eiwitten bevatte, zogenaamde 'host-cell proteins' (HCP's), waarvan één flagelline was. De tweede casus (beschreven in ***hoofdstuk 6***) betreft een recombinant, humaan plasmaeiwit. Bij dit biofarmaceuticum werd de AI reeds opgemerkt in het eerste klinische onderzoek, maar net als bij de eerste casus bleek de oorzaak gelegen in HCP's.

In ***hoofdstuk 5*** werd opnieuw een *ex vivo* volbloedincubatietest toegepast voor het aantonen van een inflammatoire reactie. Hierbij bleek een sterke IL-6- en TNF-α-respons na stimulering met ETC-216, terwijl het vernieuwde (opgeschoonde) product (MDCO-216) geen respons vertoonde. Dit verschil was statistisch significant voor alle onderzochte populaties: gezonde proefpersonen, en patiënten met stabiel en acuut coronairlijden. Nadien bevestigde een klinisch onderzoek de afwezigheid van AI na toediening van

MDCO-216 aan gezonde proefpersonen en patiënten met stabiele, coronaire hartziekte, en daarmee de succesvolle eliminatie van de oorzakelijke HCP's.

Zorgvuldigheid dient te worden betracht bij de interpretatie van de resultaten van zo een *ex vivo* test, zeker waar het de conclusie betreft dat door de toepassing van een *ex vivo* test AI had kunnen worden voorkomen. Het uitgevoerde onderzoek toont namelijk ook aan dat de reactie op ETC-216 verschilt zowel tussen als binnen populaties. Sommige verschillen kunnen worden toegeschreven aan comorbiditeit en gebruik van bepaalde medicamenten, maar hiermee worden de resultaten slecht ten dele verklaard. Juist deze verschillen benadrukken dat het vertalen van *ex vivo* uitslagen naar *in vivo* effecten lastig blijft, evenals de preklinische voorspelling van AI.

Hoewel *hoofdstuk 5* bewijst dat de AI als gevolg van bepaalde HCP's kan worden gedetecteerd in het preklinische stadium, blijft de vraag onbeantwoord waarom de in de richtlijnen voorgeschreven teststrategie de destijds opgetreden AI niet heeft kunnen verhinderen. Aan de hand van de twee casus illustreert ***hoofdstuk 6*** de belangrijkste tekortkomingen van de huidige praktijk.

De eerste tekortkoming betreft de sensitiviteit van de testen die worden toegepast voor de kwaliteitsbewaking van geneesmiddelen. Endotoxine is de enige stof waarvan de aanwezigheid altijd wordt onderzocht; ware het niet dat de vaak gebruikte limulus-amoebocyt-lysaat-test (LAL-test) bepaalde endotoxinevarianten niet kan detecteren. Zo ook detecteren veel testen voor HCP's en residuaal DNA slechts een selectie van alle aanwezige (bacteriële) restmateriaal. Aangezien de identiteit van bijvoorbeeld de gevonden HCP's in deze testen onbekend blijft, is ook de testuitslag lastig te duiden. Immers, van veel (bacteriële) producten en alle mogelijke combinaties daarvan is het klinische effect onduidelijk. Hierin ligt de tweede tekortkoming: de kwantificering in plaats van kwalificering van onzuiverheden.

Nieuwere testen daarentegen trachten de *in vivo* situatie na te bootsen door het gebruik van menselijke immuuncellen of -receptoren. Deze testen, zoals ook gebruikt in de *hoofdstukken 4 & 5*, kunnen immunostimulatoire stoffen opsporen die voorheen eerst in de kliniek zouden zijn ontdekt. Geen laboratoriumonderzoek is echter waterdicht, niet in de minste plaats vanwege de oneindig grotere complexiteit van een levend organisme en alle *in vivo* aanwezige omgevingsfactoren. Bovendien is bij voorbaat niet bekend welke weefsels en cellen een rol spelen bij het ontstaan van een bepaalde reactie.

Toxicologisch onderzoek in proefdieren kan de gevolgen van de eerste twee tekortkomingen enigszins beperken, mits het immuunsysteem van de gekozen diersoort in gelijke mate reageert op bepaalde stimuli als het menselijke. In makaken leidde ETC-216 bijvoorbeeld tot AI, maar dit werd gemist, doordat gevoelige biomarkers (*e.g.* cytokines) niet werden bepaald en doordat de metingen die in de richting van AI hadden kunnen wijzen met te grote intervallen werden verricht. Belangrijk hierbij is dat immunotoxiciteit niet routinematig wordt onderzocht en dat dit evenmin wordt vereist door de richtlijnen. Daarnaast ligt de nadruk van immunotoxicologische onderzoeken – indien uitgevoerd – op langetermijnonderdrukking of -versterking van het afweersysteem, terwijl de meeste gevallen van AI bij biofarmaceutica juist snel optreden en kortdurend zijn.

Tot slot is bekendheid met het fenomeen AI belangrijk ter voorkoming van toekomstige casus. Vanuit onwetendheid kan men ten onrechte aannemen dat AI zeldzaam is of symptomen toeschrijven aan bijvoorbeeld hypersensitiviteit, met alle gevolgen van dien. Alleen door meer openheid en door het uitwisselen van informatie over geneesmiddelen kunnen zinnige wijzigingen van de richtlijnen worden voorgesteld en bediscussieerd.

HET CENTRALE THEMA VAN DIT PROEFschrift is *sticky proteins & dirty proteins* – 'kleverige eiwitten' en 'vuile eiwitten'. De kleverigheid betreft de dynamische binding van therapeutische eiwitten aan diverse (lichaams)oppervlakten, waarmee theoretisch sommige slecht begrepen, farmacokinetische eigenschappen van biofarmaceutica kunnen worden verklaard, in het bijzonder de vertraagde t_{max} na intraveneuze toediening en de fluctuerende plasmaconcentraties. Vuile eiwitten kunnen een ongewenste afweerreactie teweegbrengen, indien het menselijke immuunsysteem een biofarmaceuticum als vijandig beschouwd. Hierbij kunnen zowel het actieve bestanddeel als onzuiverheden of vervuiling als stimulus dienen.

Ofschoon bepaalde eigenaardigheden van biofarmaceutica zich lastig laten voorspellen, vooral ten gevolge van onvoldoende inzicht in de onderliggende mechanismen, lijkt kennis van beide concepten – *sticky & dirty proteins* – onmisbaar voor klinisch farmacologen en artsen.

APPENDIX

CURRICULUM VITÆ

Joannes A.A. Reijers was born in the eldest city of the county of Holland (Dordrecht) AD 1985, and studied medicine at the eldest university of the Northern Netherlands (*Leiden University*). Both the doctoral and the medical exams were passed with honours, in respectively 2008 and 2010.

Thereafter, he remained associated with the academic hospital, the *Leiden University Medical Center*, in the function of resident at the department of internal medicine.

From 2011 through 2016, Mr. Reijers worked at the *Centre for Human Drug Research* in Leiden, where all research was conducted, which culminated in this thesis. During this period, he became a registered clinical pharmacologist and member at the *Dutch Society of Clinical Pharmacology and Biopharmacy*.

Mr. Reijers returned to clinical practice and to the *alma mater* in 2016, starting the training for rheumatologist. As part of this specialisation, he is currently following a 3-year course in internal medicine at the regional hospital in the historical city of Gouda.

BIBLIOGRAPHY

1 Wisman LAB, De Cock EPM, Reijers JAA, *et al.* A phase I dose-escalation and bioequivalence study of a trastuzumab biosimilar in healthy male volunteers. *Clin Drug Investig* 2014; **34**: 887–94.

2 Reijers JAA, Burggraaf J. Trastuzumab induces an immediate, transient volume increase in humans: a randomised placebo-controlled trial. *EBioMedicine* 2015; **2**: 953–9.

3 Kallend DG, Reijers JAA, Bellibas SE, *et al.* A single infusion of MDCO-216 (ApoA-1 Milano/POPC) increases ABCA1-mediated cholesterol efflux and pre-beta 1 HDL in healthy volunteers and patients with stable coronary artery disease. *Eur Hear journal Cardiovasc Pharmacother* 2016; **2**: 23–9.

4 Reijers JAA, van Donge T, Schepers FML, Burggraaf J, Stevens J. Use of population approach non-linear mixed effects models in the evaluation of biosimilarity of monoclonal antibodies. *Eur J Clin Pharmacol* 2016; **72**: 1343–52 (***chapter 1***).

5 Dillingh MR, Reijers JAA, Malone KE, *et al.* Clinical evaluation of Humira® biosimilar ONS-3010 in healthy volunteers: focus on pharmacokinetics and pharmacodynamics. *Front Immunol* 2016; **7**: 508.

6 Monnet E, Lapeyre G, Poelgeest E van, Jacqmin P, Graaf K, Reijers J, *et al.* Evidence of NI-0101 pharmacological activity, an anti-TLR4 antibody, in a randomized phase I dose escalation study in healthy volunteers receiving LPS. *Clin Pharmacol Ther* 2017; **101**: 200–8.

7 Reijers JA, Dane M, Malone K, Burggraaf J, Moerland M. Characterisation of immunostimulation by trastuzumab in responders and non-responders. *J Pharmacol Clin Toxicol* 2017; **5**: 1075 (***chapter 4***).

8 Reijers JAA, Kallend DG, Malone KE, *et al.* MDCO-216 does not induce adverse immunostimulation, in contrast to its predecessor ETC-216. *Cardiovasc drugs Ther* 2017; **31**: 381–9 (***chapter 5***).

9 Reijers JAA, Dane MJC, van Zonneveld AJ, Burggraaf J, Moerland M. Potential influence of endothelial adsorption on the delayed time to maximum concentration of biopharmaceuticals. *Eur J Drug Metab Pharmacokinet* 2018; **43**: 103–13 (***chapter 2***).

10 Reijers JAA, Moerland M, Burggraaf J. Remarkable pharmacokinetics of monoclonal antibodies: a quest for an explanation. *Clin Pharmacokinet* 2017; **56**: 1081–9 (***chapter 3***).

11 Ducore J, Lawrence JB, Simpson M, Boggio L, Bellon A, Burggraaf J, Stevens J, Moerland M, Frieling J, Reijers J, Wang M. Safety and dose-dependency of eptacog beta (activated) in a dose escalation study of non-bleeding congenital haemophilia A or B patients, with or without inhibitors. *Haemophilia* 2017; **23**: 844–51.

ACKNOWLEDGEMENTS

Special thanks are extended to the operational crew of CHDR, without whose tireless efforts the clinical trials – of which the data were used in chapters 1, 4, and 5 – would not have been possible. Particularly, Mr. Gerrit A. van der Luijt is acknowledged for his assistance in managing the conduct of these trials and for his overall moral as well as friendly support. Ms. Tess D. Woutman and Ms. Monique van der Linden are recognised for their roles in replicating the intravenous administration procedures described in chapter 2.

Furthermore, expressions of gratitude are offered to the scientifical staff of CHDR, especially, the *promotores &* copromotor, Ms. Annelieke C. Kruithof, Dr. Marlous R. Dillingh, Mr. Willem A.J. Birkhoff, Dr. Jan Freijer. Together with M(r)s. Helma F.M. Nederend, Mlle. Baukje du Bois, and M(r)s. Sabine G.J. Deferme, they have helped shape hypotheses and opinions – many of which formed the basis of the work presented here – during countless discussions, in-depth conversations, and memorable soirées.

AFFILIATIONS

Centre for Human Drug Research, Leiden, The Netherlands
- J. Burggraaf
- A.F. Cohen
- T. van Donge
- M. Moerland
- J.A.A. Reijers
- F.M.L. Schepers
- J. Stevens

Department of Internal Medicine (Nephrology) and the *Eindhoven Laboratory of Experimental Vascular Medicine*, *Leiden University Medical Center*, Leiden, The Netherlands
- M.J.C. Dane
- A.J. van Zonneveld

Janssen Prevention Center, Janssen Vaccines and Prevention b.v., Leiden, The Netherlands
- K.E. Malone

Leiden University Medical Center, Leiden, The Netherlands
- J.W. Jukema (*Department of Cardiology*)
- R. Verbeek (*Department of Clinical Pharmacy and Toxicology*)

The Medicines Company
- D.G. Kallend (Zürich, Switzerland)
- P.L.J. Wijngaard (Parsippany, New Jersey, USA)

Alternatives Unit, Biomedical Primate Research Centre, Rijswijk, The Netherlands
- J.J. Bajramovic